ÉCOLE DE TECHNOLOGIE SUPÉRIEURE
UNIVERSITÉ DU QUÉBEC

THÈSE PAR ARTICLES PRÉSENTÉE À
L'ÉCOLE DE TECHNOLOGIE SUPÉRIEURE

COMME EXIGENCE PARTIELLE
À L'OBTENTION DU
DOCTORAT EN GÉNIE
Ph.D.

PAR
KADDISSI, Claude

COMMANDE NONLINÉAIRE ET NON DIFFÉRENTIABLE D'UN SYSTÈME ÉLECTROHYDRAULIQUE

MONTRÉAL, LE 28 MARS 2008

CE RAPPORT DE THÈSE A ÉTÉ ÉVALUÉ

PAR UN JURY COMPOSÉ DE :

M. Jean-Pierre Kenné, directeur de thèse
Département de génie mécanique à l'École de technologie supérieure

M. Maarouf Saad, codirecteur de thèse
Département de génie électrique à l'École de technologie supérieure

M. Anh Dung Ngô, président du jury
Département de génie mécanique à l'École de technologie supérieure

M. Louis Lamarche, membre du jury
Département de génie mécanique à l'École de technologie supérieure

M. Francis Aimé Okou, examinateur externe
Département de génie électrique et informatique au Collège militaire royal du Canada, Kingston

IL A FAIT L'OBJET D'UNE SOUTENANCE DEVANT JURY ET PUBLIC

LE 29 FÉVRIER 2008

À L'ÉCOLE DE TECHNOLOGIE SUPÉRIEURE

AVANT-PROPOS

Les systèmes électrohydrauliques sont des systèmes difficiles à commander, vu leur comportement nonlinéaire et leurs paramètres qui varient en fonction de la température et de la pression. En effet, ils présentent plusieurs types de nonlinéarité ainsi qu'un aspect non-différentiable qui rendent leur commande encore plus compliquée.

À l'égard de ce qui précède, plusieurs stratégies et lois de commande ont été établies. Dans la revue de littérature, nous nous sommes intéressés en premier lieu à la commande des systèmes électrohydrauliques en général, ensuite nous avons visé les stratégies appliquées aux systèmes électrohydrauliques utilisés dans l'industrie, surtout automobile, en particulier la commande d'une suspension active électrohydraulique. Dans ce type d'application, un comportement insatisfaisant est souvent dû aux hypothèses simplificatrices qui sont imposées par les ingénieurs afin de diminuer la complexité de la loi commande. Citons par exemple le fait de linéariser le modèle mathématique et de négliger la dynamique de certains composants.

En effet, notre objectif est d'améliorer la commande des systèmes électrohydrauliques, en proposant une loi de commande nonlinéaire et robuste avec le moins d'hypothèses simplificatrices possibles. Cette loi doit assurer la stabilité du système, en tenant compte de la discontinuité du modèle mathématique, de toutes les nonlinéarités et de la variation des paramètres dans le temps. En résumé, les objectifs de cette recherche peuvent être récapitulés en cinq étapes principales :

- Concevoir un modèle mathématique qui décrit la dynamique d'un système électrohydraulique et qui couvre ses aspects nonlinéaires, afin d'avoir une représentation plus réaliste du processus physique;
- Simuler ensuite ce modèle et comparer son comportement avec le système réel;
- Développer une loi de commande nonlinéaire, plus performante et robuste que les stratégies classiques déjà employées pour ce type de systèmes et avec lesquelles les résultats obtenus ne sont pas encore très satisfaisants. Faire ensuite une analyse de stabilité de l'approche proposée;

- Valider le modèle et la loi de commande proposés, par simulation et implantation en temps réel;
- Viser une application industrielle particulière telle que la suspension active électrohydraulique.

Finalement, le but ultime recherché est d'exploiter cette stratégie de commande dans l'industrie automobile. En effet, les grands fabricants comme '*General motors*' et '*Ford*' ont récemment eu recourt aux systèmes électrohydrauliques pour le contrôle de la suspension active des voitures, du système de transmission ainsi que du système d'accélération. Ce type de commande est connu sous le nom de 'Drive By Wire' (DBW) ou 'Commande par signal électrique' et est déjà utilisé en avionique sous le nom de 'Fly By Wire' (FBW). D'où l'intérêt et l'impact industriel de ce travail.

REMERCIEMENTS

Mes sincères remerciements vont aux Professeurs Jean-Pierre Kenné et Maarouf Saad, mes directeurs de thèse, pour leur disponibilité marquée à me guider et superviser tout au long de ce cheminement, pour le soutien financier qu'il m'ont accordé et assuré, ce qui m'a permis de me concentrer plus sur ma recherche.

Un grand remerciement aussi à M. Charles Fallaha pour son aide appréciée à m'introduire au langage C, qui était pertinent pour le développement de certaines fonctions nécessaires à la partie expérimentale de la recherche.

Je souhaite aussi remercier M. Joe Sfeir pour les idées dont il m'a fait part à plusieurs reprises pendant ma thèse me permettant ainsi de mieux évaluer différentes approches.

Je remercie aussi mes parents pour leur soutien financier au début de ce long cheminement qui m'a permis de m'installer et m'intégrer rapidement au Québec.

Finalement, ce travail n'aurait pu être accompli sans le support moral de ma fiancée Chadia qui me donnait toujours l'encouragement et l'enthousiasme pour continuer lorsque toutes les solutions semblaient impossibles.

COMMANDE NONLINÉAIRE ET NON-DIFFÉRENTIABLE D'UN SYSTÈME ÉLECTROHYDRAULIQUE

KADDISSI, Claude

RÉSUMÉ

Cette thèse traite la modélisation, l'identification et la commande des systèmes électrohydrauliques et leur intégration dans des processus industriels tels que la suspension active des véhicules. Le travail est réparti sur trois phases. Dans une première étape une étude est menée sur le modèle mathématique d'un système électrohydraulique générique et la commande utilisée en temps réel, qui est basée sur l'approche du backstepping nonlinéaire. L'emphase est essentiellement sur la disposition des paramètres du contrôleur et la façon dont ils influencent la dynamique de l'erreur. Malgré que le backstepping assure la stabilité asymptotique globale du système, les paramètres du contrôleur affectent néanmoins considérablement la saturation et l'allure du signal de commande et par conséquent, la dynamique de l'erreur. Le backstepping est un choix incontestable parce qu'il constitue une technique nonlinéaire puissante et robuste. Les résultats expérimentaux, obtenus à ce stade, sont comparés à ceux d'un contrôleur PID, afin de montrer que les contrôleurs linéaires classiques n'assurent pas l'efficacité requise, surtout lorsque l'actionneur du système hydraulique fonctionne à charge maximale. En deuxième lieu, la variation des paramètres hydrauliques du système, en fonction de la pression et de la température, ainsi que son effet sur la dégradation de l'efficacité du contrôleur, est étudiée. En conséquence, il est conclu qu'une stratégie de commande adaptative est nécessaire afin de mettre à jour le contrôleur avec la variation des paramètres. En effet, le backstepping adaptatif indirect est employé : d'abord, parce qu'il permet l'identification des valeurs réelles des paramètres du système; ensuite, il permet en même temps de profiter de la robustesse et de la stabilité qu'offre le backstepping. Les résultats expérimentaux à ce niveau sont comparés à ceux d'un contrôleur backstepping non-adaptatif appliqué au même banc d'essai, dans les mêmes conditions. L'efficacité de l'approche proposée, en termes de stabilité garantie et erreur de poursuite négligeable, en présence de paramètres variables, est bien démontrée. La troisième et dernière étape, étudie la commande d'une suspension active électrohydraulique, basée sur une combinaison de backstepping et de forwarding. Le modèle mathématique d'une suspension active électrohydraulique peut être classifié parmi les systèmes entrelacés. Ceci signifie que le modèle d'état est formé d'équations en 'feedback' et en 'feedforward'. Par conséquent, le backstepping et le forwarding forment une stratégie de commande appropriée pour stabiliser ce type de systèmes. L'avantage ultime de cette dernière est qu'elle ne laisse aucune dynamique interne, contrairement à d'autres stratégies. Il sera démontré, que le backstepping combiné avec le forwarding est une stratégie de commande propice pour compenser l'effet des perturbations routières sur la stabilité des véhicules. Les résultats sont comparés à ceux d'un PID classique et d'un contrôleur par mode de glissement, pour prouver que le contrôleur proposé surpasse une gamme de contrôleurs existants, pour une gamme de perturbations.

Mots clés: Systèmes électrohydraulique, suspension active, commande nonlinéaire, backstepping et integrator forwarding.

NONLINEAR AND NON-DIFFERENTIABLE CONTROL OF AN ELECTROHYDRAULIC SYSTEM

KADDISSI, Claude

ABSTRACT

This thesis studies the modeling, identification and control of electrohydraulic servo systems and their integration in industrial processes such as cars active suspension. The work is divided into three major stages. In a first step the focus is on the mathematical model of a generic electrohydraulic system and the real-time control that is being employed, which is based on the nonlinear backstepping approach. Emphasis is essentially on the tuning parameters effect and on how they influence the errors dynamic behavior, as will be shown. While backstepping control ensures the global asymptotic stability of the system, the tuning parameters of the controller nonetheless do greatly affect the saturation and chattering in the control signal, and consequently, the errors dynamic. Backstepping is used here because it is a powerful and robust nonlinear strategy. The experimental results are compared to those obtained with a real-time PID controller, to prove that classic linear controllers fail to achieve a good tracking of the desired output, especially, when the hydraulic actuator operates at the maximum load. Secondly, the variation of the electrohydraulic system parameters due changes in the system pressure and temperature as well as the effect of this variation on degrading the controller efficiency, is carried on. Consequently, it was concluded that an adaptive control strategy is needed in order to update the controller with the parameters variation. In such case, indirect adaptive backstepping was used: first, because it allows the identification of the system parameters real values; second, because it permits to benefit of the backstepping robustness and stability at the same time. The out coming results are compared to those obtained from a non-adaptive backstepping controller applied to the same electrohydraulic test-bench, under the same conditions. The effectiveness of the proposed approach, in terms of guaranteed stability and negligible tracking error, in the presence of varying parameters, is well revealed in the results. The third and final step, studies the control of an electrohydraulic car active suspension, based on a combination of backstepping and integrator forwarding. The mathematical model of an electrohydraulic active suspension can be classified among interlaced systems. This means that the state space model is a sequence of feedback and feedforward equations. Therefore, interlaced backstepping and integrator forwarding is an optimal control strategy to stabilize this class of systems. The foremost advantage carried on by this interlaced strategy is that it leaves no internal dynamic, as is the case of others. As it will be demonstrated, the interlaced backstepping and integrator forwarding is an outstanding control strategy to compensate the effect of chaotic roads on cars stability. The results are compared with a classic PID and a sliding mode controller, to show that the proposed controller outperform a range of other existing ones for a range of perturbation signals.

Keywords: Electrohydraulic systems, active suspension, nonlinear control, backstepping and integrator forwarding.

TABLE DES MATIÈRES

Page

LISTE DES TABLEAUX

Page

LISTE DES FIGURES

Page

LISTE DES ABRÉVIATIONS, SIGLES ET ACRONYMES

LP	Linear Parameter (Linéaire en Paramètres)
PID	Proportional – Integral – Derivative (Proportionnel – Intégral – Dérivée)
SCADA	Supervisory Control And Data Acquisition (Contrôle supervisé et acquisition de données)
NCD	Nonlinear Control Design (Conception de commande nonlinéaire)
SQP	Sequential Quadratic Programming (Programmation séquentielle quadratique)
LQG	Linear – Quadratic – Gaussian (Linéaire – Quadratique – Gaussien)
PDF	Pseudo – Derivative Feedback (Rétroaction pseudo dérivative)
LPV	Linear Parameters Varying system (Système linéaire à paramèters variables)

LISTE DES SYMBOLES ET UNITÉS DE MESURE

A	Section du piston du vérin hydraulique, cm^2
A_v	Ouverture de l'orifice de la servovalve, cm^2
a	Constante exponentielle, *sans dimension*
B	Coefficient de frottement visqueux du moteur hydraulique, *daN.cm.s*
B_p	Coefficient de frottement visqueux de la suspension passive, *daNs/cm*
B_r	Coefficient d'amortissement du pneu, *daNs/cm*
C_d	Coefficient d'écoulement, *sans dimension*
C_L	Coefficient de fuite interne du moteur hydraulique, $cm^5/daN.s$
D_m	Cylindrée du moteur hydraulique, cm^3/rad
J	Inertie du moteur hydraulique, $daN.s^2.cm$
K	Gain constant de la servovalve, cm^2/V
K_p	Rigidité de la suspension passive, *daN/cm*
K_r	Rigidité du pneu, *daN/cm*
L	Coefficient de fuite interne du vérin hydraulique, $cm^5/daN.s$
M_r	Masse de l'ensemble suspension-pneu, *kg*
M_v	Masse du corps du véhicule, *kg*
$P_{1,2}$	Pression dans les deux chambres de l'actionneur hydraulique, daN/cm^2
P_L	Pression différentielle à la charge, daN/cm^2
P_s	Pression à la sortie de la pompe, daN/cm^2
Q, $Q_{1,2}$	Débits à travers les orifices de la servovalve, cm^3/sec
T_L	Couple résistif, *daN.cm*

u	Signal d'entrée de la servovalve, V
V	Volume d'huile dans une des chambres du moteur ou vérin hydraulique à une position quelconque, cm^3
V_0	Volume d'huile dans une des chambres du vérin hydraulique à 50% de la course du piston, cm^3
x	Position verticale du pneu du véhicule, m
x_r	Perturbations de la route, m
x_s	Position verticale du corps du véhicule, m
β	Coefficient de compressibilité de l'huile, daN/cm^2
θ, θ_p	Position angulaire du moteur hydraulique, rad
ρ	Masse volumique de l'huile, g/cm^3
τ, τ_v	Constante de temps de la servovalve, sec

INTRODUCTION

De nos jours, les systèmes électrohydrauliques sont très populaires dans la majorité des processus industriels comme la machinerie lourde, la robotique, l'avionique et l'industrie automobile. Ceci est dû principalement au rapport élevé puissance – volume qu'ils sont capables de fournir, en étant moins encombrants que les moteurs électriques de même puissance. Par contre au niveau commande, la nonlinéarité et la singularité du modèle mathématique des systèmes électrohydrauliques rendent la plupart des contrôleurs classiques à gains constants inadéquats.

En effet, un système électrohydraulique est composé de plusieurs éléments, à savoir :

- Une pompe qui alimente le circuit en fluide, souvent de l'huile qui est refoulée au système à une pression constante dite pression source.
- Un réservoir contenant le fluide.
- Un accumulateur qui joue le rôle d'une source d'énergie complémentaire ou d'un absorbeur des chocs dus aux coups de bélier.
- Une valve de régulation qui assure une pression source constante.
- Un actionneur hydraulique linéaire (vérin) ou rotatif (moteur) selon le type de déplacement désiré.
- Une servovalve dont le rôle est de déterminer la direction du mouvement du moteur ainsi que sa vitesse et son accélération; ceci en réglant par la position de son tiroir le débit d'huile dans les chambres d'admission et de refoulement de l'actionneur hydraulique. L'huile refoulée par ce dernier est acheminée à travers la servovalve au réservoir.

En général, la fonction principale d'un tel système est de déplacer une charge à une position donnée ou suivant une trajectoire désirée à une vitesse et accélération bien déterminées. L'élément principal de ces systèmes est la servovalve ; en effet il en existe deux types principaux : les servovalves à un seul étage ou à commande directe et les servovalves à deux étages ou à commande indirecte. Dans le premier type, le tiroir est actionné directement par un moteur électromagnétique (solénoïde) ; le point faible de ce modèle est sa dynamique réduite qui n'offre pas une grande manœuvrabilité. Tandis que le second type est composé

d'un étage piloté par l'action d'un moteur électromagnétique qui crée une différence de pression au niveau d'un étage principal formé du tiroir principal ce qui cause son déplacement; cette configuration offre une plus grande manoeuvrabilité.

La complexité des systèmes électrohydrauliques est surtout due à la servovalve. En fait, l'expression du débit du fluide à travers cette dernière est nonlinéaire et non-différentiable. D'un coté, le débit est proportionnel à la racine carrée de la pression; d'un autre côté, son expression contient une fonction 'signe' qui prend la valeur 1 ou -1 et vice versa, dépendamment du sens de l'écoulement. En outre, d'autres nonlinéarités peuvent aussi apparaître au niveau de la servovalve. Citons par exemple :

- L'expression du champ magnétique du solénoïde ;
- La force d'action du solénoïde ;
- La section des orifices qui est considérée rectangulaire, alors qu'en réalité elle est circulaire, étant plus facile à usiner. Ceci ramène la section de l'orifice à un arc de cercle, difficile à évaluer, puisqu'elle varie de façon nonlinéaire avec la position du tiroir.

D'un autre côté, les paramètres de tels systèmes sont sujets à des fluctuations à cause des variations de température et de pression ; ce qui diminue l'efficacité du système de commande. Effectivement, quand les systèmes électrohydrauliques sont utilisés dans des procédés simples, les commandes linéaires classiques de placement de pôles, par retour d'états ainsi que les commandes robustes par synthèse H_2 ou H_∞, donnent des résultats acceptables et même très satisfaisants dans plusieurs cas. Cependant l'utilisation accrue des systèmes électrohydrauliques dans des applications industrielles, où une grande précision du mouvement et un faible temps de réponse sont requis, rend indispensable la nécessité de trouver un modèle mathématique qui puisse bien décrire leur comportement nonlinéaire et non-différentiable, pour ensuite établir une loi de commande qui tient compte de ces aspects avec le moins d'hypothèses simplificatrices.

En effet la loi de commande que nous adoptons et qui constitue la clé de la solution, est basée sur le backstepping nonlinéaire et la théorie de Lyapunov. Cette approche, avec le modèle

mathématique que nous avons établi et les améliorations apportées a permis de résoudre la problématique précédemment définie et à laquelle nous nous sommes engagés au cours de notre recherche. Ceci nous a ouvert alors l'horizon pour pousser nos recherches dans les applications industrielles.

Dans l'industrie automobile, on exploite de plus en plus ce genre de système, surtout pour profiter des différents composants hydrauliques qui sont déjà disponibles dans une voiture, comme : l'huile, la pompe entraînée par le moteur thermique, le réservoir et les tuyauteries. Ceci permet de sauvegarder plus d'espace au lieu d'installer à nouveau des actionneurs électriques et assurer leur alimentation.

Dans le cadre de notre recherche nous nous sommes intéressés à la suspension active électrohydraulique. En effet, au niveau de la commande de la suspension active, les lois de commande nonlinéaires sont encore peu exploitées et les recherches se concentrent plus sur la fiabilité des composants mécaniques et hydrauliques.
En ce qui concerne la suspension active, le problème principal est que le confort des passagers est souvent amélioré au détriment de la tenue de route du véhicule et vice-versa.

De plus, le modèle mathématique de la suspension active n'a pas une structure triangulaire inférieure (condition nécessaire pour l'application du backstepping); mais, une partie en est triangulaire inférieure et l'autre est triangulaire supérieure, ce qui fait que le backstepping à lui seul ne suffit plus.

La solution proposée est une combinaison du backstepping et d'une autre approche qui est le forwarding. Cette dernière est l'équivalent du backstepping pour les systèmes qui ont un modèle mathématique à structure triangulaire supérieure.
Ceci a permis d'assurer un contrôle global de la suspension et un très bon compromis entre le confort et la tenue de route.

Le reste de ce rapport de thèse est constitué de quatre chapitres et d'une conclusion.

Dans un premier chapitre, nous présentons une revue de littérature pour illustrer la contribution des travaux précédents à l'élaboration de notre thèse, ainsi que l'originalité de nos principales contributions. Les trois chapitres suivants correspondent à trois articles. Ils constituent une contribution originale de l'auteur de cette thèse et de ses directeurs.

L'article du deuxième chapitre a été publié dans la revue IEEE/ASME Transactions On Mechatronics :
« Kaddissi, C., J.-P. Kenné, et M. Saad (2007). "Identification and Real-Time Control of an Electrohydraulic Servo System Based on Nonlinear Backstepping." Mechatronics, IEEE/ASME Transactions on **12**(1): 12-22. »

Comme son titre l'indique, dans cet article nous présentons l'approche du backstepping appliqué, en temps réel, à un système électrohydraulique générique en présentant une façon particulière d'introduire les paramètres de contrôle.

L'article du troisième chapitre, est soumis à la revue IEEE/ASME Transactions On Mechatronics :
« Kaddissi, C., J.-P. Kenné, et M. Saad (2007). "Real-time Indirect Adaptive Control of an Electrohydraulic Servo System Based on Nonlinear Backstepping." Submitted to the Mechatronics, IEEE/ASME Transactions on »

Dans cet article nous présentons le backstepping adaptatif indirect appliqué, en temps réel, à un système électrohydraulique générique afin d'identifier la variation des paramètres hydrauliques du système et de les réinjecter dans le contrôleur.

L'article du quatrième chapitre, est accepté pour publication dans la revue Journal of Vibration and Control (JVC) :
« Kaddissi, C., M. Saad, et J.-P. Kenné (2007). "Interlaced Backstepping and Integrator Forwarding for Nonlinear Control of an Electrohydraulic Active Suspension." Accepted in the Journal of Vibration and Control (JVC). »

Dans ce dernier article nous présentons la commande entrelacée basée sur le backstepping et le forwarding, appliquée à un modèle de suspension active électrohydraulique.

Les trois articles sont présentés dans leur version originale telle qu'acceptée par la revue correspondante. Pour cela, nous avons prévu à la fin de ce rapport trois annexes qui expliquent et montrent en détail tous les développements concernant ces trois articles. Ces annexes sont répartis de la manière suivante : L'annexe A correspond au chapitre 2 (premier article) ; l'annexe B correspond au chapitre 3 (deuxième article) et l'annexe C correspond au chapitre 4 (troisième article).

Finalement, une conclusion récapitule le travail et les contributions principales apportées.

CHAPITRE 1

REVUE DE LITTÉRATURE

1.1 Introduction à la modélisation des systèmes électrohydrauliques

Les systèmes électrohydrauliques sont employés fréquemment en aéronautique et dans la fabrication de machine-outil. Par conséquence beaucoup d'analyses ont été faites pour établir les facteurs qui en affectent le comportement dynamique dans les régimes transitoires et permanents. La figure 1.1 montre la configuration générique d'un tel système et identifie ses composants. L'élément de base est la servovalve qui contrôle le débit du fluide hydraulique à travers l'actionneur. Cette valve est à l'origine de la complexité de ces systèmes en modélisation et en commande.

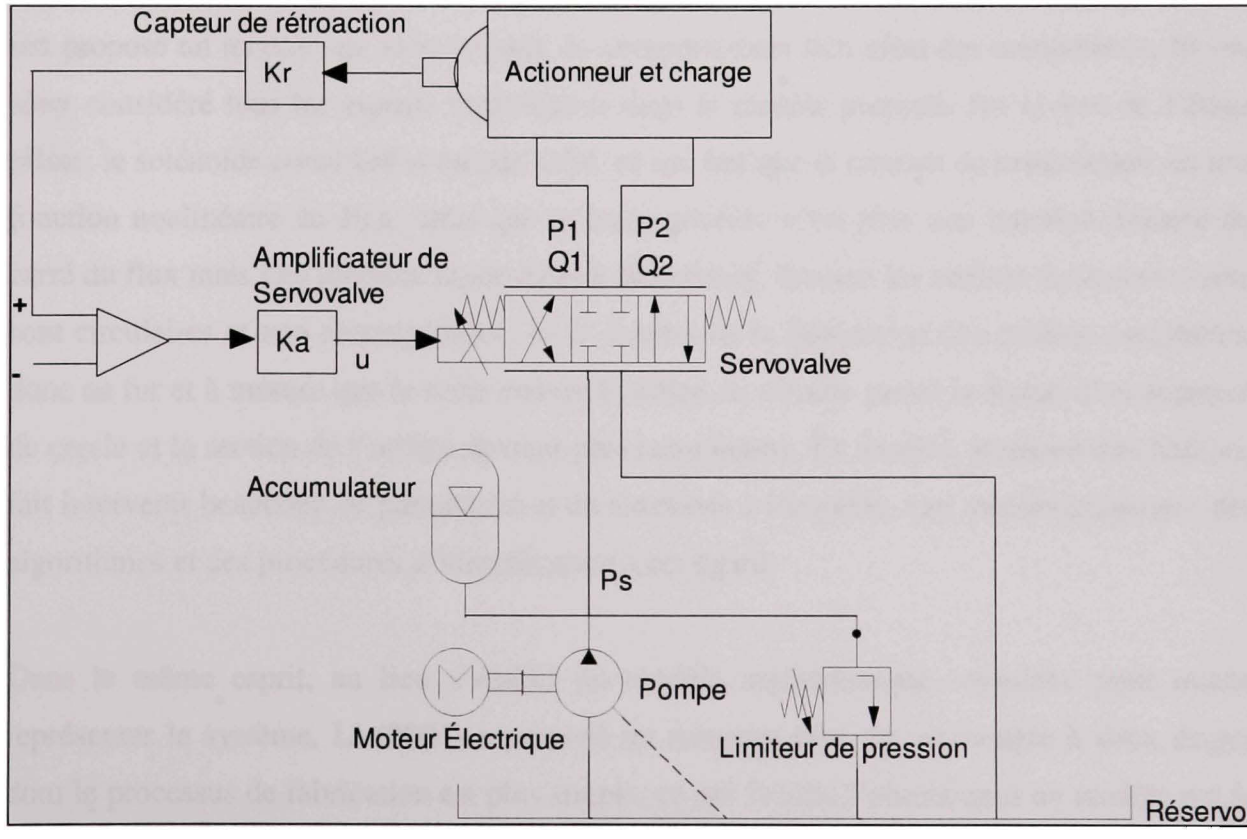

Figure 1.1 ***Schémas d'un système électrohydraulique.***

La base de la modélisation des différents composants d'un système électrohydraulique a été établie par Merritt (1967). En se basant sur la mécanique de fluide, il a dérivé l'expression du débit à travers l'orifice d'une servovalve et la dynamique de pression dans les deux chambres d'une servovalve à deux étages ainsi que dans les chambres d'admission et de refoulement d'un actionneur hydraulique. Cependant, ces modèles portaient sur des linéarisations afin d'écrire le système sous forme de fonction de transfert et d'en simplifier l'expression. Ceci n'est pas idéal quand un système électrohydraulique est utilisé dans une tâche complexe, à cause des phénomènes nonlinéaires qui peuvent apparaître; surtout que son fonctionnement dans ce cas n'est plus restreint autour d'un seul point d'opération. En plus, nous remarquons que l'inertie des tiroirs d'une servovalve est négligée relativement à celle de l'actionneur, ce qui induit une dynamique non modélisée dont l'effet peut devenir significatif à des fréquences élevées. De nos jours, ces aspects sont de plus en plus pris en considération à cause de la haute précision requise dans les processus qui emploient ces systèmes.

En ce qui concerne les servovalves à deux étages et à action pilotée, Zavarehi et al. (1999), ont proposé un modèle qui tient compte du comportement non idéal des composants. Ils ont alors considéré tous les aspects nonlinéaires dans le modèle proposé. Au niveau de l'étage pilote, le solénoïde considéré n'est pas idéal, ce qui fait que le courant de restauration est une fonction nonlinéaire du flux, ainsi que la force générée n'est plus une fonction linéaire du carré du flux mais une fonction nonlinéaire à déterminer. Ensuite les orifices de la servovalve sont circulaires et non rectangulaires, vu la facilité de la fabrication des orifices circulaires, donc au fur et à mesure que le tiroir couvre l'orifice, ce dernier prend la forme d'un segment de cercle et la section de l'orifice devient plus compliquée. Ce modèle, pourtant très réaliste, fait intervenir beaucoup de paramètres et de fonctions à identifier. Les auteurs proposent des algorithmes et des procédures d'identification à cet égard.

Dans le même esprit, au lieu d'établir un modèle mathématique complexe pour mieux représenter le système, Li (2001) a proposé un nouveau type de servovalve à deux étages dont le processus de fabrication est plus simple, ce qui facilite l'obtention d'un modèle qui la représente correctement et qui n'engendre pas trop de paramètres comme dans le modèle de

Zavarehi et al. (1999). En fait l'étage principal est formé de deux tiroirs séparés qui règlent indépendamment les débits entrant et sortant de la servovalve; l'avantage de cette configuration est la facilité de fabrication et d'assemblage, puisque les dimensions sont plus faciles à ajuster, par conséquent elle tend à être moins chère. Cependant, malgré ces avantages, la dynamique de ce type de servovalve est limitée par rapport à celle des servovalves conventionnelles. Ceci est dû à la manière dont la servovalve est interconnectée. Une telle connexion peut créer un zéro responsable d'une bande passante de largeur réduite. L'auteur propose une amélioration de la dynamique, par l'étude du lieu des racines et l'ajustement des paramètres nécessaires pour minimiser l'effet dominant du zéro.

D'une façon très différente, Habibi et Goldenberg (2000) ont présenté une nouvelle conception des systèmes électrohydrauliques illustrée dans la figure 1.2 ci-dessous,

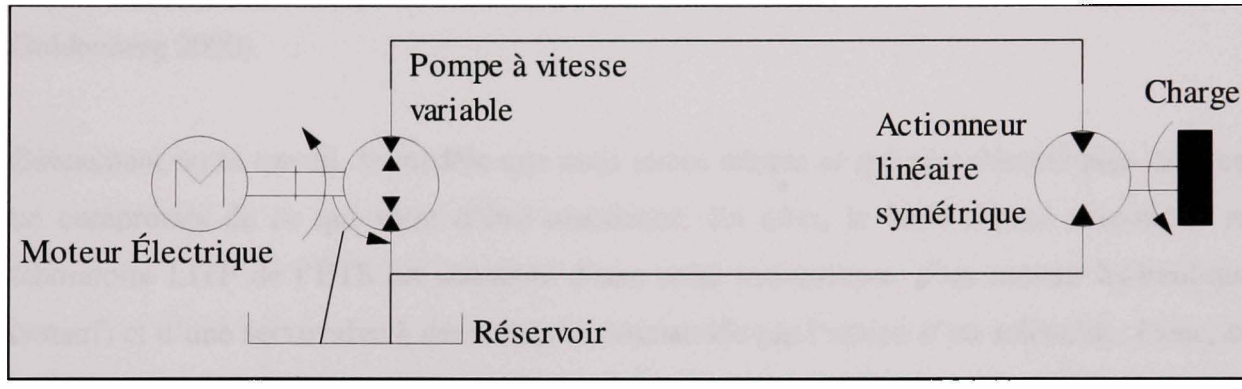

Figure 1.2 ***Nouvelle conception sans servovalve.***

La chose la plus remarquable est l'absence de la servovalve, qui est la source de complexité de ces systèmes. Son rôle, qui est de préciser la direction et le débit du fluide, a été remplacé par une pompe bidirectionnelle et à vitesse variable. Ceci élimine le désavantage de la configuration conventionnelle, qui est jugée inefficace puisque la pompe travaillait continûment et à vitesse constante indépendamment du mouvement de l'actionneur. Le problème qui apparaît au niveau de cette conception est l'effet de la zone morte. Cette dernière engendre des problèmes de précision à chaque changement de vitesse ou de direction. En premier lieu, il existe une zone morte au niveau de la pompe et du moteur électrique qui l'entraîne. En second lieu, au niveau de la connexion entre la pompe et

l'actionneur hydraulique; cette zone morte est due surtout aux fuites au niveau de la pompe et à la perte de charge à travers la connexion pompe – actionneur. Le plus important, est que dans une telle configuration on ne peut plus contrôler la différence de pression due à la charge, ce qui était faisable avant grâce à la servovalve. Cette conception demeure toutefois une bonne alternative pour des applications simples où une grande précision n'est pas requise, vu les jeux et les tolérances qui existent au niveau de la pompe et ses connexions.

Nous remarquons de ce qui précède, que récemment beaucoup de travaux et d'études se font au niveau de la modélisation des systèmes électrohydrauliques dont le comportement possède des aspects difficiles à être représentés mathématiquement. Le problème est qu'une amélioration donnée a toujours ses inconvénients; le fait de considérer tous les détails du système, (Zavarehi et al. 1999), donne un modèle complexe. Alors qu'une conception d'un système plus simple engendre des problèmes de précision, (Li 2001) et (Habibi and Goldenberg 2000).

Concernant notre travail, le modèle que nous avons adopté et qui sera détaillé plus tard, est un compromis de ce qui vient d'être mentionné. En effet, le banc d'essai disponible au laboratoire LITP de l'ÉTS est constitué d'une unité hydraulique, d'un moteur hydraulique (rotatif) et d'une servovalve à deux étages commandée par l'action d'un solénoïde. Donc, ce modèle tient compte de toutes les nonlinéarités et surtout de l'aspect non différentiable du système. La servovalve, quant à elle, est modélisée par une fonction de transfert du premier ordre, en considérant des orifices symétriques rectangulaires et en négligeant l'inertie du tiroir par rapport à celle de l'actionneur et de la charge.

1.2 Introduction à la commande des systèmes électrohydrauliques

En ce qui concerne la commande des systèmes électrohydrauliques, nous allons décrire et commenter les résultats des approches les plus utilisées. Nous allons viser par la suite une application qui nous intéresse dans l'industrie automobile, et qui occupe une première place

dans les recherches des grands fabricants automobile: le contrôle de la suspension active électrohydraulique.
En général, nous avons remarqué que pour les commandes linéaires ou lorsque le modèle était linéarisé, le succès des résultats se limitait aux basses fréquences vu les divers phénomènes de résonances et de nonlinéarités qui peuvent apparaître dans la région des harmoniques élevés.

1.2.1 Systèmes électrohydrauliques en général

Concernant les commandes classiques, le simple placement de pôles a été employé par Lim (1997) sur un modèle linéaire. Théoriquement les pôles peuvent être choisis dans n'importe quelle position désirée, cependant il y a en pratique des limites qui sont liées à la dynamique du système, outre le fait que linéariser le modèle induit un manque de précision. Les résultats ont montré une performance limitée et une erreur en régime permanent qui subsistait toujours.

Une autre alternative est la commande par retour de sortie qui a été utilisée par Ayalew et al. (2005). Elle consiste à linéariser le modèle mathématique du système hydraulique pour contrôler la force de l'actionneur. Malgré le fait que le retour de sortie ne donne aucune information sur le comportement des autres variables d'états, même si la sortie est stable, cette approche s'est révélée aussi efficace que la commande par retour d'état.
D'autre part, la commande adaptative indirecte a été employée par Yu et Kuo (1997) pour le contrôle d'un système électrohydraulique. Les paramètres du modèle linéaire cherché sont estimés par la méthode des moindres carrés avec zone morte; le contrôleur adaptatif est alors formulé par placement de pôles. La commande obtenue a été comparée avec celle d'un contrôleur PID classique et s'est avérée bien plus satisfaisante et robuste. Cependant, les paramètres estimés ont convergé vers les vraies valeurs avec un certain biais, vu l'existence d'incertitude.

Zeng et Hu (1999) ont utilisé l'algorithme PDF (Pseudo – Derivative Feedback), qui diffère de la commande PID classique à retour de sortie par le fait que le terme intégrateur est placé en chaîne directe, alors que toute dérivation nécessaire pour la stabilité du système doit être placée dans la chaîne de retour (rétroaction), ce qui assure une plus grande stabilité et permet d'éviter des commandes saturées. La faiblesse de cette approche réside dans la limitation de sa validité seulement aux voisinages d'un point fixe afin de garder la structure linéaire du système.
D'un autre côté, des méthodes plus robustes et nonlinéaires ont été employées. Comparées avec les stratégies classiques, elles se sont révélées plus performantes.

L'approche par mode de glissement (Hassan 2002) prend une place importante dans la commande des systèmes électrohydrauliques et les résultats expérimentaux correspondant sont souvent très satisfaisants. Cependant, malgré la robustesse offerte par cette stratégie, il faut être prudent en l'utilisant, vu qu'il existe des conditions à vérifier et quelques désavantages à considérer. En fait, le signal de commande qui assure la stabilité asymptotique du système est discontinu et change de signe à une fréquence infinie, ce qui peut nuire aux composants du système. Des techniques existent pour adoucir ce signal de commande; par contre avec ces techniques la stabilité n'est garantie qu'à l'extérieur d'un certain espace fermé. Enfin, lorsque des incertitudes ou perturbations sont considérées, il faut que l'image de la perturbation soit contenue dans celle du signal de contrôle; ce qu'on appelle 'matching conditions', sinon la stabilité n'est pas garantie. À cet égard, Sun et Chiu (1999) ont utilisé cette approche où les perturbations étaient estimées par un observateur du second ordre, pour le contrôle de la force de l'actionneur hydraulique. Dans leur application, la discontinuité du modèle mathématique n'a pas été traitée, ce qui rend cette approche valide seulement dans certaines conditions. De plus, Hwang (1996) et Chen et al. (2005) ainsi que Ha et al. (1998) ont traité l'atténuation de la discontinuité du signal de commande d'un contrôleur par mode de glissement. Dans le premier cas, une fonction de saturation avec des paramètres de commutation qui varient avec le temps ont été employés. De très bons résultats sont obtenus avec cette approche, mais la surface de glissement présentait des oscillations sévères quand les incertitudes et la charge externe étaient prises en considération. Dans le

second cas, la composante oscillante du signal de commande est atténuée par un signal synthétisé par des règles en logique floue, précisant à quels moments le terme discontinu doit être d'une amplitude importante ou non. Ceci rendait le choix des paramètres de contrôle assez critique.

En effet, l'avantage majeur de la commande basée sur la logique floue, outre sa robustesse, est le fait que la connaissance de la dynamique du système à commander n'est pas nécessaire. Cependant l'implantation des règles de décision n'est pas toujours évidente. À titre d'exemple, dans le but de compenser les nonlinéarités du système électrohydraulique et d'assurer sa stabilité, le contrôle par logique floue a été employé par Yongqian et al. (1998). Contrairement au mode de glissement précédent, on ne se soucie plus du modèle dynamique et des incertitudes. Le contrôleur utilisé est basé sur une matrice de règles de décision de l'erreur. De bons résultats de suivi de trajectoire, caractérisés par un temps de réponse réduit ont été obtenus, mais une erreur en régime permanent, due au nombre insuffisant de règles de décision, subsistait toujours. À cet égard, un terme d'intégration fut ajouté en parallèle pour en éliminer l'effet. Dans le même esprit, Deticek (1999) a utilisé la même technique, son contrôleur s'adaptait rapidement aux variations des paramètres du système. En fait, le contrôleur est basé sur deux séries de règles de décision: la première séries de règles, constitue les règles conventionnelles alors que la deuxième série constitue des règles capables de modifier ceux de la première série afin de les adapter aux changements du système électrohydraulique. La simulation a donné des résultats très satisfaisants avec une légère erreur de poursuite. Mais avec un tel contrôleur, nous remarquons que le nombre de variables est de 13 ce qui donne 169 (13x13) règles de décision et rend l'implantation en temps réel très complexe.

L'efficacité des résultats de la stratégie de commande précédente, est très proche de celle obtenue par le contrôleur à réseaux de neurones artificiels et apprentissage en ligne utilisé par Kandil et al. (1999). Dans ce mode de contrôle, l'apprentissage est fait par rétro propagation de l'erreur de sortie et par conséquent la connaissance de la dynamique du système, encore une fois, n'était pas nécessaire.

Dans les deux approches précédentes, nous ne pouvons pas ignorer l'existence d'une légère erreur de poursuite en régime permanent due à la zone morte du contrôleur. En plus, étant donné que la stabilité du système dans ces approches (logique floue et réseaux de neurones) est étudiée sur un domaine discret, elle n'est garantie que sur les frontières du domaine d'étude considéré.

Une autre technique, qui prend de l'ampleur dans la commande des systèmes électrohydrauliques est le backstepping nonlinéaire (Hassan 2002) et (Miroslav et al. 1995). En fait, plusieurs applications montrent l'efficacité et la robustesse de cette approche; son utilisation dans les systèmes électrohydrauliques est assez récente.

Alleyne et Liu (2000) ont utilisé la commande basée sur le backstepping en version adaptative pour le contrôle de la force d'un actionneur hydraulique. L'approche consiste à écrire le modèle du système en forme triangulaire et à construire un signal de contrôle qui stabilise chaque état séparément. Les essais expérimentaux ont montré que la version adaptative a apporté des améliorations remarquables.
D'ailleurs, la même approche est utilisée par Ursu et al. (2004) et (2006), avec un modèle mathématique à quatre variables d'état dans le premier cas et un modèle à cinq variables d'état dans le second cas. Dans ce dernier, au lieu de la différence de pression due à la charge, ils ont considéré les deux pressions en amont et en aval de l'actionneur hydraulique séparément. Le but était le contrôle de la force et de la position à partir du contrôle de la force seulement, d'où le l'application du backstepping à une partie du modèle de ce système. Les résultats montrent une erreur de poursuite presque nulle, ainsi qu'une grande stabilité dans le comportement transitoire du système. Cependant, seule les trajectoires positives ont été considérées afin de contourner la discontinuité dans le modèle mathématique et par suite dans la loi de commande. Notons qu'aucune amélioration n'est remarquée dans le second cas par rapport au premier.

Mais en fait, le potentiel du backstepping ne se limite pas à ces résultats. Cette stratégie présente les avantages suivants :

- L'expression des trajectoires désirées et du signal de commande est analytique, ce qui évite les dérivées numériques et par conséquence les bruits (Miroslav et al. 1995).
- Cette approche nous rend capables d'être sélectifs envers la gestion des nonlinéarités. Ainsi nous pouvons éliminer les nonlinéarités nuisibles à la commande et conserver celles qui sont utiles et qui permettent d'éviter des commandes saturées et à amplitude élevée (Khalil 2002).
- Cette approche allège les 'matching conditions' imposées sur les incertitudes, comme dans le mode de glissement, et garantit donc la stabilité même pour des incertitudes dites 'unmatched' (Khalil 2002).

Dans nos travaux de recherche, nous avons adopté cette approche, comme dans (Kaddissi et al. 2007) et (Kaddissi et al. 2006). En fait, le backstepping est utilisé dans notre cas pour le contrôle de la position ainsi que de la force d'un système électrohydraulique générique.

1.2.2 Application industrielle

Dans ce travail de recherche, nous nous intéressons à appliquer nos résultats dans l'industrie automobile où les systèmes électrohydrauliques sont de plus en plus exploités. Nous avons visé le contrôle de la suspension active électrohydraulique représentée à la figure 1.3. En fait, les grands fabricants ainsi que les chercheurs, poussent assez largement leurs études dans cette application, étant donné la compétition qui existe pour combiner le confort des passagers et l'adhérence sur la route en même temps. Il existe plusieurs modèles mathématiques et plusieurs stratégies de contrôle dans la littérature pour les suspensions actives électrohydrauliques.

Parmi les stratégies de commande classique, le placement de pôles a été utilisé par Leite et Peres (2002), mais dans leur approche la dynamique de l'actionneur hydraulique était négligée. Dans les commandes robustes, Abdellahi et al (2000) ont employé la synthèse par H_2 et H_∞, les résultats obtenus étaient très satisfaisants, sauf que ces stratégies utilisent des modèles mathématiques linéarisés, qui ne sont valides qu'autour d'un certain point de

fonctionnement et par suite ne prennent pas en considération toute la dynamique du système. De même un contrôleur LQG avec la méthode des perturbations singulières a été implanté par Ando et Suzuki (1996). Cependant là aussi, la dynamique de l'actionneur a été négligée ce qui réduisait par conséquent l'efficacité du contrôle.

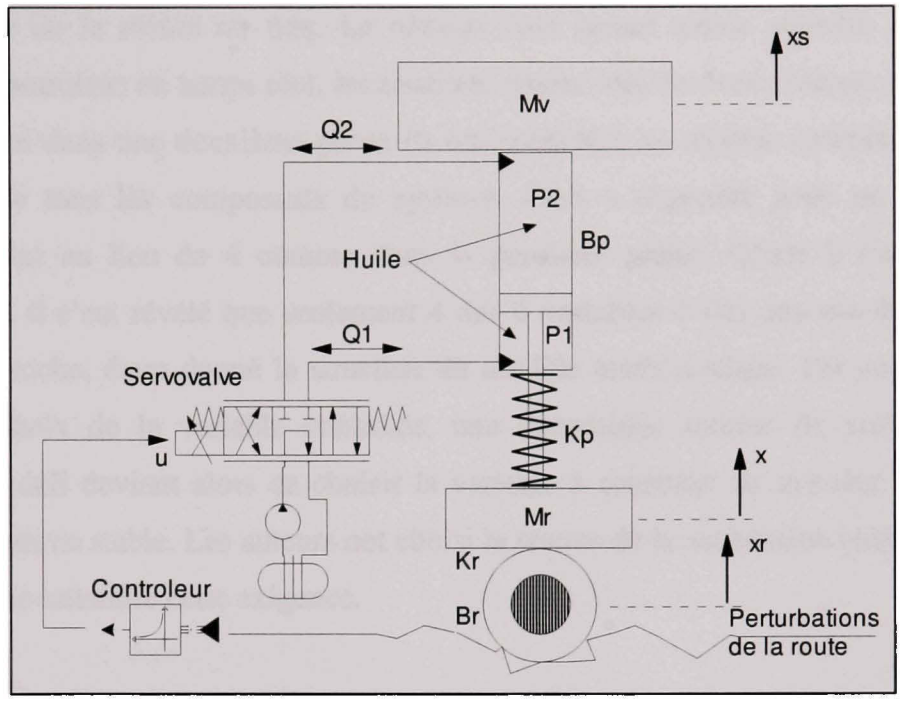

Figure 1.3 ***Schéma d'une suspension active électrohydraulique.***

Dans le cadre des stratégies de commande nonlinéaire, Le mode de glissement a été utilisé par Sam et al. (2003) en comparaison avec un régulateur LQG. Au niveau du confort des passagers et de la force qui leur était transmise, le contrôleur par mode de glissement a donné de meilleurs résultats. Toutefois, le signal de commande généré engendrait beaucoup d'oscillation à fréquences élevées; ceci reste toujours le point faible du mode de glissement.

Toujours dans la commande nonlinéaire, Fialho et Balas (2002) ont utilisé la commande LPV combinée avec le backstepping, pour une suspension active. Le LPV consiste à écrire le système variant, linéairement en fonction de ses paramètres et à utiliser ensuite une certaine stratégie de commande, qui était le backstepping dans ce cas. Ce dernier est classé parmi les stratégies de commande nonlinéaire les plus robustes. Les auteurs Lin et Kanellakopoulos

(1997) se sont basés sur cette approche pour la commande d'une suspension active électrohydraulique. En effet, ils ont analysé le problème de tous les côtés, en considérant au début un modèle mathématique simplifié, et ensuite un modèle nonlinéaire plus complet. Dans la première phase, ils ont établi un modèle linéaire simple en négligeant la dynamique de l'actionneur. Le but était de vérifier si l'absence de cette dynamique éloigne le modèle mathématique de la réalité ou non. Le résultat était quand même attendu; quand ils ont implanté le contrôleur en temps réel, les résultats étaient loin de ceux obtenus en simulation. C'est pourquoi dans une deuxième phase ils ont considéré un modèle complet qui inclut la dynamique de tous les composants du système. Ceci a engendré avec un système à 6 variables d'état au lieu de 4 comme dans la première phase. Quant à l'application du backstepping, il s'est révélé que seulement 4 des 6 variables d'état peuvent être stabilisées par cette approche, étant donné la structure du modèle mathématique. Par conséquent, peu importe le choix de la variable contrôlée, une dynamique interne du second ordre va subsister. Le défi devient alors de choisir la variable à contrôler de manière à obtenir une dynamique interne stable. Les auteurs ont choisi la course de la suspension comme variable à contrôler, pour satisfaire cette exigence.

Suite à ce qui précède nous nous sommes fixés comme objectif de développer une loi de commande qui rejoint les avantages des approches mentionnées plus haut. Ceci a été possible en jumelant le backstepping au forwarding (Sepulchre et al. 1997). En effet, le forwarding est le complément du backstepping. En d'autres termes, il s'applique aux systèmes où le backstepping ne s'applique pas ou s'applique partiellement, ce qui est notre cas. Nous nous sommes inspirés du travail de Krstic (2004), qui décrit dans plusieurs cas la théorie de cette approche et les algorithmes numériques qui aident à sa résolution. Par conséquent, en combinant le backstepping et le forwarding, nous avons réussi à stabiliser tous les états du modèle d'une suspension active électrohydraulique indépendamment du choix de la variable à contrôler qui dans notre cas était la position verticale du véhicule. Comme il sera montré dans le quatrième chapitre, cette approche assure une stabilité définitive du système pour des perturbations bornées et finies, et le signal de commande résultant est doux et d'une faible amplitude.

1.3 Contributions originales

Au meilleur de notre connaissance les contributions suivantes sont originales et sont résumées ci-dessous.

a) Au niveau des systèmes électrohydrauliques génériques :

- Un modèle mathématique qui tient compte de toutes les nonlinéarités du système, sans toutefois être très complexe, est développé. Ceci par l'entremise des hypothèses simplificatrices suivantes :
    - Les fuites externes au niveau des actionneurs hydrauliques sont négligées;
    - Le frottement sec au niveau des actionneurs hydrauliques est négligé;
    - L'inertie du tiroir de la servovalve est négligée;
    - La section des orifices de la servovalve est considérée rectangulaire.
- La non-différentiabilité du modèle mathématique (fonction signe), qui représente le changement du sens d'écoulement du fluide dans le circuit hydraulique, est prise en considération dans la loi de commande et est approximée par une sigmoïde. Ceci élimine les problèmes de dérivation d'un côté et rend possible la poursuite de toutes sortes de trajectoire d'un autre côté.
- À chaque étape de la loi de commande, basée sur le backstepping, les expressions des trajectoires désirées et du signal de commande sont rendues purement analytiques. Ceci assure un calcul en temps réel plus rapide et plus rigoureux. Ces mêmes expressions sont développées explicitement en fonction des erreurs de poursuite des différentes variables d'état et de la trajectoire désirée de l'actionneur hydraulique. Ceci facilite l'analyse de l'effet des divers paramètres sur la convergence de ces erreurs vers zéro.
- Un mécanisme particulier pour l'introduction des paramètres de contrôle dans la fonction de Lyapunov est conçu de manière à accélérer la convergence et la stabilité du système, moyennant un faible signal de commande et par conséquent une faible énergie. Ce mécanisme consiste à :
    - Introduire les paramètres de contrôle dans le dénominateur de la fonction de Lyapunov à chaque étape du backstepping;

- Introduire ces mêmes paramètres de contrôle dans la trajectoire désirée qui rend négative la dérivée de cette fonction de Lyapunov, en les multipliant par l'erreur correspondante.

- Le modèle mathématique nonlinéaire développé est exprimé sous forme LP. Ceci constitue une clé pour l'identification des paramètres du système. En effet, un système sous forme LP, même nonlinéaire, peut être identifié avec des algorithmes d'identification linéaires comme les moindres carrés récursifs sans avoir recours à linéariser le système.

b) Au niveau de la suspension active électrohydraulique :

- Le modèle mathématique établi est basé sur le modèle que nous avons développé pour les systèmes électrohydrauliques génériques. Il devient donc possible de construire facilement le modèle d'une application industrielle qui utilise les systèmes électrohydrauliques à partir du modèle générique.
- Le modèle mathématique possède une structure mixte feedback/feedforward. Afin de pouvoir contrôler le système avec la commande entrelacée, un changement de variable au niveau du modèle mathématique est fait pour que le système puisse être classé parmi les systèmes entrelacés. Ces derniers peuvent être stabilisés par des séquences de 'backstepping' et de 'integrator forwarding' ; ce qui est connu sous le nom de commande entrelacée.
- Le nouveau modèle obtenu après changement de variable, nous a permis de contrôler toutes les variables d'état du système sans laisser aucune dynamique interne. En effet, dans le cas où elle est présente, la dynamique interne du modèle d'une suspension active électrohydraulique a un comportement oscillant. Par suite, une stratégie de commande qui laisserait une dynamique interne dans le système, ne garantirait pas la stabilité de ce dernier.
- Finalement, la commande entrelacée, qui est élaborée et développée dans cette partie de la recherche, est basée sur une séquence de 'backstepping' et de 'integrator forwarding'. Cette stratégie jusqu'à présent n'a été appliquée que sur des modèles purement

mathématiques et théoriques qui n'ont aucune signification physique. En outre, les références qui expliquent cette stratégie de commande sont très rares et peu détaillées.

CHAPITRE 2

IDENTIFICATION AND REAL-TIME CONTROL OF AN ELECTROHYDRAULIC SERVO SYSTEM BASED ON NONLINEAR BACKSTEPPING

Claude Kaddissi, *Member, IEEE*, Jean-Pierre Kenné and Maarouf Saad, Associate *Member, IEEE*
École de technologie supérieure, 1100 Notre-Dame Street West, Monreal, Quebec H3C 1K3, Canada
Email: claude.kaddissi@etsmtl.ca

Abstract

This paper studies the identification and the real-time control of an electrohydraulic servo system. The control strategy is based on the nonlinear Backstepping approach. Emphasis is essentially on the tuning parameters effect and on how it influences the errors dynamic behavior, as will be shown. While Backstepping control ensures the global asymptotic stability of the system, the tuning parameters of the controller nonetheless do greatly affect the saturation and chattering in the control signal, and consequently, the errors dynamic. In fact, electrohydraulic systems are known to be highly nonlinear and non-differentiable due to many factors, such as leakage, friction, and especially, the fluid flow expression through the servovalve. These nonlinear terms appear in the closed loop errors dynamic. Their values are so large that in the presence of a poor design, they can easily overwhelm the effect of the controller parameters. Backstepping is used here because it is a powerful and robust nonlinear strategy. The experimental results are compared to those obtained with a real-time PID controller, to prove that classic linear controllers fail to achieve a good tracking of the desired output, especially, when the hydraulic actuator operates at the maximum load. Before going through the controller design, the system parameters are identified. Despite the nonlinearity of the system, identification is based on the recursive least squares method. This is done by rewriting the mathematical model of the system in an LP (Linear in Parameters) form. Finally, the experimental results will show the effectiveness of the proposed approach in terms of guaranteed stability and zero tracking error.

Index Terms – Backstepping, Electrohydraulic systems, Nonlinear control.

2.1 Introduction

A brief depiction of electrohydraulic systems is necessary in order to understand their behavior. An electrohydraulic system is basically composed of the following components: a pump that feeds the system with hydraulic fluid oil from a tank; an accumulator, located on the discharge side of the pump, which acts as a supporting source of energy in case of an abrupt need for additional power; a relief valve, installed next to the accumulator, to limit the maximum operating pressure; a hydraulic actuator that drives loads at desired specifications, and a servovalve, which directs the oil flow through the appropriate position of its spool, and consequently determines the direction of the motion and speed of the hydraulic actuator. A broader and more detailed description of electrohydraulic systems can be found in (Merrit 1967).

Electrohydraulic systems have recently become increasingly popular in many types of industrial equipment and processes. Such applications include rolling and paper mills, aircrafts and all kinds of automation, including in the automobile industry, where linear movements, fast response, and accurate positioning with heavy loads are needed. This is principally due to the high-power density and system solution that they can offer, being less bulky than DC and AC motors. However, as a result of the ever increasing complexity of such applications, considering nonlinearity and mathematical model singularity, linear models and traditional constant-gain controllers have become inadequate.

Although building a mathematical model that includes all the system dynamics is not a trivial matter, several improvements have been made in the domain. Habibi and Goldenberg (2000), proposed a new design for linear hydraulic actuators. The work done by Li (2001) and Zavarehi et al.(1999) put forward a dynamic redesign for servovalves; in fact, due to its nonlinear behavior, this component is responsible for the complexity of such systems. The mathematical model that we propose in this work is similar to the one presented by LeQuoc et al.(1990); however, the latter is dimensionless while this one deals with dimensional quantities.

Regarding control, three major types of strategies can be depicted: robust linear control, robust nonlinear control and intelligent control strategies.

Starting with linear control, the author Lim (1997) applied a simple poles placement to a linearized model of an electrohydraulic system. In Plahuta et al.(1997) and Zeng and Hu (1999), classic cascaded loops and PID controllers were employed respectively for the position control of a hydraulic actuator. Experiments and simulations carried out in previous works showed that factors resulting in dynamic variations are beyond the capacity of these controllers. There are also many such factors that must be taken into account, such as load variations, changes in the characteristics of transducers and in the properties of the hydraulic fluid, changes in the dynamics of servo components and in other system components, etc. As a result, many robust and adaptive control methods have been used.

An indirect adaptive controller, based on pole placement for the speed and position feedback of electrohydraulic systems is used by Yu and Kuo (1996) and (1997). However, the controller is based on a linear model of the plant, which imposes certain limitations on the efficiency and robustness of the controller. Sliding mode control was used by the authors Fink and Singh (1998) to regulate the drop in pressure across the hydraulic actuator due to the load; the resulting control signal involved high-frequency chattering because of the switching function. The latter problem was handled by Chen et al. (2005) where the controller is based on varying boundary layers, instead of fixed boundary layers of the sliding surface, in order to avoid chattering. Another case is the one in Alleyne and Hedrick (1995), where the sliding mode was applied for the control of an electrohydraulic active suspension, with the controller here being a special case of feedback linearization. System performance was enhanced by the use of an adaptive version of the controller. Input-output linearization control was also adopted by Hahn et al. (1994) and Ayalew and Kulakowski (2005) to compensate for the global nonlinearities of the electrohydraulic system. While this strategy is very suitable for the use of linear control, its resulting control signal is however often a high amplitude voltage because of the cancellation of nonlinear terms. Conversely, Lyapunov-based nonlinear controllers are widely used, with their main advantage being the lack of restrictions in manipulating system nonlinearities. A good example is examined by Liu and

Alleyne (2000), where an electrohydraulic actuator is provided with good force tracking. Backstepping is a particular component of Lyapunov-based controllers. It constitutes a powerful control strategy for handling nonlinearities. It was employed on electrohydraulic systems by the authors Ursu et al. (2003) and Kaddissi et al.(2004), as well as on electrohydraulic active suspensions, by Lin and Kanellakopoulos (1997) and Kaddissi et al. (2005).

Intelligent control as fuzzy logic was adopted by Yongqian et al. (1998), and the controller was based on a decision rules matrix of the error. Results very closely mirrored those of a neural network-based controller, used by Kandil et al. (1999), where learning was accomplished through output error retropropagation. While simulation results in these advanced strategies were very successful in most cases, stability is however not guaranteed using these approaches. This is because in such cases, it is studied on discrete domains, and the system behavior cannot be predicted at limits.

This paper proposes a Backstepping approach for the position control of an electrohydraulic servo system as well as a simple method for parameter identification. Our previous works, Kaddissi et al. (2004) and (2005), were based on simulations, with the focus put on accounting for all system nonlinearities and on solving the problem of non-differentiability in the mathematical model. The current work is based on real-time experiments, with its main focus placed on the chosen parameter for the Backstepping controller and on the way they are designed to appear in the Lyapunov function. While a major advantage of the backstepping approach is its flexibility in building a control law by avoiding the cancellation of useful nonlinearities, electrohydraulic systems however always pose a major problem. In fact, the errors dynamic involves quantities that are a function of system pressure and pressure drop. The values of these pressures can become so high that they will crush the effect of the controller tuning parameters, as presented by Lee and Tsao (2002), for example. The problem is solved in this paper by choosing the Lyapunov function such that the matrix of the errors dynamic becomes parameterized. As will be demonstrated, our choice brings flexibility by rendering the matrix triangular, and as a result, only the controller parameters

will affect the errors dynamic. Moreover, with such a choice, the use of Backstepping ensures the global stability of the system, and generates low amplitude and a chatter-free control signal.

The rest of the paper is organized as follows. The motivation for this work is presented in section 2. Section 3 presents a complete description of the mathematical model used. Section 4 deals with the identification of the system parameters. The design of the Backstepping controller and the choice of the Lyapunov function is the subject of Section 5; design details are given at the end of the paper in Appendix *A2.4*. Section 6 contains a brief description of the Rt-Lab system used to implement the real-time work on our electrohydraulic workbench. In Section 7, experimental results are compared with those obtained by a real-time PID controller. Finally, some conclusions and remarks bring this work to a close in Section 8.

2.2 Motivation

Electrohydraulic systems have many applications, especially in the automobile industry, which is of great interest to us. However, controlling such systems poses several important problems for control engineers and researchers.

It is well known, in control systems, that the key to a successful control is an accurate mathematical model. In electrohydraulic systems, this implies complexity and involvedness in both, identification and control, because of the highly nonlinear and non-differentiable expressions used. That is why the tendency has always been to make use of linear models. Nevertheless, in advanced applications involving high-frequency signals and perturbations, the ignored dynamics in linear models will surface and degrade the system behavior regardless of the control strategy used.

The mathematical model that we have built in this paper encloses all the dynamics of the electrohydraulic system; however, certain assumptions are used to lighten its complexity. The maximum allowed value of the supply pressure is set at P_s; with the relief valve used,

leaks are supposed to be minor, and the dynamic of the servovalve is fast enough to allow it to be depicted with a first-order differential equation; as well, the non-differentiable term is approximated with a sigmoid function for verification of Lipschitz conditions. Furthermore, the system is written in LP form in order to enable it to be identified using classic methods.

Regarding control, it can be seen from the introduction that finding an ideal strategy free of weak spots is not a clear-cut endeavor. However, studies have shown that Lyapunov-based approaches are the best strategies for systems with complex dynamics. This is because the Lyapunov function is based on the system dynamic itself, thus offering more flexibility in building the control signal. Backstepping is a very robust and powerful Lyapunov-based control strategy, especially in applications where perturbations and uncertainties are well pronounced. Firstly, Backstepping relaxes the 'matching conditions' as explained by Khalil (2002), which means that the perturbation signal or the uncertainties in the system model are not restricted to show in the state equation that contains the input of the system as in other control strategies. A good example is the electrohydraulic automobile active suspension, where road disturbance is the perturbation signal, and appears in states that do not contain the input signal as in Kaddissi et al. (2005). Secondly, Backstepping avoids the cancellation of useful nonlinearities and takes advantage of the useful ones to increase system stability and reduce the amplitude of the control signal in order to avoid saturation. The only problem, which must be carefully examined, is the introduction of the tuning parameters into the Lyapunov function, as explained in the last section of the introduction. In fact, this choice plays a major role in the errors dynamic behavior, as will be demonstrated. This is why it is very important to improve the Backstepping control strategy in order to fully benefit from all its advantages.

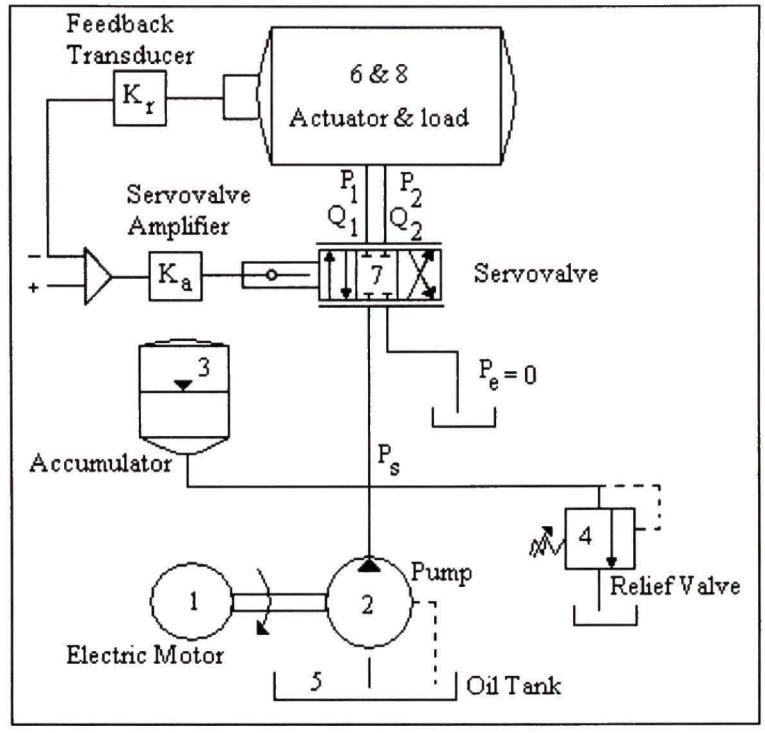

Figure 2.1 ***Schematic of hydraulic servo-system.***

2.3 System Modeling

A symbolic representation of an electrohydraulic system is shown in Figure 2.1. Figure 2.2, on the other hand, shows the experimental workbench on which the work was achieved. In the latter, the electric motor that drives the pump at a constant speed is DC-based. The pump itself has a fixed displacement, and delivers oil flow from the tank to the rest of the components. Normally, the pressure P_s at the pump discharge is kept constant by means of the accumulator and the relief valve. The installed accumulator is relatively small, and is used as an additional source of hydraulic fluid and a water hammer absorber. The relief valve is set to P_s and compensates for pressure increases due to large loads by returning a required additional amount of flow to the tank. The displacement of the rotary hydraulic actuator that drives the load is constant; its direction of motion, speed and acceleration are determined by the two stage servovalve, through the convenient position of its spool. The load is generated using pump, which is driven by the hydraulic actuator and another servovalve that creates a desired restriction at the pump discharge. All necessary data are collected through the

different installed sensors; i.e., torque meter, tachometer and pressure sensors. The control signal generated by the controller designed in this paper actuates the servovalve spool to the proper position. The dynamic equation for a servovalve spool movement can be given by :

$$\tau_v \dot{A}_v + A_v = Ku \tag{2.1}$$

Where u is the control input, K is the servovalve constant, τ_v is its time constant and A_v is the valve opening area. The flow rates to and from the servovalve, through the valve orifices, assuming a small leakage, are given as:

$$Q_1 = Q_2 = C_d A_v \sqrt{\frac{P_s - sign(A_v)P_L}{\rho}} \tag{2.2}$$

where, P_L and P_s are the pressure differential due to load and the pressure discharge of pump respectively, (Abdellahi et al.)

$$\begin{cases} P_L = P_1 - P_2 \\ P_s = P_1 + P_2 \end{cases} \tag{2.2'}$$

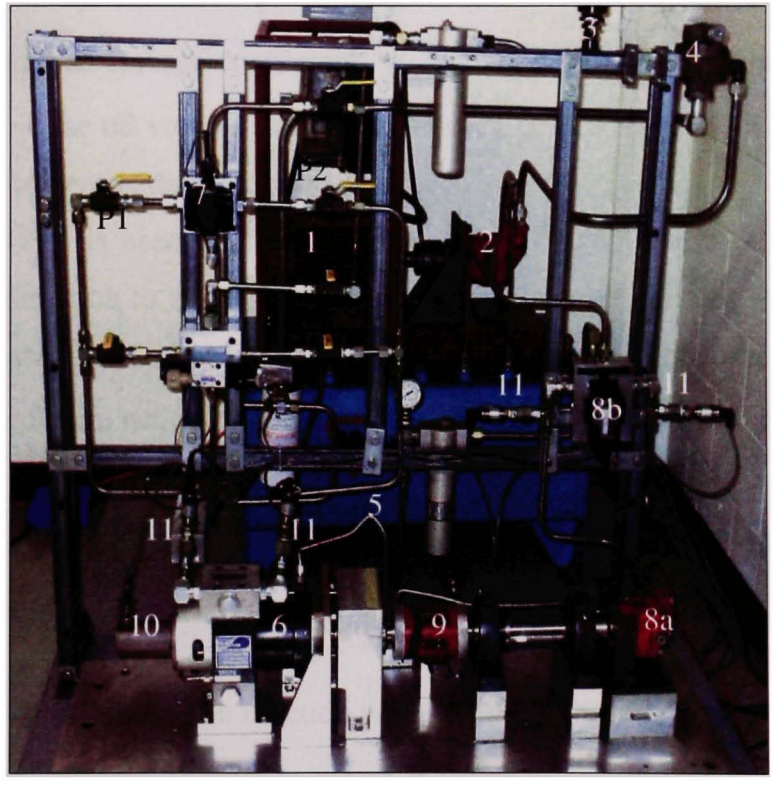

Figure 2.2 ***Experimental Electrohydraulic Workbench.***

1—electric motor; 2—pump; 3— accumulator; 4—relief valve; 5—tank; 6— rotary hydraulic actuator; 7—two stage servovalve; 8a—pump; 8b—servovalve; 9—torque meter; 10—tachometer; and 11—pressure sensors.

C_d is the flow discharge coefficient and ρ is the fluid oil mass density. Equalities, (2.1), (2.2) and (2.2') are held knowing that the servovalve is critically centered and the orifices are matched and symmetrical, (Merritt 1967).

The *sign* function in (2.2) stands for change of the fluid flow direction through the servovalve. In fact, when the actuator is rotating in a positive direction P_L is positive and the servovalve is in parallel ways position; while in the negative direction of rotation, P_L is negative and the servovalve is in cross ways position. This *sign* function gives rise to the non-differentiability problem, especially when dealing with bi-directional applications.
Since oil viscosity might vary with temperature, it should be considered in the actuator dynamics along with oil leakage. Thus we give the compressibility equation as:

$$\frac{V}{2\beta}\dot{P}_L = C_d A_v \sqrt{\frac{P_s - sign(A_v)P_L}{\rho}} - D_m\dot{\theta} - C_L P_L \tag{2.3}$$

We define C_L as the load leakage coefficient, β is the fluid bulk modulus, θ is the output angular position, V is the oil volume under compression in one chamber of the actuator, and D_m is the actuator volumetric displacement.
The derivative of (2.3) is needed in building the control signal; in most cases, motion is considered in one direction to avoid the differentiation problems. In fact, for a model of the form $\dot{x} = f(x)$ an essential factor of its validity is the continuous dependence of its solutions on the data of the problem, which can be stated by the Lipschitz inequality given by:

$$\|f(x) - f(y)\| \le L\|x - y\| \tag{2.4}$$

To satisfy (2.4), we estimated the *sign* function with a *sigmoid* function of the form:

$$sigm(x) = \frac{1 - e^{-ax}}{1 + e^{-ax}} \tag{2.5}$$

This is a continuously differentiable function with the following properties,

$$a > 0 \quad \text{and} \quad sigm(x) = \begin{cases} 1 \ if \ \ ax \to \infty \\ 0 \ if \ \ ax \to 0 \\ -1 \ if \ \ ax \to -\infty \end{cases} \tag{2.5'}$$

The previous estimation guarantees the existence of the solution and extends the control of electrohydraulic systems to bi-directional applications, thus avoiding differentiability problems.

Let us now consider the hydraulic actuator equation of motion given by Newton's second law. Neglecting the Coulomb frictional torque, we have:

$$J\ddot{\theta} = D_m(P_1 - P_2) - B\dot{\theta} - T_L \tag{2.6}$$

T_L is the load torque, B the viscous damping coefficient, and J the actuator inertia.

Finally, choosing, $x_1 = \theta, x_2 = \omega = \dot{\theta}$, $x_3 = P_L$, $x_4 = A_v$ as state variables; the system can be easily described with a 4th order nonlinear state-space model.

$$\begin{cases} \dot{x}_1 = x_2 \\ \dot{x}_2 = w_a x_3 - w_b x_2 - w_c \\ \dot{x}_3 = p_a x_4 \sqrt{P_s - x_3 . sigm(x_4)} - p_b x_3 - p_c x_2 \\ \dot{x}_4 = -r_a x_4 + r_b u \end{cases} \tag{2.7}$$

Or, in matrix form,

$$\boxed{\begin{pmatrix} \dot{x}_1 \\ \dot{x}_2 \\ \dot{x}_3 \\ \dot{x}_4 \end{pmatrix} = \begin{pmatrix} 0 & 1 & 0 & 0 \\ 0 & -w_b & w_a & 0 \\ 0 & -p_c & -p_b & p_a\sqrt{P_s - x_3 . sigm(x_4)} \\ 0 & 0 & 0 & -r_a \end{pmatrix} \begin{pmatrix} x_1 \\ x_2 \\ x_3 \\ x_4 \end{pmatrix} + \begin{pmatrix} 0 & 0 \\ 0 & -1 \\ 0 & 0 \\ r_b & 0 \end{pmatrix} \begin{pmatrix} u \\ w_c \end{pmatrix}} \tag{2.7'}$$

where r_a, r_b, p_a, p_b, p_c, w_a, w_b, w_c, are appropriate constants given by,

$$r_a = \frac{1}{\tau_v},\ r_b = \frac{K}{\tau_v},\ p_a = \frac{2\beta C_d}{V\sqrt{\rho}},\ p_b = \frac{2\beta C_L}{V}$$

$$p_c = \frac{2\beta D_m}{V},\ w_a = \frac{D_m}{J},\ w_b = \frac{B}{J},\ w_c = \frac{T_L}{J} \tag{2.8}$$

In this first step, the mathematical model of the electrohydraulic system was fully designed and established. The next step involves setting up an identification algorithm for the system parameters, which is done in the following section.

2.4 System Identification

Examining the system model (2.7), it can be seen that the parameters to be identified are those in the last three equations. Besides, the last equation represents the dynamic of the servovalve, and so the parameters of the latter can be determined from the data sheet provided by the manufacturer. This leads to the conclusion that only parameters in the second and third equations of system (2.7) need to be identified, (i.e., w_a, w_b, w_c, p_a, p_b and p_c in the following equations).

$$\begin{cases} \dot{x}_2 = w_a x_3 - w_b x_2 - w_c \\ \dot{x}_3 = p_a x_4 \sqrt{P_s - x_3 . sigm(x_4)} - p_b x_3 - p_c x_2 \end{cases} \tag{2.9}$$

Assuming a zero load, (w_c=0), the equations in (2.9) can be rewritten in matrix form, as follows:

$$\begin{pmatrix} \dot{x}_2 \\ \dot{x}_3 \end{pmatrix} = \begin{pmatrix} x_3 & -x_2 & 0 & 0 & 0 \\ 0 & 0 & x_4 . \sqrt{P_s - x_3 . sigm(x_4)} & -x_3 & -x_2 \end{pmatrix} \begin{pmatrix} w_a \\ w_b \\ p_a \\ p_b \\ p_c \end{pmatrix} \tag{2.10}$$

It can be seen that the subsystem (2.10) has linear parameters, which is a sufficient condition for those parameters to be identified through the continuous Recursive Least Square method with constant trace as in Astrom and Wittenmark (1989). Now let:

$$y(t) = \begin{pmatrix} \dot{x}_2 \\ \dot{x}_3 \end{pmatrix}$$

$$\varphi(t)^T = \begin{pmatrix} x_3 & -x_2 & 0 & 0 & 0 \\ 0 & 0 & x_4 . \sqrt{P_s - x_3 . sigm(x_4)} & -x_3 & -x_2 \end{pmatrix}$$

$$\theta = \begin{pmatrix} w_a \\ w_b \\ p_a \\ p_b \\ p_c \end{pmatrix} \tag{2.11}$$

Then,

$$y(t) = \varphi(t)^T \theta \tag{2.12}$$

This is the classic form of a system that has an LP structure, where y is the observed vector of variable, φ is the matrix of regression variables and θ is the vector of unknown parameters. We then define the least square error $V(\theta)$ and the matrix $P(t)$ follows,

$$\begin{aligned} V(\theta) &= \int_0^t e^{\alpha(t-s)}\left(y(s)-\varphi(s)^T\theta\right)^2 ds \quad ; \quad 0<\alpha<1 \\ P(t) &= \left(\int_0^t \varphi(s)^T\varphi(s)ds\right)^{-1} \end{aligned} \tag{2.13}$$

Finally, the parameter estimate $\hat{\theta}$ that minimizes the least square error must satisfy,

$$\boxed{\begin{aligned} \frac{d\hat{\theta}}{dt} &= P(t)\varphi(t)e(t) \\ e(t) &= y(t)-\varphi(t)^T\hat{\theta}(t) \\ \frac{dP(t)}{dt} &= \alpha P(t)-P(t)\varphi(t)\varphi(t)^T P(t) \end{aligned}} \tag{2.14}$$

Through (2.14), we can now identify the system parameters in (2.8), and consequently, start the design of the Backstepping controller.

2.5 Backstepping Nonlinear Control

In this section, the Backstepping controller is designed based on Krstic, Kanellakopoulos et al. (1995). A complete list of the intermediate variables and functions, used to alleviate the expressions of the system model and the controller equations, is given in Appendix *A2.3*. A detailed description of the controller design and the proof of the following proposition are given in Appendix *A2.4* as well, at the end of this work.

- Proposition:

Consider the following nonlinear model of the electrohydraulic system written in state-space:

$$\begin{cases} \dot{x}_1 = x_2 \\ \dot{x}_2 = w_a x_3 - w_b x_2 - w_c \\ \dot{x}_3 = p_a x_4 g(.) - p_b x_3 - p_c x_2 \\ \dot{x}_4 = -r_a x_4 + r_b u \end{cases} \tag{2.15}$$

Let $e_i = x_i - x_{id}$, for $i = 1,2,3,4$, be the tracking error between every state variable and its desired value, with x_{1d} as the desired position to be reached. If there are three stabilizing state feedback functions (Steps 1, 2 and 3 of Appendix *A2.4*):

$$\begin{cases} x_{2d} = \Theta(e_1, x_{1d}) \\ x_{3d} = \Omega(e_1, e_2, \dot{x}_{1d}, \ddot{x}_{1d}) \\ x_{4d} = \Psi(e_1, e_2, e_3, \dot{x}_{1d}, \ddot{x}_{1d}, \dddot{x}_{1d}) \end{cases} \tag{2.16}$$

where Θ, Ω and Ψ are functions designed such as to stabilize the subsystem $\dot{x}_1, \dot{x}_2, \dot{x}_3$ of (2.15); along with $x_{id}(0) = 0$. Then:

- Choosing the following positive definite Lyapunov function,

$$V_4(e_1, e_2, e_3, e_4) = \frac{1}{2\rho_1} e_1^2 + \frac{1}{2\rho_2} e_2^2 + \frac{1}{2\rho_3} e_3^2 + \frac{1}{2\rho_4} e_4^2 \tag{2.18}$$

with $\rho_1, \rho_2, \rho_3, \rho_4 > 0$.

- Choosing the control input u as follows (final step of Appendix *A2.4*),

$$u = \Lambda(e_1, e_2, e_3, e_4, \dot{x}_{1d}, \ddot{x}_{1d}, \dddot{x}_{1d}, x_{1d}^{(4)}) \tag{2.17}$$

where Λ is a function designed to stabilize the full system (2.15), will guarantee a zero tracking error situation and the global asymptotic stability of the errors dynamic, since we will have:

$$\begin{cases} \dot{V}_4 = -e_1^2 - e_2^2 - e_3^2 - e_4^2 < 0, \ \ \forall \{e_1, e_2, e_3, e_4\} \neq 0 \\ \dot{V}_4 = 0 \text{ for } e_1 = e_2 = e_3 = e_4 = 0 \end{cases} \tag{2.19}$$

In fact, if we rewrite the state-space equations of (2.15) in terms of the tracking errors (last section of Appendix *A2.4*), the errors dynamic is then found to be:

$$\begin{cases} \dot{e}_1 = -\rho_1 e_1 + e_2 \\ \dot{e}_2 = -\dfrac{\rho_2}{\rho_1} e_1 - \rho_2 e_2 + w_a e_3 \\ \dot{e}_3 = -\dfrac{\rho_3}{\rho_2} w_a e_2 - \rho_3 e_3 + p_a C_d g(.) e_4 \\ \dot{e}_4 = -\dfrac{\rho_4}{\rho_3} p_a C_d g(.) e_3 - \rho_4 e_4 \end{cases} \tag{2.20}$$

Or, in matrix form,

$$\begin{pmatrix} \dot{e}_1 \\ \dot{e}_2 \\ \dot{e}_3 \\ \dot{e}_4 \end{pmatrix} = \underbrace{\begin{pmatrix} -\rho_1 & 1 & 0 & 0 \\ -\frac{\rho_2}{\rho_1} & -\rho_2 & w_a & 0 \\ 0 & -\frac{\rho_3}{\rho_2} w_a & -\rho_3 & p_a C_d g(.) \\ 0 & 0 & -\frac{\rho_4}{\rho_3} p_a C_d g(.) & -\rho_4 \end{pmatrix}}_{A} \begin{pmatrix} e_1 \\ e_2 \\ e_3 \\ e_4 \end{pmatrix} \tag{2.21}$$

As we can see from (2.21), the controller parameters, as expected, appear on the diagonal of matrix *A*. Their effect on the error convergence to zero is obvious. Larger values of the tuning parameters yield to a faster convergence. However, very large values often result in a saturated control signal that involves chattering, because of the physical limitations of the system. Consequently a compromise has to be made in the tuning parameters choice. Unfortunately, in electrohydraulic systems, this compromise is very hard to find. In fact, the values of w_a and $p_a.C_d.g(.)$ are very large, especially the second term because it depends on the system pressure. This makes those terms crush the effect of the tuning parameters, which cannot be as large as them. The previous problem was solved in this paper with the proper choice of the Lyapunov function and the way tuning parameters were introduced, which made them appear in ratios in the first sub-diagonal.

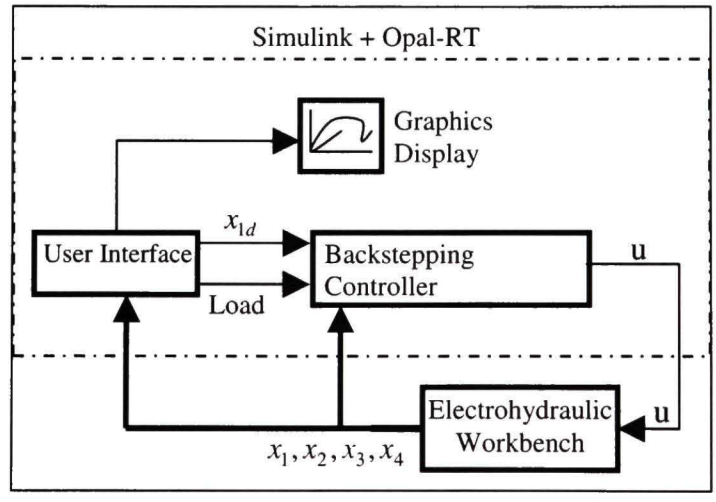

Figure 2.3 ***Block scheme of the Backstepping controller under Simulink and Rt- Lab.***

With this choice, the ratios ρ_2/ρ_1, $\rho_3 w_a/\rho_2$ and $p_a C_d g(.)\rho_4/\rho_3$ can be rendered very small with fairly large values of the tuning parameters ρ_1, ρ_2, ρ_3 and ρ_4. The smaller these ratios are with respect to the tuning parameters, the more the latter tend to be the eigenvalues of matrix A, and the tracking errors convergence is sped up.

2.6 Experimental Workbench and Settings

The implementation of the Backstepping controller on the electrohydraulic workbench, shown in Figure 2.2, was done on the OPAL-RT system under the QNX operating system. Through the RT-LAB Library, the OPAL-RT communicates with the controller built in SIMULINK. The OPAL-RT system has six Intel Pentium IV targets, four of which are for calculations and the remaining two dedicated to receiving and sending real-time signals. Figure 2.3 shows a block scheme of the controller, the electrohydraulic workbench and the user interface.

The master block SM_control is the Backstepping controller that generates the electric control signal u for the servovalve. The console block SC_userInterface is the block for data acquisition and graphics visualization, in addition to the desired actuator position and load that can be manipulated in real time through a signal generator and a slider gain, respectively. Data are acquired in this block every 0.1 *ms*. The save block SS_electrohydraulic communicates with the input/output 'OP-SCM-AIO-16A' analog cards.

The signals that are being acquired from the OP-SCM-AIO-16A analog output card are the angular velocity, the pressure P_1 at the hydraulic actuator inlet, the pressure P_2 at the hydraulic actuator outlet and the fluid flow through the servovalve; whereas the signals that are being sent to the OP-SCM-AIO-16A analog input card are the control input signal to the servovalve and the load that is determined by an electric signal raging from -10 *V* to +10 *V*. Both cards have a voltage limit ranging from -17 *V* to +17 *V*, which are beyond the voltage limit of the servovalve, which ranges from -5 *V* to +5 *V*.

2.7 Experimental Results

This section presents and analyzes the experimental results obtained from the Backstepping controller versus those obtained by a real-time classic PID controller. While it might seem unfair to compare a nonlinear controller with a PID controller, we do make it however because the PID is the most popular and widespread controller used in industry. We therefore held it as a reference for comparison. The goal is to evaluate the system transient response and steady state behavior. The maximum working pressure, during all experiments, is set at 1250 *psi*, which is the pressure threshold for the relief valve to open.

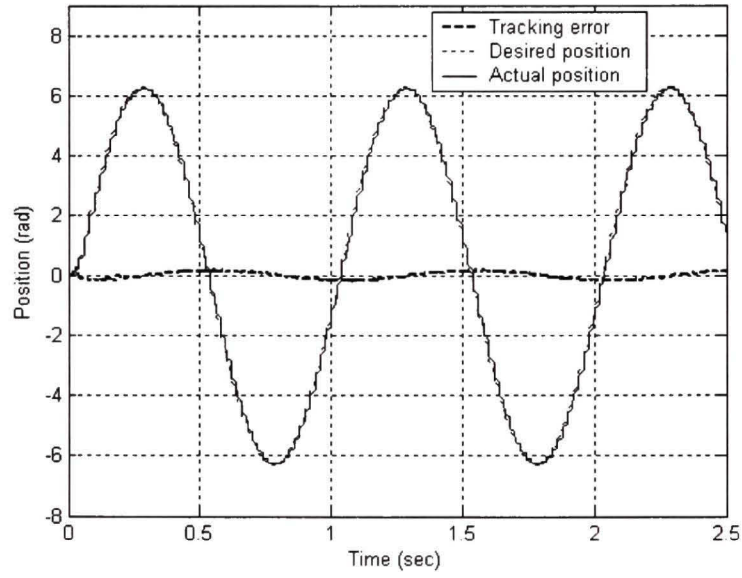

Figure 2.4 ***Experimental position and tracking error for Backstepping controller with load applied on the hydraulic actuator.***

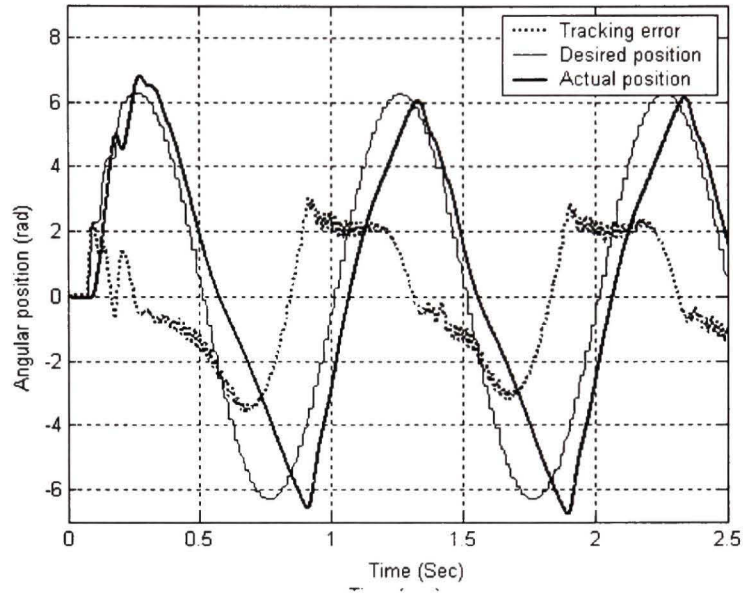

Figure 2.5 ***Experimental position and tracking error for PID with maximum load applied on the hydraulic actuator.***

2.7.1 Identification

The online identification of the system parameters is based on the recursive least square algorithm, with constant trace. The identification procedure is achieved in an open-loop system. In fact, the input signal that is being sent to the servovalve is a sine wave with a *3*Hz frequency and 0.5 Volts amplitude, with a low power white noise added to include all frequencies. During identification, the sampling time was set to 0.1 *ms* to ensure accuracy in derivative calculation. After 15 *sec* of identification, the system parameters became fairly constant and were set at the following values during the control process:

$$w_a = 27.34 cm^2/(s^2.daN);\ w_b = 10.23 s^{-1};$$
$$p_a = 27.79\sqrt{daN}/(cm^3.s);\ p_b = 4.62 s^{-1};$$
$$p_c = 32.02 daN/cm^2$$

Using the relations in (2.8), the physical parameters of the system can be figured out. The servovalve parameters are deduced from its data sheet. The installed servovalve is 760 valves series MOOG 760-103A. Its constant gain, time constant and discharge coefficient are respectively:

$$K = 0.0265 cm^2 / V$$
$$\tau_v = 0.01 \sec$$
$$C_d = 0.63$$

The oil physical properties are quite standard for the density and bulk modulus, respectively:

$$\rho = 85/(981 \times 10^5)\ daN.s^2/cm^4$$
$$\beta = 7995 daN / cm^2$$

The rest of the parameters resulting from the identification process are:

- Hydraulic actuator chamber volume: $V = 389.3 cm^3$
- Hydraulic actuator displacement: $D_m = 0.78 cm^3 / rad$
- Actuator and load moment of inertia: $J = 0.0285 daN.s^2.cm$
- Leakage coefficient: $C_L = 0.11 cm^5 / daN.s$
- Viscous friction: $B = 0.0285 daN.s.cm$

A complete list of the hydraulic system parameters, with their corresponding nomenclatures and dimensions, is given in Appendix *A2.1*.

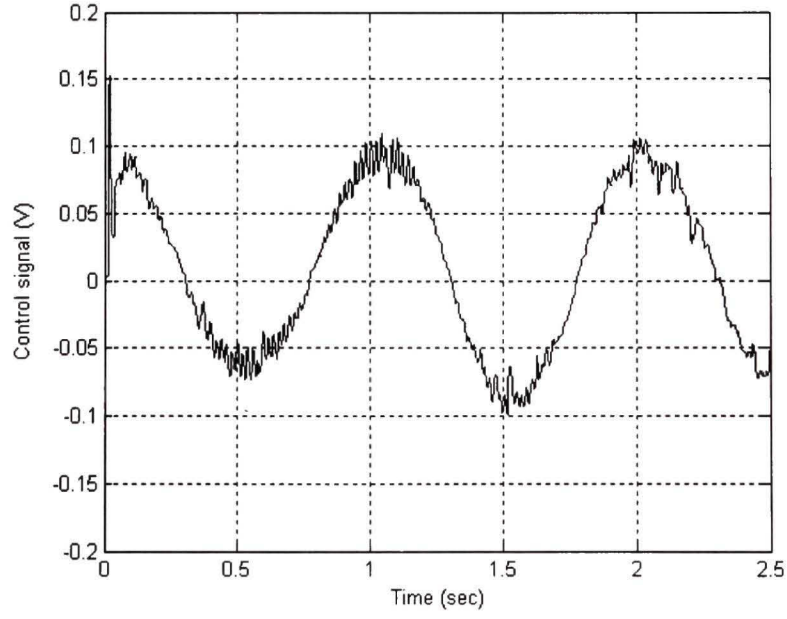

Figure 2.6 ***Experimental control signal of the Backstepping controller with maximum load on the hydraulic actuator.***

2.7.2 Real-Time Control and Comparisons

The real-time controller was implemented on the electrohydraulic workbench, and the results were compared to those obtained by a real-time PID controller. All the tests were performed under the same conditions. The parameters of the Backstepping controller were chosen such as to bring the matrix of the errors dynamic close to an inferior triangular one (Appendix *A2.2*); thus, only the controller parameters will affect the error convergence to zero.

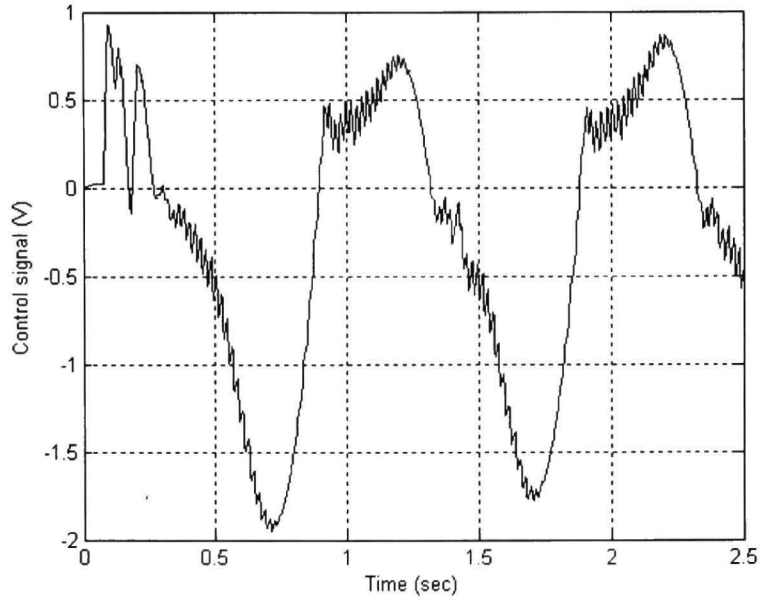

Figure 2.7 ***Control signal for PID controller with maximum load applied on the hydraulic actuator.***

As explained in the previous section, fairly large parameter values lead to a faster convergence, and consequently to a better transient state. On the other hand, the three gains of the PID controller were optimized using the 'NCD Outport' of the 'NCD Blockset' library of Matlab–Simulink. The 'NCD (Nonlinear Control Design) Outport' uses a nonlinear optimization algorithm; it converts time-domain constraints into a constrained optimization problem, and then solves the problem using state-of-the-art optimization routines taken from the Optimization Toolbox. The routine uses a Sequential Quadratic Programming (SQP) method.

The desired position to be tracked is a sine wave with a frequency of 1 Hz frequency and a 2π rad amplitude. In other words, the hydraulic actuator is made to rotate twice in a positive

direction and twice in a negative direction. The experiments were done, for both controllers, with a maximum load applied on the hydraulic actuator, which constitutes the worst case. Another test with no load applied to the hydraulic actuator was conducted for the PID controller to determine its efficiency margin.

Figure 2.4 shows the desired position, the actual position and the tracking error, for the real-time Backstepping controller. It can be seen that an excellent transient state is achieved and the tracking error is negligible. Figure 2.5 illustrates the same quantities, under the same conditions, for the real-time PID controller. In this case, only the angular position of the hydraulic actuator is fed back to the controller, unlike with Backstepping, where the four states constitute the feedback signals. As can be seen, tracking is far from achieved, especially in the negative direction of motion, because the load was applied in that way. Figures 6 and 7 show the control signals, in volts, which are generated by the Backstepping and the PID controllers, respectively, and then sent to the servovalve. We can see a very low amplitude and fairly smooth control signal in Figure 2.6, while Figure 2.7 confirms that classic linear controllers require more power to achieve tracking. This is a very important issue, since energy minimization is a fundamental criterion in control systems. Figure 2.8 indicates the desired angular velocity, the actual angular velocity and the tracking error of the hydraulic actuator resulting from the Backstepping controller. The trajectory of the desired velocity is generated by the Backstepping controller itself, based on the position tracking error, as can be seen from x_{2d} in (16) or as detailed in Step 1 of Appendix *A2.4*. It can be seen that the transient regime is very good, and lasts less than 0.05 *sec*. On the other hand, the tracking error is very small; however there are small peaks whenever the actuator changes its direction of motion. This can be interpreted as the effect of static friction, though its influence is insignificant. However, in some cases and applications, the PID controller can produce satisfactory results, even for nonlinear systems. This is shown in Figure 2.9, where the desired position, actual position and tracking error when no load is applied to the hydraulic actuator are plotted for the PID controller. It is clear that the tracking error is significantly bigger than that of the Backstepping controller, and the transient state is much

worse. However, the tracking is very acceptable though it will worsen gradually with a load increase. In this paper, we presented the two extreme cases.

2.8 Conclusion

In this work, a complete study was done of the modeling, identification and control of an electrohydraulic system. The mathematical model accounted for all the system dynamics, apart from few trivial assumptions that were put together to alleviate the complexity of the expressions. System identification was rendered very simple by rewriting the system model in an LP form, which allowed the use of the recursive least square algorithm for this purpose. On the other hand, nonlinear Backstepping control was employed for position tracking.

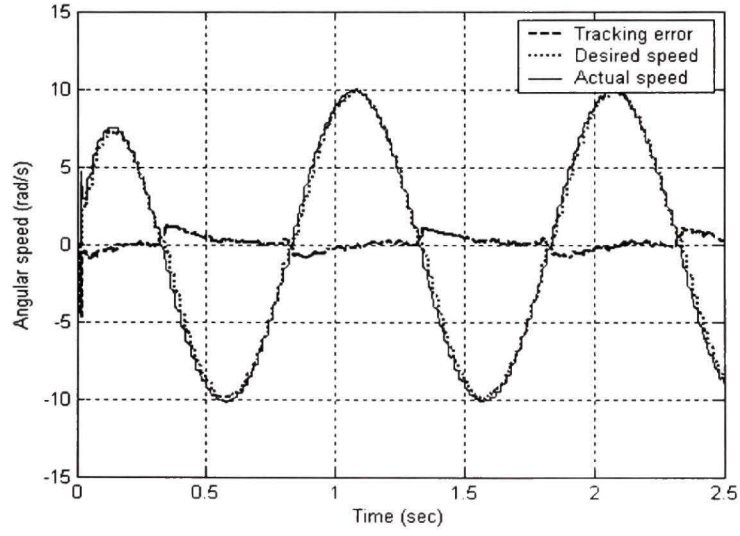

Figure 2.8 ***Experimental velocity and tracking error for Backstepping controller with maximum load applied on the hydraulic actuator.***

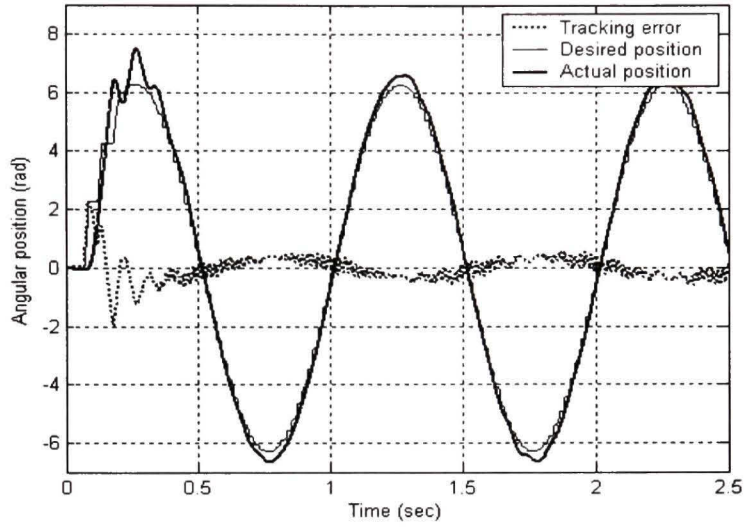

Figure 2.9 ***Experimental Position and tracking error for PID controller with no load applied.***

The emphasis was laid on the Lyapunov function choice. This was carried out such that the controller parameters appear in the errors dynamic, not only in the diagonal, but also in form of ratios at some other locations; this thus provides greater flexibility to control the error convergence to zero. Finally, a PID controller was implemented in order to compare transient state behavior, error tracking and the load effect. Our future works will include the real-time control of electrohydraulic active suspension using Backstepping control and theoretical improvements of nonlinear control for feedback and feedforward systems.

Appendix

Tableau A 2.1

List of system parameters

Name	Symbol	Unit
Valve orifice opening area	A_v	cm^2
Viscous damping coefficient	B	$daN.cm.sec$
Discharge coefficient	C_d	$dimensionless$
Leakage coefficient	C_L	$cm^5 / daN.s$
Actuator displacement	D_m	cm^3 / rad
Actuator and load inertia	J	$daN.s^2.cm$
Servovalve constant gain	K	$cm^2/Volt$
Pressures in actuator chambers	$P_{1,2}$	daN/cm^2
Load pressure	P_L	daN/cm^2
Supply pressure	P_s	daN/cm^2
Flow rates in/out of actuators	$Q_{1,2}$	cm^3/sec
Actuator load torque	T_L	$daN.cm$
Servovalve control input	u	$Volt$
Oil volume under compression	V	cm^3
Fluid bulk modulus	β	daN/cm^2
Fluid mass density	ρ	g/cm^3
Servovalve time constant	τ_v	sec
Actuator angular position	θ	rad

Tableau A 2.2

List of controller parameters

Tuning parameters	Value	Observations
P_1	50	---
ρ_2	150	$\rho_2 > \rho_1$ for speed must converge faster than position
ρ_3	40	$\rho_3 < \rho_2$ to minimize the effect of $w_a = 27.34$
ρ_4	0.001	$\rho_4 << \rho_3$ to minimize the effect of $p_a C_d g(.) \sim 10^4$

Tableau A 2.3

List of constants/variables of the stabilizing functions and control signal

Constant/variable	Value	Constant/variable	Value
$A2$	$\frac{\rho_2}{\rho_1 w_a} + \frac{(w_b - \rho_1)\rho_1}{w_a}$	c_2	$b_3 + \rho_3$

Constant/variable	Value	Constant/variable	Value
a_2	$\frac{\rho_1 - w_b + \rho_2}{w_a}$	$h(.)$	$-b_1 e_1 - c_1 e_2 - c_2 e_3 + b_4 \dot{x}_{1d} + b_5 \ddot{x}_{1d} + \frac{\dddot{x}_{1d}}{w_a} + \frac{p_b w_c}{w_a}$
b_1	$p_b a_1 + p_c \rho_1 - a_1 \rho_1 - \frac{\rho_2}{\rho_1}$	$f(.)$	$\frac{2ae^{-ax_4}}{(1+e^{-ax_4})^2}$
b_2	$p_b a_2 - p_c + a_1 - \rho_2 a_2$	d_1	$b_1 \rho_1 + \frac{\rho_2 c_1}{\rho_1}$
b_3	$w_a a_2 - p_b$	d_2	$-b_1 + c_1 \rho_2 + \frac{\rho_3 c_2 w_a}{\rho_2}$
b_4	$\frac{p_b w_b}{w_a} + p_c$	d_3	$-c_1 w_a + c_2 \rho_3$
b_5	$\frac{p_b + w_b}{w_a}$	$J(.)$	$d_1 e_1 + d_2 e_2 + d_3 e_3 - c_2 p_a C_d g(.) e_4 + b_4 \ddot{x}_{1d} + b_5 \dddot{x}_{1d} + \frac{x_{1d}^{(4)}}{w_a}$
c_1	$b_2 + \frac{\rho_3 w_a}{\rho_2}$	$g(.)$	$\sqrt{P_s - x_3 . sigm(x_4)}$

A 2.4 Backstepping design and proposition proof

Step 1: Let $V_1 = \frac{1}{2\rho_1} e_1^2$ be a candidate Lyapunov function for subsystem $\dot{x}_1 = x_2$. Then,

$$\dot{V}_1 = \frac{e_1}{\rho_1}(\dot{x}_1 - \dot{x}_{1d}) = \frac{e_1}{\rho_1}(e_2 + x_{2d} - \dot{x}_{1d}) \cdot$$

If we choose the following stabilizing function,

$$x_{2d} = \Theta(e_1, x_{1d}) = \dot{x}_{1d} - \rho_1 e_1 \tag{2.22}$$

This will yield to

$$\dot{V}_1 = -e_1^2 < 0 \tag{2.23}$$

Step 2: Let $V_2 = \frac{1}{2\rho_1} e_1^2 + \frac{1}{2\rho_2} e_2^2$ be a candidate Lyapunov function for subsystem $\dot{x}_2 = w_a x_3 - w_b x_2 - w_c$. Then,

$$\dot{V}_2 = -e_1^2 + e_2 \left[\frac{w_a}{\rho_2} x_3 + \left(\frac{1}{\rho_1} + \frac{(w_b - \rho_1)\rho_1}{\rho_2} \right) e_1 + \frac{(\rho_1 - w_b)}{\rho_2} e_2 - \frac{w_b}{\rho_2} \dot{x}_{1d} - \frac{\ddot{x}_{1d}}{\rho_2} - \frac{w_c}{\rho_2} \right]$$

Now, if we choose the following stabilizing function,

$$x_{3d} = \Omega(e_1, e_2, \dot{x}_{1d}, \ddot{x}_{1d}) = -a_1 e_1 - a_2 e_2 + \frac{w_b}{w_a}\dot{x}_{1d} + \frac{\ddot{x}_{1d}}{w_a} + \frac{w_c}{w_a} \tag{2.24}$$

This will yield to

$$\dot{V}_2 = -e_1^2 - e_2^2 < 0 \tag{2.25}$$

Step 3: Let $V_3 = \frac{1}{2\rho_1}e_1^2 + \frac{1}{2\rho_2}e_2^2 + \frac{1}{2\rho_3}e_3^2$ be a candidate Lyapunov function for subsystem $\dot{x}_3 = p_a x_4 g(.) - p_b x_3 - p_c x_2$. Then,

$$\dot{V}_3 = -e_1^2 - e_2^2 + e_3\left[\frac{p_a C_d x_4 g(.)}{\rho_3} + \frac{b_1}{\rho_3}e_1 + (\frac{b_2}{\rho_3} + \frac{w_a}{\rho_2})e_2 + \frac{b_3}{\rho_3}e_3 - \frac{b_4}{\rho_3}\dot{x}_{1d} - \frac{b_5}{\rho_3}\ddot{x}_{1d} - \frac{\dddot{x}_{1d}}{\rho_3 w_a} - \frac{p_b w_c}{\rho_3 w_a}\right]$$

Now, if we choose the following stabilizing function,

$$\begin{aligned} x_{4d} &= \Psi(e_1, e_2, e_3, \dot{x}_{1d}, \ddot{x}_{1d}, \dddot{x}_{1d}) \\ &= \frac{1}{p_a C_d g(.)}\left[-b_1 e_1 - (b_2 + \frac{\rho_3 w_a}{\rho_2})e_2 - b_3 e_3 + b_4\dot{x}_{1d} + b_5\ddot{x}_{1d} + \frac{\dddot{x}_{1d}}{w_a} + \frac{p_b w_c}{w_a} - \rho_3 e_3\right] \\ &= \frac{1}{p_a C_d g(.)}\left[-b_1 e_1 - (b_2 + \frac{\rho_3 w_a}{\rho_2})e_2 - b_3 e_3 + b_4\dot{x}_{1d} + b_5\ddot{x}_{1d} + \frac{\dddot{x}_{1d}}{w_a} + \frac{p_b w_c}{w_a} - \rho_3 e_3\right] \end{aligned} \tag{2.26}$$

This will yield to

$$\dot{V}_3 = -e_1^2 - e_2^2 - e_3^2 < 0 \tag{2.27}$$

At this stage, the stabilizing functions, which are the desired trajectories of all the state variables, have been generated. Every stabilizing function depends on the tracking errors of the variables of the previous state, on the desired position, and its derivatives.

Final step: The final step involves the building of the control signal of the system, which is the electric signal that actuates the servovalve spool to the right position.

Let, $V_4 = \frac{1}{2\rho_1}e_1^2 + \frac{1}{2\rho_2}e_2^2 + \frac{1}{2\rho_3}e_3^2 + \frac{1}{2\rho_4}e_4^2$ be a candidate Lyapunov function for subsystem $\dot{x}_4 = -r_a x_4 + r_b u$. Then,

$$\dot{V}_4 = -e_1^2 - e_2^2 - e_3^2 + e_4\left\{\begin{array}{l}\frac{r_b}{\rho_4}\left(1 - \frac{x_3 f(.)h(.)}{2p_a C_d \rho . g(.)^3}\right)u + \frac{p_a C_d g(.)e_3}{\rho_3} - \frac{r_a}{\rho_4}x_4 - \frac{J(.)}{\rho_4 p_a C_d g(.)} \\ -\frac{1}{2p_a C_d \rho_4 \rho . g(.)^3}\begin{pmatrix}\dot{x}_3 sgm(x_4) \\ -r_a x_3 x_4 f(.)\end{pmatrix}h(.)\end{array}\right\}$$

Now, if we choose the control signal u as follows,

$$u = \Lambda(e_1, e_2, e_3, e_4, \dot{x}_{1d}, \ddot{x}_{1d}, \dddot{x}_{1d}, x_{1d}^{(4)}) = \frac{\left[-\frac{\rho_4}{\rho_3} p_a C_d g(.) e_3 + r_a x_4 + \frac{J(.)}{p_a C_d g(.)} + \frac{1}{2 p_a C_d \rho . g(.)^3} \begin{pmatrix} \dot{x}_3 sgm(x_4) \\ -r_a x_3 x_4 f(.) \end{pmatrix} h(.) - \rho_4 e_4 \right]}{r_b \left(1 - \frac{x_3 f(.) h(.)}{2 p_a C_d \rho . g(.)^3} \right)} \tag{2.28}$$

This will yield to

$$\dot{V}_4 = -e_1^2 - e_2^2 - e_3^2 - e_4^2 < 0 \tag{2.29}$$

Equation (2.29) shows that the error dynamic is globally asymptotically stable, because any error signal will converge to zero.

Errors dynamic:

The effect of the controller tuning parameters and the weight of the Lyapunov function choice can be seen by examining the errors dynamic of the closed loop system. The latter is found by calculating $\dot{e}_i = \dot{x}_i - \dot{x}_{id}$ and replacing x_i with $e_i + x_{id}$ for $i = 1,2,3,4$. $\dot{x}_1, \dot{x}_2, \dot{x}_3$ and $\dot{x}_4$ are found directly from the system model (2.15); whereas $\dot{x}_{1d}, \dot{x}_{2d}, \dot{x}_{3d}$ and $\dot{x}_{4d}$ are the analytical derivatives of x_{1d}, x_{2d}, x_{3d} and x_{4d} that were found in steps 1, 2, and 3. Therefore, we have:

$$\begin{aligned} \dot{e}_1 &= \dot{x}_1 - \dot{x}_{1d} = x_2 - \dot{x}_{1d} \\ &= e_2 + x_{2d} - \dot{x}_{1d} = e_2 + (-\rho_1 e_1 + \dot{x}_{1d}) - \dot{x}_{1d} \\ &= -\rho_1 e_1 + e_2 \end{aligned} \tag{2.30}$$

$$\begin{aligned} \dot{e}_2 &= \dot{x}_2 - \dot{x}_{2d} = (w_a x_3 - w_b x_2 - w_c) - (-\rho_1 \dot{e}_1 + \ddot{x}_{1d}) \\ &= -\frac{\rho_2}{\rho_1} e_1 - \rho_2 e_2 + w_a e_3 \end{aligned} \tag{2.31}$$

$$\begin{aligned} \dot{e}_3 &= \dot{x}_3 - \dot{x}_{3d} \\ &= (p_a x_4 g(.) - p_b x_3 - p_c x_2) + a_1 \dot{e}_1 + a_2 e_2 - \frac{w_b}{w_a} \ddot{x}_{1d} - \frac{\dddot{x}_{1d}}{w_a} \\ &= -\frac{\rho_3}{\rho_2} w_a e_2 - \rho_3 e_3 + p_a C_d g(.) e_4 \end{aligned} \tag{2.32}$$

$$\dot{e}_4 = \dot{x}_4 - \dot{x}_{4d} = (-r_a x_4 + r_b u) - \dot{x}_{4d} = -\frac{\rho_4}{\rho_3} p_a C_d g(.) e_3 - \rho_4 e_4 \tag{2.33}$$

References

Alleyne, A. and J. K. Hedrick (1995). "Nonlinear adaptive control of active suspensions." Control Systems Technology, IEEE Transactions on 3(1): 94-101.

Astrom, K. J. and B. Wittenmark (1989). Adaptive Control. Addison-Wesley, United States.

Ayalew, B. and B. T. Kulakowski (2005). Nonlinear decentralized position control of electrohydraulic actuators in road simulation. Proceedings of the ASME Design Engineering Division 2005, Nov 5-11 2005, Orlando, FL, United States, American Society of Mechanical Engineers, New York, NY 10016-5990, United States.

Chen, H.-M., J.-C. Renn, and J.-P. Su (2005). "Sliding mode control with varying boundary layers for an electro-hydraulic position servo system." International Journal of Advanced Manufacturing Technology 26(1-2): 117-123.

Fink, A. and T. Singh (1998). Discrete sliding mode controller for pressure control with an electrohydraulic servovalve. Control Applications, 1998. Proceedings of the 1998 IEEE International Conference on.

Habibi, S. and A. Goldenberg (2000). "Design of a new high-performance electrohydraulic actuator." Journal of Mechatronics, IEEE/ASME Transactions 5(2): 158-164.

Hahn, H., A. Piepenbrink, and K.-D. Leimbach, (1994). Input/output linearization control of an electro servo-hydraulic actuator. Control Applications, 1994., Proceedings of the Third IEEE Conference on.

Kaddissi, C., J.-P. Kenné, and M. Saad (2004). Position Control of an Electro-Hydraulic Servosystem - A Non-Linear Backstepping Approach. ICINCO - Intrernational Conference on Infornatics in Control, automation and robotoics, Setubal - Portugal.

Kaddissi, C., J.-P. Kenné, and M. Saad (2005). Drive by wire Control of an Electro-Hydraulic Active Suspension, a Backstepping approach. CCA - Proceedings of the 2005 IEEE Conference on Control Applications, August 28-31, 2005 - pp. 1581-1587, Toronto - Canada.

Kandil, N., S. LeQuoc, and M. Saad (1999). "On-Line Trained Neural Controllers for Nonlinear Hydraulic System." 14th World Congress of IFAC: 323-328.

Khalil, H. K. (2002). Nonlinear systems. New Jersey, Upper Saddle River, N.J: Prentice Hall, c2002.

Krstic, M., I. Kanellakopoulos, and P. V. Kokotovic,. (1995). Nonlinear and adaptive control design, New York, N.Y. J. Wiley and Sons, c1995.

Lee, S. J. and T.-C. Tsao (2002). Nonlinear backstepping control of an electrohydraulic material testing system. 2002 American Control COnference, May 8-10 2002, Anchorage, AK, United States, Institute of Electrical and Electronics Engineers Inc.

LeQuoc, S., R. M. H. Cheng, and K.H. Leung, (1990). "Tuning an electrohydraulic servovalve to obtain a high amplitude ratio and a low resonance peak." Journal of Fluid Control 20(3Mar): 30-49.

Li, P. Y. (2001). "Dynamic Redesign of a Flow Control Servovalve Using a Pressure Control Pilot." Journal of Dynamic Systems, Measurement and Control 124(3): 428-34.

Lim, T. J. (1997). Pole placement control of an electro-hydraulic servo motor. Proceedings of the 1997 2nd International Conference on Power Electronics and Drive Systems, PEDS. Part 1 (of 2), May 26-29 1997, Singapore, Singapore, IEEE, Piscataway, NJ, USA.

Lin, J.-S. and I. Kanellakopoulos (1997). "Nonlinear design of active suspensions." IEEE Control Systems Magazine 17(3): 45-59.

Liu, R. and A. Alleyne (2000). "Nonlinear force/pressure tracking of an electro-hydraulic actuator." Journal of Dynamic Systems Measurement and Control-Transactions of the Asme 122(1): 232-237.

Merrit, H. E. (1967). Hydraulic Control Systems, New York, N.Y.: J. Wiely and sons.

Plahuta, M. J., M. A. Franchek, and H. Stern (1997). "Robust controller design for a variable displacement hydraulic motor." American Society of Mechanical Engineers, The Fluid Power and Systems Technology Division (Publication) FPST. Proceedings of the 1997 ASME International Mechanical Engineering Congress and Exposition, Nov 16-21 1997 4: 169-176.

Ursu, I., F. Popescu, and F. Ursu (2003). Control synthesis for electrohydraulic servo mathematical model. Proceedings of the CAIM 2003, the 11th International Conference on Applied and Industrial Mathematics, Oradea, Romania.

Yongqian, Z., S. LeQuoc, and M. Saad (1998). Nonlinear fuzzy control on a hydraulic servo system. American Control Conference, 1998. Proceedings of the 1998.

Yu, W.-S. and T.-S. Kuo (1996). "Robust indirect adaptive control of the electrohydraulic velocity control systems." IEE Proceedings: Journal of Control Theory and Applications 143(5): 448-454.

Yu, W.-S. and T.-S. Kuo (1997). "Continuous-time indirect adaptive control of the electrohydraulic servo systems." Journal of Control Systems Technology, IEEE Transactions on Control Systems Technology 5(2): 163-177.

Zavarehi, M. K., P. D. Lawrence, and F. Sassani(1999). "Nonlinear modeling and validation of solenoid-controlled pilot-operated servovalves." IEEE/ASME Transactions on Mechatronics Journal 4(3Sep): 324-334.

Zeng, W. and J. Hu (1999). "Application of intelligent PDF control algorithm to an electrohydraulic position servo system." IEEE/ASME International Conference on Advanced Intelligent Mechatronics (AIM '99), Sep 19-Sep 23 1999: 233-238.

INTRODUCTION AU BACKSTEPPING ADAPTATIF INDIRECT

Dans le chapitre précédent, une étude complète a été faite sur la modélisation, l'identification et la commande d'un système électrohydraulique. Le modèle développé tenait compte de toute la dynamique du système, mis à part quelques approximations infimes qui étaient nécessaires pour alléger la complexité de certaines expressions mathématiques. Malgré son aspect nonlinéaire, le système était très facilement identifié à l'aide de l'algorithme des moindres carrés récursifs et ceci en réécrivant le modèle du système sous une forme linéaire en paramètres ou LP. D'autre part, la commande nonlinéaire basée sur le Backstepping a été utilisée dans le but d'obtenir une poursuite précise de la position angulaire désirée du moteur hydraulique. L'emphase concernait surtout le choix de la fonction de Lyapunov ainsi que la manière dont les paramètres d'ajustement du contrôleur y étaient introduits de façon à accélérer la convergence de la dynamique de l'erreur vers zéro. Finalement, un contrôleur industriel du type PID a été mis en application afin de comparer les résultats avec le Backstepping au niveau de la dynamique de l'erreur et l'effet de la variation de la charge sur cette dernière.

Comme mentionné dans la conclusion du chapitre précédent (article), nos travaux futurs viseront une amélioration plus poussée de cette technique de Backstepping appliquée à la commande d'un système électrohydraulique. Par conséquent, le chapitre suivant (article) élabore une version adaptative du Backstepping. En effet, durant les différentes expériences achevées au laboratoire LITP de l'ÉTS, il a été constaté que pour des charges élevées sur le moteur hydraulique, dans des conditions d'opération identiques, le système électro-hydraulique et son modèle mathématique ne se suivaient plus. Ceci explique une variation au niveau des paramètres hydrauliques du système; notamment le coefficient de frottement visqueux de l'actionneur ainsi que le module de Bulk du fluide. De ce fait, une nécessité d'identifier continuellement les paramètres du système et de les injecter dans le contrôleur afin de le mettre à jour, s'impose. Le choix du Backstepping adaptatif indirect vient du fait qu'il permet d'identifier la valeur physique et réelle des paramètres du système, permettant ainsi au moteur hydraulique de suivre la position désirée imposée dans toutes les conditions.

CHAPITRE 3

REAL TIME INDIRECT ADAPTIVE CONTROL OF AN ELECTROHYDRAULIC SERVO SYSTEM BASED ON NONLINEAR BACKSTEPPING

Claude Kaddissi, *Member, IEEE*, Jean-Pierre Kenné, and Maarouf Saad, *Associate Member, IEEE*
École de Technologie Supérieure, 1100 Notre-Dame West street, Quebec H3C 1K3, Canada
Email: jean-pierre.kenne@etsmtl.ca

Abstract

This paper studies the real-time position control of an electrohydraulic system using indirect adaptive backstepping. In fact, electrohydraulic systems are known to be highly nonlinear and non-differentiable due to many factors as leakage, friction and especially the fluid flow expression through the servovalve. Backstepping is used for being a powerful, robust nonlinear strategy and for its ability to ensure a global asymptotic stability of the controlled system without canceling useful nonlinearities. On the other hand, hydraulic parameters are prone to variations, particularly fluid viscosity and bulk modulus that increase with pressure and decrease with temperature. This in turn, results in a varying viscous friction coefficient. Hence, it is interesting to employ an adaptive control strategy in order to update the controller with the parameters variation. In such case, indirect adaptive control is highly recommended, because it has the benefit of identifying the real values of the system parameters. Emphasis in this work is also on the tuning parameters effect and their influence on the error dynamic behavior, in addition to the smoothness of the control signal.

The out coming results are compared to those obtained from a non-adaptive backstepping controller applied to the same electrohydraulic test-bench. The effectiveness of the proposed approach, in terms of guaranteed stability and negligible tracking error, in the presence of varying parameters, is well revealed in the results.

Index Terms: Electrohydraulic systems, Backstepping, Adaptive Control, Nonlinear Control.

3.1 Introduction

Currently, electrohydraulic systems are very popular in most of the industrial processes such as heavy machinery, robotics, aircrafts and automotive industry. This is principally due to the high power to volume ratio that they can offer, by being less bulky than electrical motors. However, in control system applications, the nonlinearities and the mathematical model singularity of electrohydraulic systems causes traditional constant gain controllers to be inadequate.

The electrohydraulic test-bench that was used to achieve the current work is represented in figure 3.1 and is composed of:

- A fixed displacement pump driven by an electric motor
- A hydrostatic tank from where the pump carries fluid oil
- A small accumulator located at the discharge side of the pump that acts as a water hammer arrestor in case of an urgent shut down or a sudden load increase.
- A relief valve installed next to the accumulator to limit the maximum operating pressure
- A hydraulic actuator that drives a certain load
- A servovalve that directs the oil flow according to the appropriate position of its spool, and consequently determines the direction of motion and speed of the hydraulic actuator.

More details about hydraulic components and electrohydraulic systems can be found in Merritt (1967).

According to what was mentioned in the previous paragraph there are two issues to deal with when it comes to electrohydraulic systems: The accuracy of the mathematical model and the effectiveness of the control strategy. Regarding the first issue, several improvements were made. In Habibi and Goldenberg (2000), a new design for asymmetric linear hydraulic actuators is elaborated. A dynamic redesign for a nonlinear servovalve is considered in the of

papers Li (2001) and Zavarehi et al. (1999). In fact, the complication of hydraulic systems is mainly caused by the nonlinear behavior of this component. However, the mathematical model that we adopted in this work is similar to one in LeQuoc et al. (1990) except minor differences that will be discussed later.

Concerning the control issue, several classical and advanced strategies can be encountered in literature. Beginning with linear control, simple poles placement was employed to the linearized model of an electrohydraulic system. The authors Lim (1997) and Zeng and Hu (1999) used cascaded PID controllers to monitor the position of hydraulic actuators. The dynamic variations depicted in the previous works, through experiments, lead to the conclusion that such phenomena are beyond the capacity of these controllers. Those dynamic variations that should be taken into account in the control strategy are due to:

- Load variations ;
- Changes of transducers characteristic ;
- Changes of the hydraulic fluid properties ;
- Changes in the servo components dynamic, etc.

All the previous observations were behind the use and the development of many robust and adaptive control methods. Indirect adaptive control, for speed and position feedback of hydraulic actuators was used by Yu and Kuo (1996) and (1997). However, the controller efficiency and robustness, in both cases, was limited by the fact that it is based on a linear model of the system. Sliding mode control was used by Fink and Singh (1998), to regulate the differential pressure, across the hydraulic actuator; however the resulting control signal involved high frequency chattering because of the switching function. On the other side, the paper of Chen et al. (2005) dealt with the previous chattering problem, in fact the controller there is based on variable sliding surfaces, in order to avoid chattering. For the use of linear control methods on nonlinear systems, Input-output linearization is very convenient and was adopted by Hahn et al. (1994) to compensate the nonlinearities of the electrohydraulic system. The drawback of this method is that it leads to the cancellation of useful nonlinearities that would enhance the system stability and reduce the control signal amplitude

in their presence. Conversely, backstepping is a very potent control strategy, able to handle nonlinearities. It was applied to an electrohydraulic system by Ursu (2004) and Kaddissi et al. (2007); as well as to an electrohydraulic active suspension by Lin and Kanellakopoulos (1997) and Kaddissi et al. (2005). Intelligent control like fuzzy logic and neural network were adopted by Yongqian et al. (1998) and Kandil et al. (1999) respectively. The results quality was very satisfactory in both cases. The main disadvantage that could be detected is that stability is not guaranteed in these approaches because it is studied on discrete domains and the system behavior cannot be predicted at limits.

This paper proposes an indirect adaptive backstepping approach for position control of an electrohydraulic servo system. This allows taking advantage of the backstepping strategy on one side and considers the variation of the system parameters on the other. The benefit of using indirect adaptive control is that it guaranties the convergence of the system parameters to their real physical values and ensures the system stability at the same time.

The rest of the paper is organized as follow. The motivation for this work is presented in section 2. Section 3 is a brief description of the mathematical model. Section 4 deals with the identification algorithm and the adaptive controller design that is being employed. In section 5, the experimental results are compared with there counterparts of a non-adaptive backstepping controller. Finally, some conclusions and remarks bring this work to an end in section 6.

3.2 Motivation

Electrohydraulic systems have many applications that are of great interest to us. However, their control brings to engineers and researchers several difficulties that are not trivial to solve. In fact, it is thorny to find an ideal control strategy that combines all the solutions. This is why in our previous work, Kaddissi et al. (2007), the focus was on the nonlinear and non-differentiable aspects of the mathematical model and how they were managed by the backstepping controller. Another issue was the fine tuning of the controller parameters to

ensure a good tracking of the reference signal. On the other hand, the current work focuses on the hydraulic system parameters and the effect of their variation on the closed loop system behavior. This is why we found it intriguing to develop an indirect adaptive version of the backstepping controller, in order to take care of cases where a variable load on the hydraulic actuator or different ambient conditions or any irregularities could result in a variation of the system parameters and affect its stability. Figure 3.2 illustrates a block diagram of the whole closed loop system, which will be discussed further in detail. Therefore, in the upcoming sections we will be going through the description of each of its blocks.

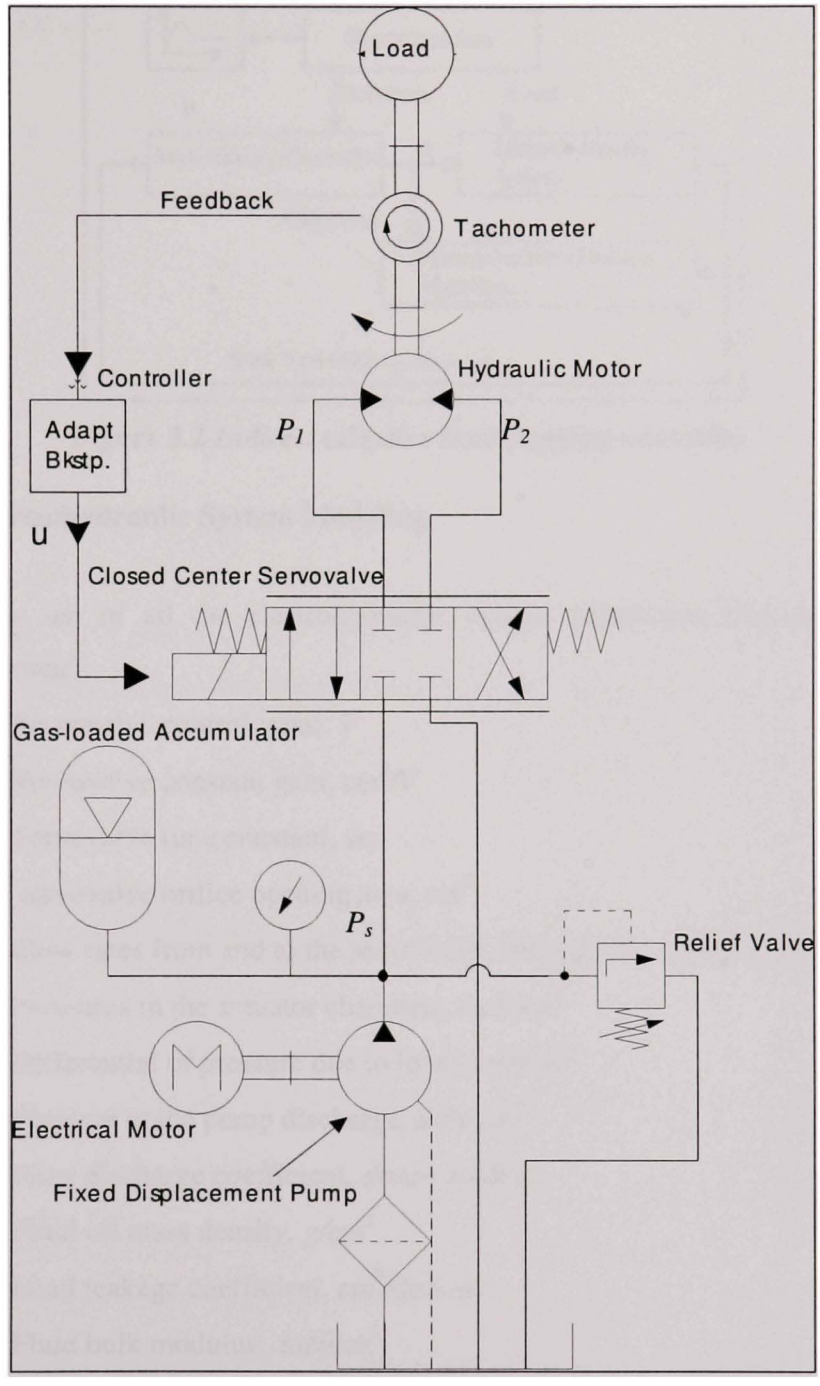

Figure 3.1 ***Schematic of hydraulic servo-system.***

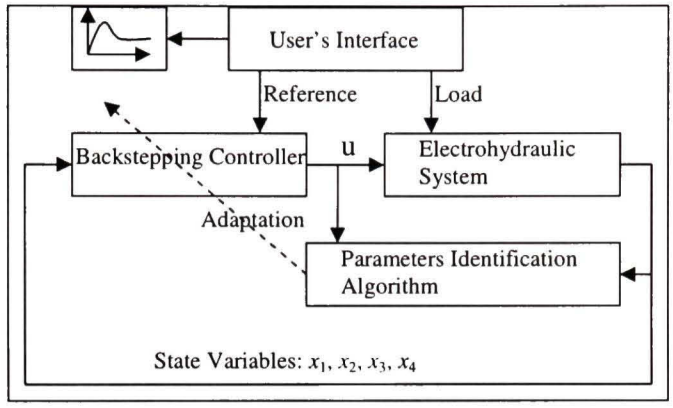

Figure 3.2 ***Indirect adaptive Backstepping controller.***

3.3 Electrohydraulic System Modeling

Following is a list of all the electrohydraulic system parameters that are used in the mathematical model:

- u: Servovalve control input, V
- K: Servovalve constant gain, cm^2/V
- τ_v: Servovalve time constant, *sec*
- A_v: Servovalve orifice opening area, cm^2
- Q: Flow rates from and to the servovalve, through the valve orifices, cm^3/sec
- $P_{1,2}$: Pressures in the actuator chambers, daN/cm^2
- P_L : Differential of pressure due to load, daN/cm^2
- P_s: Pressure at the pump discharge, daN/cm^2
- C_d: Flow discharge coefficient, *dimensionless*
- ρ: Fluid oil mass density, g/cm^3
- C_L: Load leakage coefficient, $cm^5/daN.sec$
- β: Fluid bulk modulus, daN/cm^2
- V : Oil volume in one chamber of the actuator, cm^3
- D_m Actuator volumetric displacement, cm^3/rad
- T_L Load torque, *daN.cm*
- B: Viscous damping coefficient, *daN.cm.sec*
- J: Actuator inertia, $daN.sec^2.cm$

- θ_p: Actuator angular position, *rad*

The flow through the servovalve is given by,

$$Q = C_d A_v \sqrt{\frac{P_s - P_L}{\rho}} \qquad \text{if } \theta_p > 0 \tag{3.1}$$

$$Q = C_d A_v \sqrt{\frac{P_s + P_L}{\rho}} \qquad \text{if } \theta_p < 0 \tag{3.2}$$

Therefore, since $sign(A_v) = sign(\theta_p)$ we can write,

$$Q = C_d A_v \sqrt{\frac{P_s - sign(A_v) P_L}{\rho}} \tag{3.3}$$

With $P_s = P_1 + P_2$ and $P_L = P_1 - P_2$.

Now, in order to avoid numerical problems due the non-differentiable term in (3.3), the sign function is approximated with a sigmoid function that has the following properties:

$$sigm(x) = \frac{1 - e^{-ax}}{1 + e^{-ax}} \qquad \forall x \in \Re \tag{3.4}$$

This is a continuously differentiable function with,

$$a > 0 \quad \text{and} \quad sigm(x) = \begin{cases} 1 \ if \ ax \to \infty \\ 0 \ if \ ax \to 0 \\ -1 \ if \ ax \to -\infty \end{cases} \tag{3.5}$$

Consequently,

$$Q = C_d A_v \sqrt{\frac{P_s - sigm(A_v) P_L}{\rho}} \tag{3.6}$$

This approximation guarantees the existence of a solution independently of the rotation direction of the actuator, avoiding thus the non-differentiability problem.

Since oil has a certain degree of compressibility that is more pronounced at high pressures, it should be considered in the actuator dynamic. Thus, we give the compressibility equation as,

$$\frac{V}{2\beta} \dot{P}_L = C_d A_v \sqrt{\frac{P_s - sigm(A_v) P_L}{\rho}} - D_m \dot{\theta} - C_L P_L \tag{3.7}$$

Let us now consider the hydraulic actuator equation of motion given by Newton's second law. By neglecting the Coulomb frictional torque, we have,

$$J \ddot{\theta}_p = D_m (P_1 - P_2) - B \dot{\theta}_p - T_L \tag{3.8}$$

The final remaining component is the servovalve, which dynamic equation is a first order one, since its spool inertia has been neglected for simplification purposes. It is given by,

$$\tau_v \dot{A}_v + A_v = Ku \tag{3.9}$$

Now if we choose, $x_1 = \theta_p$, $x_2 = \omega = \dot{\theta}_p$, $x_3 = P_L$, $x_4 = A_v$ as state variables, the system can be easily written in a 4th order nonlinear state-space model.

$$\boxed{\begin{cases} \dot{x}_1 = x_2 \\ \dot{x}_2 = w_a x_3 - w_b x_2 - w_c \\ \dot{x}_3 = p_a x_4 \sqrt{P_s - x_3 . sigm(x_4)} - p_b x_3 - p_c x_2 \\ \dot{x}_4 = -r_a x_4 + r_b u \end{cases}} \tag{3.10}$$

Where r_a, r_b, p_a, p_b, p_c, w_a, w_b, w_c, are the systems parameters given by,

$$r_a = \frac{1}{\tau_v}, \quad r_b = \frac{K}{\tau_v}, \quad p_a = \frac{2\beta C_d}{V\sqrt{\rho}}, \quad p_b = \frac{2\beta C_L}{V}$$

$$p_c = \frac{2\beta D_m}{V}, \quad w_a = \frac{D_m}{J}, \quad w_b = \frac{B}{J}, \quad w_c = \frac{T_L}{J}$$

The parameters aimed by the identification process are: p_a, p_b, p_c, w_a, w_b and w_c. Although w_c is proportional to the resistive torque T_L, it is still unknown since it depends on the actuator inertia J. Those parameters will be continuously identified during the control process, and then will be injected in the backstepping controller as shown in figure 3.2. This way, the parameters variation can be tracked and taken into consideration at any time. On the other hand, the parameters r_a and r_b are provided by the servovalve datasheet. The next step is to set up and design the indirect adaptive backstepping controller.

3.4 Indirect Adaptive Backstepping Controller

By referring to figure 3.2, the control of the electrohydraulic system is achieved as follow:

- The state variables x_1, x_2, x_3 and x_4 are sent to the parameters identification block along with the control signal u.
- Once the system parameters are identified, they are introduced in the backstepping controller block as well as the 4 state variables in order to generate the control signal.

- The control signal is brought to electrohydraulic system so that the hydraulic actuator could track its desired position x_r while taking into consideration the load torque.

The previous sequence is repeated at every sampling time of the control process. Based on (3.10) we can write,

$$\begin{cases} \dot{x}_2 = w_a x_3 - w_b x_2 - w_c \\ \dot{x}_3 = p_a x_4 \underbrace{\sqrt{P_s - x_3 sigm(x_4)}}_{g(.)} - p_b x_3 - p_c x_2 \end{cases} \tag{3.11}$$

Or in matrix from,

$$\begin{pmatrix} \dot{x}_2 \\ \dot{x}_3 \end{pmatrix} = \begin{pmatrix} x_3 & 0 \\ -x_2 & 0 \\ -1 & 0 \\ 0 & x_4 g(.) \\ 0 & -x_3 \\ 0 & -x_2 \end{pmatrix}^T \times \begin{pmatrix} w_a \\ w_b \\ w_c \\ p_a \\ p_b \\ p_c \end{pmatrix} \tag{3.12}$$

It can be seen that the subsystem (3.12) is linear with respect to its parameters, which is a sufficient condition for those parameters to be identified through the continuous Recursive Least Square method as in Astrom and Wittenmark (1989). Now, let:

$$\begin{cases} y(t) = \begin{pmatrix} \dot{x}_2 \\ \dot{x}_3 \end{pmatrix} \\ \varphi(t) = \begin{pmatrix} x_3 & -x_2 & -1 & 0 & 0 & 0 \\ 0 & 0 & 0 & x_4 g(.) & -x_3 & -x_2 \end{pmatrix} \\ \theta(t)^T = \begin{pmatrix} w_a & w_b & w_c & p_a & p_b & p_c \end{pmatrix} \end{cases} \tag{3.13}$$

Where: $y(t)$ is the observation vector, $\varphi(t)$ is the matrix of regressors and $\theta(t)$ is the vector of unknown parameters that are now time dependent, since they are continuously identified and might vary in time. Then,

$$y(t) = \varphi(t)\theta(t) \tag{3.14}$$

Next, we define the least square error $V(\theta)$ and the matrix $P(t)$ as well according to Astrom and Wittenmark (1989),

$$\begin{cases} V(\theta) = \int_0^t e^{\alpha(t-s)}\left(y(s) - \varphi(s)\theta(s)\right)^2 ds \quad ; \; 0 < \alpha < 1 \\ P(t) = \left(\int_0^t \varphi(s)\varphi(s)^T ds\right)^{-1} \end{cases} \tag{3.15}$$

Finally, the parameter estimate $\hat{\theta}(t)$ that minimizes the least square error, according to Astrom and Wittenmark (1989), must satisfy,

$$\boxed{\begin{cases} \dfrac{d\hat{\theta}(t)}{dt} = P(t)\varphi(t)^T e(t) \\ e(t) = y(t) - \varphi(t)\hat{\theta}(t) \\ \dfrac{dP(t)}{dt} = \alpha P(t) - P(t)\varphi(t)^T \varphi(t) P(t) \end{cases}} \tag{3.16}$$

With, $\hat{\theta}(t)^T = \begin{pmatrix} \hat{w}_a & \hat{w}_b & \hat{w}_c & \hat{p}_a & \hat{p}_b & \hat{p}_c \end{pmatrix}$

By integrating the first equation of (3.16), we get the estimates of the system parameters and thus update the backstepping controller at every sampling time.

Finally, to close the loop in figure 3.2, the design of the backstepping block follows. The controller is designed with the estimated system parameters; its tuning parameters and the intermediate variables and functions used to alleviate the calculations are listed in appendices *A3.1* and *A3.2* respectively.

Consider the nonlinear model of the electrohydraulic system in (3.10), and let $e_i = x_i - x_{id}$, for $i = 1,2,3,4$, be the tracking error between every state variable and its desired value, with $x_{1d} = x_r$ the desired position of the hydraulic actuator to be tracked.

Step 1: Let $V_1 = \dfrac{1}{2\rho_1} e_1^2$ be a candidate Lyapunov function for subsystem $\dot{x}_1 = x_2$ of (3.10). Then,

$$\dot{V}_1 = \frac{e_1}{\rho_1}(\dot{x}_1 - \dot{x}_{1d}) = \frac{e_1}{\rho_1}(e_2 + x_{2d} - \dot{x}_{1d}) \tag{3.17}$$

If we choose the following stabilizing function,

$$x_{2d}(e_1, x_{1d}) = \dot{x}_{1d} - \rho_1 e_1 \tag{3.18}$$

This will yield to

$$\dot{V}_1 = -e_1^2 < 0 \tag{3.19}$$

Step 2: Let $V_2 = \frac{1}{2\rho_1}e_1^2 + \frac{1}{2\rho_2}e_2^2$ be a candidate Lyapunov function for subsystem $\dot{x}_2 = \hat{w}_a x_3 - \hat{w}_b x_2 - \hat{w}_c$ of (3.10). Then,

$$\dot{V}_2 = -e_1^2 + e_2\left[\frac{\hat{w}_a}{\rho_2}x_3 + \left(\frac{1}{\rho_1} + \frac{(\hat{w}_b - \rho_1)\rho_1}{\rho_2}\right)e_1 + \frac{(\rho_1 - \hat{w}_b)}{\rho_2}e_2 - \frac{\hat{w}_b}{\rho_2}\dot{x}_{1d} - \frac{\ddot{x}_{1d}}{\rho_2} - \frac{\hat{w}_c}{\rho_2}\right] \tag{3.20}$$

Now, if we choose the following stabilizing function,

$$x_{3d}(e_1, e_2, \dot{x}_{1d}, \ddot{x}_{1d}) = \left(-a_1 e_1 - a_2 e_2 + \frac{\hat{w}_b}{\hat{w}_a}\dot{x}_{1d} + \frac{\ddot{x}_{1d}}{\hat{w}_a} + \frac{\hat{w}_c}{\hat{w}_a}\right) \tag{3.21}$$

This will yield to

$$\dot{V}_2 = -e_1^2 - e_2^2 < 0 \tag{3.22}$$

Step 3: Let $V_3 = \frac{1}{2\rho_1}e_1^2 + \frac{1}{2\rho_2}e_2^2 + \frac{1}{2\rho_3}e_3^2$ be a candidate Lyapunov function for subsystem $\dot{x}_3 = \hat{p}_a x_4 g(.) - \hat{p}_b x_3 - \hat{p}_c x_2$ of (3.10). Then,

$$\dot{V}_3 = -e_1^2 - e_2^2 + e_3\left\{\begin{array}{l}\frac{\hat{p}_a C_d x_4 g(.)}{\rho_3} + \frac{b_1}{\rho_3}e_1 \\ +(\frac{b_2}{\rho_3} + \frac{\hat{w}_a}{\rho_2})e_2 + \frac{b_3}{\rho_3}e_3 - \frac{b_4}{\rho_3}\dot{x}_{1d} \\ -\frac{b_5}{\rho_3}\ddot{x}_{1d} - \frac{\dddot{x}_{1d}}{\rho_3\hat{w}_a} - \frac{\hat{p}_b\hat{w}_c}{\rho_3\hat{w}_a}\end{array}\right\} \tag{3.23}$$

Now, if we choose the following stabilizing function,

$$x_{4d}(e_1, e_2, e_3, \dot{x}_{1d}, \ddot{x}_{1d}, \dddot{x}_{1d}) = \frac{1}{\hat{p}_a C_d g(.)}\left\{\begin{array}{l}-b_1 e_1 - (b_2 + \frac{\rho_3\hat{w}_a}{\rho_2})e_2 - b_3 e_3 + b_4\dot{x}_{1d} \\ +b_5\ddot{x}_{1d} + \frac{\dddot{x}_{1d}}{\hat{w}_a} + \frac{p_b\hat{w}_c}{\hat{w}_a} - \rho_3 e_3\end{array}\right\} \tag{3.24}$$

This will yield to

$$\dot{V}_3 = -e_1^2 - e_2^2 - e_3^2 < 0 \tag{3.25}$$

At this stage, the stabilizing functions, which are the desired trajectories of all the state-variables, have been designed. Every stabilizing function depends on the tracking error of the previous states, on the desired position and its derivatives.

Final step: The final step involves the design of the closed loop control law, which is in other words the electric signal that actuates the servovalve spool to the appropriate position, according to the angular position of the hydraulic actuator.

Let, $V_4 = \frac{1}{2\rho_1}e_1^2 + \frac{1}{2\rho_2}e_2^2 + \frac{1}{2\rho_3}e_3^2 + \frac{1}{2\rho_4}e_4^2$ be a candidate Lyapunov function for subsystem $\dot{x}_4 = -r_a x_4 + r_b u$ of (3.10). Then,

$$\dot{V}_4 = -e_1^2 - e_2^2 - e_3^2 + e_4 \left\{ \begin{array}{l} \frac{r_b}{\rho_4}\left(1 - \frac{x_3 f(.)h(.)}{2\hat{p}_a C_d \rho . g(.)^3}\right)u + \frac{\hat{p}_a C_d g(.)e_3}{\rho_3} - \frac{r_a}{\rho_4}x_4 - \frac{J(.)}{\rho_4 \hat{p}_a C_d g(.)} \\ -\frac{1}{2\hat{p}_a C_d \rho_4 \rho . g(.)^3}\left(\dot{x}_3 sgm(x_4) - r_a x_3 x_4 f(.)\right)h(.) \end{array} \right\} \tag{3.26}$$

Now, if we choose the control signal u as follows,

$$u(e_1, e_2, e_3, e_4, \dot{x}_{1d}, \ddot{x}_{1d}, \dddot{x}_{1d}, x_{1d}^{(4)}) = \frac{\left[-\frac{\rho_4}{\rho_3}\hat{p}_a C_d g(.)e_3 + r_a x_4 + \frac{J(.)}{\hat{p}_a C_d g(.)} + \frac{1}{2\hat{p}_a C_d \rho . g(.)^3}\left(\dot{x}_3 sgm(x_4) - r_a x_3 x_4 f(.)\right)h(.) - \rho_4 e_4 \right]}{r_b\left(1 - \frac{x_3 f(.)h(.)}{2\hat{p}_a C_d \rho . g(.)^3}\right)} \tag{3.27}$$

This will yield to

$$\dot{V}_4 = -e_1^2 - e_2^2 - e_3^2 - e_4^2 < 0 \tag{3.28}$$

Equation (3.28) shows that the error dynamic is globally asymptotically stable, because any error signal will converge to zero.

Finally, if we rewrite the state-space equations of (3.10) in terms of the tracking errors $e_i = x_i - x_{id}$, then the errors dynamic is found to be: (refer to appendix *A3.3* for more details)

$$\begin{pmatrix} \dot{e}_1 \\ \dot{e}_2 \\ \dot{e}_3 \\ \dot{e}_4 \end{pmatrix} = \underbrace{\begin{pmatrix} -\rho_1 & 1 & 0 & 0 \\ -\frac{\rho_2}{\rho_1} & -\rho_2 & \hat{w}_a & 0 \\ 0 & -\frac{\rho_3}{\rho_2}\hat{w}_a & -\rho_3 & \hat{p}_a C_d g(.) \\ 0 & 0 & -\frac{\rho_4}{\rho_3}\hat{p}_a C_d g(.) & -\rho_4 \end{pmatrix}}_{A} \begin{pmatrix} e_1 \\ e_2 \\ e_3 \\ e_4 \end{pmatrix} \tag{3.29}$$

As we can see from (3.29) the controller parameters, as expected, appear on the diagonal of matrix *A*. Their effect, on the error convergence to zero, is obvious. Larger values of the tuning parameters yield to a faster convergence. However, very large values result often in a high amplitude saturated control signal because of the physical limitations of the system. Consequently a compromise is to be made in the tuning parameters choice (refer to appendix *A3.1*).

3.5 Experimental Results

The implementation of the block diagram in figure 3.2, was done on a SCADA system. Data are updated from the electrohydraulic system every 0.1 *ms*. The signals that are being acquired from the analog output card are the angular velocity of the actuator, the pressure P_1 at the hydraulic actuator inlet, the pressure P_2 at the hydraulic actuator outlet, and the fluid flow through the servovalve. Whereas the signals that are being sent to the analog input card are the control input signal of the servovalve and the resistive torque. Both cards have a voltage limit ranging from –17 *V* to +17 *V*, which is beyond the maximum voltage of the servovalve that ranges from –5 *V* to + 5 *V*. The desired angular position trajectory is a sine function with 2π *rad* amplitude and 2 *Hz* frequency. A low power white noise signal is added to the desired position in order to provide the signal with a wide range of frequencies without, however, perturbing the system output. This is crucial for a good identification. Figure 3.3 shows the angular position, the desired position and the tracking error.

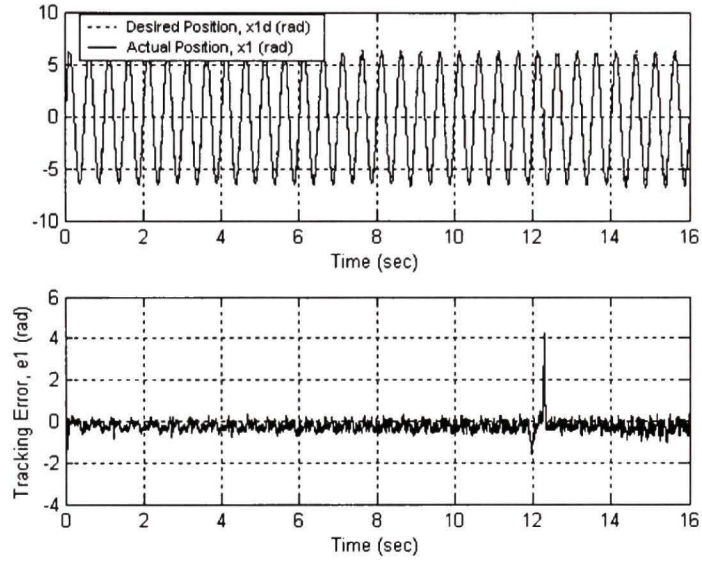

Figure 3.3 ***Angular position, desired position and tracking error, when using the indirect adaptive backstepping.***

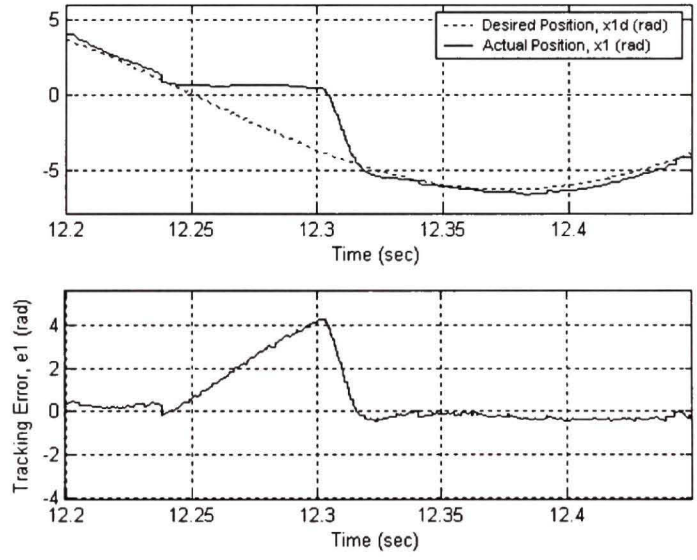

Figure 3.4 ***Zoom in of figure 3.3 during sudden load increase.***

As we can see, the adaptive controller achieves very good tracking with a maximum error of $1/10\pi$ *rad*. At instant 12.24 *sec* the load on the actuator is increased abruptly 10 times of its actual value. The effect of the perturbation is well pronounced at this moment in the tracking error of figure 3.4. However, because of the adaptive control the desired position is reached again rapidly in 0.07 *sec*.

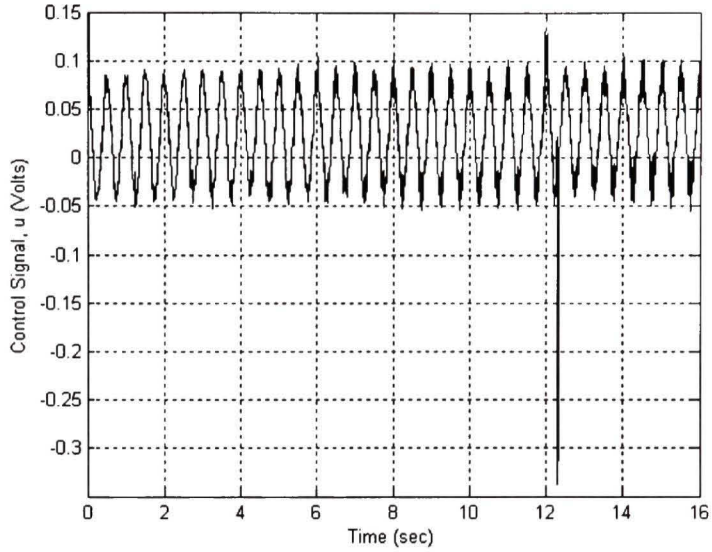

Figure 3.5 ***Control signal generated by the indirect adaptive backstepping controller.***

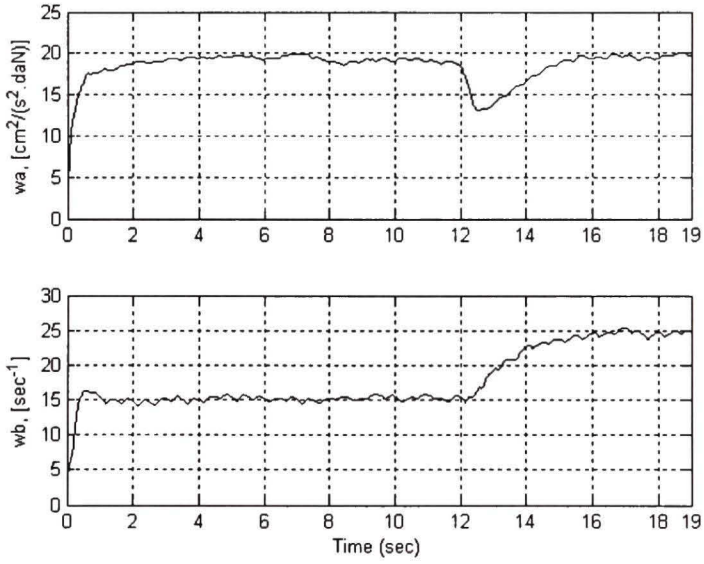

Figure 3.6 ***Parameters of the hydraulic motor (motor displacement & friction coefficient).***

On the other hand, at the same instant, we can notice in figure 3.5 the peak of voltage (-0.34 Volts), in the control signal, due to the load increase; and the ability of the adaptive controller to restore the former signal amplitude. Let us now examine the parameters identification and their behavior during the sudden load increase. Figure 3.6 illustrates the convergence of the

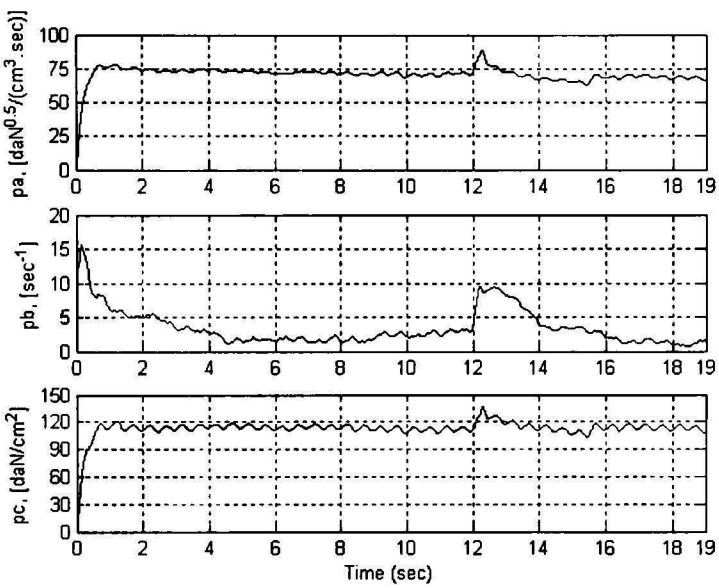

Figure 3.7 ***Hydraulic parameters (proportional to the oil bulk modulus).***

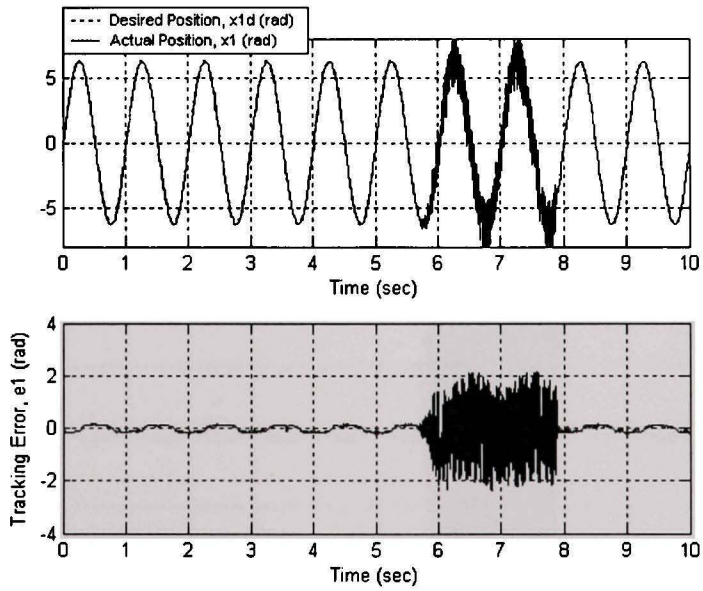

Figure 3.8 ***Angular position, desired position and tracking error when using a non-adaptive backstepping.***

hydraulic motor parameters w_a and w_b that are proportional to the motor displacement and friction coefficient respectively. It is clear that the identification process achieved a good convergence of the parameters toward their physical values. Moreover, w_a regains its value shortly after the sudden load increase; however w_b converges towards a higher value since

the friction coefficient increases with load and consequently with the system pressure. On the other side, figure 3.7 shows the hydraulic parameters that are proportional to the oil bulk modulus. The latter is known to increase with the oil pressure. In fact, at the moment where the perturbation occurs the three parameters p_a, p_b and p_c increase suddenly then converge toward a slightly different value. This is because it takes a very big pressure difference to create a significant change in the bulk modulus coefficient, while the pressure variation in our case, when setting the load to 10 times its initial value, is relatively small ~ 700 *psi*. Finally, in figures 3.8 and 3.9 the behavior of a non-adaptive backstepping controller is studied. The desired position in this case is smoother and has a frequency of 1 *Hz*. This makes the signal easier to track, which can be seen from the tracking error curve. However, although the signal is smooth, when the load on the hydraulic actuator is set to 10 times its current value (during 2 *sec*), the tracking is lost during this period and the actuator oscillates continuously being unable to regain its desired position. This is because of the control signal that turns to be almost saturated as shown in figure 3.9.

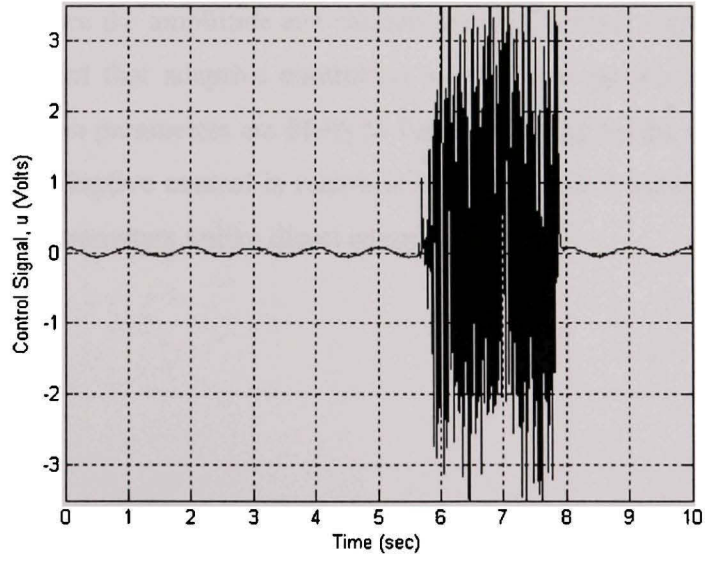

Figure 3.9 ***Control signal generated by the non-adaptive backstepping controller.***

3.6 Conclusion

In this paper, a real-time indirect adaptive backstepping controller was designed for an electrohydraulic system. It is well known that parameters in electrohydraulic systems are subjected to variations depending on the system load and pressure; especially the friction coefficient that is affected by both. For that reason, in this experiment, we chose to vary the load acting on the hydraulic actuator in order to increase the system pressure and see the variation of the system parameters especially the friction coefficient. The latter tends to increase with both pressure and load. The results were compared to those obtained with a real time non-adaptive backstepping controller, similar to the one in Kaddissi, Kenné et al. (2007). We saw that during the parameters variation, the adaptive controller was able to track the desired reference signal with a slight transient behavior after the parameters variation. On the other hand, the non-adaptive controller was unable to keep the system on track; it ended up with large oscillations and instability. Regarding the controller design, we introduced the controller tuning parameters in the Lyapunov function in such a way to obtain a triangular matrix in the errors dynamic. This is to accelerate the states convergence to their desired trajectories and to reduce the amplitude and saturation of the control signal. Finally, based on this work, it is apparent that adaptive controllers are the best option in hydraulic systems control, since the system parameters are likely to vary depending on the operating conditions. Particularly, indirect adaptive control is recommended, because it leads to the real physical values of the system parameters unlike direct adaptive control.

Appendix

Tableau A 3.1

List of the controller tuning parameters

Tuning parameters	Value	Observations
ρ_1	50	---
ρ_2	150	$\rho_2 > \rho_1$ for speed must converge faster than position
ρ_3	40	$\rho_3 < \rho_2$ to minimize the effect of w_a
ρ_4	0.001	$\rho_4 << \rho_3$ to minimize the effect of $p_a C_d g(.)$

Tableau A 3.2

List of intermediate constants and functions
used to alleviate the mathematical expressions

Constant/variable	Value	Constant/variable	Value
$A2$	$\frac{\rho_2}{\rho_1 \hat{w}_a} + \frac{(\hat{w}_b - \rho_1)\rho_1}{\hat{w}_a}$	c_2	$b_3 + \rho_3$
a_2	$\frac{\rho_1 - \hat{w}_b + \rho_2}{\hat{w}_a}$	$h(.)$	$-b_1 e_1 - c_1 e_2 - c_2 e_3 + b_4 \dot{x}_{1d} + b_5 \ddot{x}_{1d} + \frac{\dddot{x}_{1d}}{\hat{w}_a} + \frac{p_b \hat{w}_c}{\hat{w}_a}$
b_1	$\hat{p}_b a_1 + \hat{p}_c \rho_1 - a_1 \rho_1 - \frac{\rho_2}{\rho_1}$	$f(.)$	$\frac{2ae^{-ax_4}}{(1+e^{-ax_4})^2}$
b_2	$\hat{p}_b a_2 - \hat{p}_c + a_1 - \rho_2 a_2$	d_1	$b_1 \rho_1 + \frac{\rho_2 c_1}{\rho_1}$
b_3	$\hat{w}_a a_2 - p_b$	d_2	$-b_1 + c_1 \rho_2 + \frac{\rho_3 c_2 \hat{w}_a}{\rho_2}$
b_4	$\frac{\hat{p}_b \hat{w}_b}{\hat{w}_a} + \hat{p}_c$	d_3	$-c_1 \hat{w}_a + c_2 \rho_3$
b_5	$\frac{\hat{p}_b + \hat{w}_b}{\hat{w}_a}$	$J(.)$	$d_1 e_1 + d_2 e_2 + d_3 e_3 - c_2 \hat{p}_a C_d g(.) e_4 + b_4 \ddot{x}_{1d} + b_5 \dddot{x}_{1d} + \frac{x_{1d}^{(4)}}{\hat{w}_a}$

Constant/variable	Value	Constant/variable	Value
c_1	$b_2 + \frac{\rho_3 \hat{w}_a}{\rho_2}$	$g(.)$	$\sqrt{P_s - x_3.sigm(x_4)}$

A 3.3 Errors dynamic

The effect of the controller tuning parameters and the influence of the Lyapunov function choice can be seen by examining the errors dynamic of the closed loop system. The latter is found by calculating $\dot{e}_i = \dot{x}_i - \dot{x}_{id}$ and replacing x_i with $e_i + x_{id}$ for $i = 1,2,3,4$. $\dot{x}_1, \dot{x}_2, \dot{x}_3$ and $\dot{x}_4$ are found directly from the system model (3.10); whereas $\dot{x}_{1d}, \dot{x}_{2d}, \dot{x}_{3d}$ and $\dot{x}_{4d}$ are the analytical derivatives of x_{1d}, x_{2d}, x_{3d} and x_{4d} that were found in steps 1, 2, and 3 of section IV. Therefore, we have:

$$\begin{aligned} \dot{e}_1 &= \dot{x}_1 - \dot{x}_{1d} = x_2 - \dot{x}_{1d} \\ &= e_2 + x_{2d} - \dot{x}_{1d} = e_2 + (-\rho_1 e_1 + \dot{x}_{1d}) - \dot{x}_{1d} \\ &= -\rho_1 e_1 + e_2 \end{aligned} \tag{3.30}$$

$$\begin{aligned} \dot{e}_2 &= \dot{x}_2 - \dot{x}_{2d} = (\hat{w}_a x_3 - \hat{w}_b x_2 - \hat{w}_c) - (-\rho_1 \dot{e}_1 + \ddot{x}_{1d}) \\ &= -\frac{\rho_2}{\rho_1} e_1 - \rho_2 e_2 + \hat{w}_a e_3 \end{aligned} \tag{3.31}$$

$$\begin{aligned} \dot{e}_3 &= \dot{x}_3 - \dot{x}_{3d} \\ &= (\hat{p}_a x_4 g(.) - \hat{p}_b x_3 - \hat{p}_c x_2) + a_1 \dot{e}_1 + a_2 e_2 - \frac{\hat{w}_b}{\hat{w}_a} \ddot{x}_{1d} - \frac{\dddot{x}_{1d}}{\hat{w}_a} \\ &= -\frac{\rho_3}{\rho_2} \hat{w}_a e_2 - \rho_3 e_3 + \hat{p}_a C_d g(.) e_4 \end{aligned} \tag{3.32}$$

$$\begin{aligned} \dot{e}_4 &= \dot{x}_4 - \dot{x}_{4d} = (-r_a x_4 + r_b u) - \dot{x}_{4d} \\ &= -\frac{\rho_4}{\rho_3} \hat{p}_a C_d g(.) e_3 - \rho_4 e_4 \end{aligned} \tag{3.33}$$

References

Astrom, K. J. and B. Wittenmark (1989). Adaptive Control. Addison-Wesley, United States.

Chen, H.-M., J.-C. Renn, and J.-P. Su (2005). "Sliding mode control with varying boundary layers for an electro-hydraulic position servo system." International Journal of Advanced Manufacturing Technology 26(1-2): 117-123.

Fink, A. and T. Singh (1998). Discrete sliding mode controller for pressure control with an electrohydraulic servovalve. Proceedings of the 1998 IEEE International Conference on Control Applocations. Part 1 (of 2), Sep 1-4 1998, Trieste, Italy, IEEE, Piscataway, NJ, USA.

Habibi, S. and A. Goldenberg (2000). "Design of a new high-performance electrohydraulic actuator." Mechatronics, IEEE/ASME Transactions on 5(2): 158-164.

Hahn, H., A. Piepenbrink, and K.-D. Leimbach, (1994). Input/output linearization control of an electro servo-hydraulic actuator. Proceedings of the 1994 IEEE Conference on Control Applications. Part 2 (of 3), Aug 24-26 1994, Glasgow, UK, IEEE, Piscataway, NJ, USA.

Kaddissi, C., J.-P. Kenné, and M. Saad. (2005). Drive by wire control of an electro-hydraulic active suspension a backstepping approach. Control Applications, 2005. CCA 2005. Proceedings of IEEE Conference on.

Kaddissi, C., J.-P. Kenné, and M. Saad (2007). "Identification and Real-Time Control of an Electrohydraulic Servo System Based on Nonlinear Backstepping." Mechatronics, IEEE/ASME Transactions on 12(1): 12-22.

Kandil, N., S. LeQuoc, and M. Saad (1999). On-line Trained Neural Controllers for Nonlinear Hydraulic System. 14th World Congress of IFAC, pp.323-328.

Khoshzaban Zavarehi, M., P. D. Lawrence, and F. Sassani (1999). "Nonlinear modeling and validation of solenoid-controlled pilot-operated servovalves." Mechatronics, IEEE/ASME Transactions on 4(3): 324-334.

LeQuoc, S., R. M. H. Cheng, and K.H. Leung, (1990). "Tuning an electrohydraulic servovalve to obtain a high amplitude ratio and a low resonance peak." Journal of Fluid Control 20(3): 30-49.

Li, P. Y. (2001). Dynamic redesign of a flow control servo-valve using a pressure control pilot. 2001 ASME International Mechanical Engineering Congress and Exposition, Nov 11-16 2001, New York, NY, United States, American Society of Mechanical Engineers.

Lim, T. J. (1997). Pole placement control of an electro-hydraulic servo motor. Proceedings of the 1997 2nd International Conference on Power Electronics and Drive Systems, PEDS. Part 1 (of 2), May 26-29 1997, Singapore, Singapore, IEEE, Piscataway, NJ, USA.

Lin, J.-S. and I. Kanellakopoulos (1997). "Nonlinear design of active suspensions." IEEE Control Systems Magazine 17(3): 45-59.

Merrit, H. E. (1967). Hydraulic Control Systems, New York, N.Y.: J. Wiely and sons.

Ursu, I. and F. Ursu (2004). "New results in control synthesis for electrohydraulic servos." International Journal of Fluid Power 5(3): 25-38.

Yongqian, Z., S. LeQuoc, and M. Saad (1998). Nonlinear fuzzy control on a hydraulic servo system. American Control Conference. Proceeding of the.

Yu, W.-S. and T.-S. Kuo (1996). "Robust indirect adaptive control of the electrohydraulic velocity control systems." IEE Proceedings: Control Theory and Applications 143(5): 448-454.

Yu, W.-S. and T.-S. Kuo (1997). "Continuous-time indirect adaptive control of the electrohydraulic servo systems." IEEE Transactions on Control Systems Technology 5(2): 163-177.

Zeng, W. and J. Hu (1999). "Application of intelligent PDF control algorithm to an electrohydraulic position servo system." Proceedings of the 1999 IEEE/ASME

International Conference on Advanced Intelligent Mechatronics (AIM '99), Sep 19-Sep 23 1999: 233-238 BN - 0-7803-5038-3.

INTRODUCTION À LA SUSPENSION ACTIVE ÉLECTROHYDRAULIQUE

Au cours du chapitre précédent (2ème article), l'étude du contrôle adaptif indirect d'un système électrohydraulique a été faite en se basant sur la technique du backstepping, déjà employée au premier chapitre. En effet, étant donné que les paramètres d'un système électrohydraulique sont sujets à des variations qui dépendent de la charge entraînée par le moteur hydraulique ainsi que de la pression résultante; le backstepping adaptatif indirect était un choix incontestable :

- Il permet d'avoir une poursuite de trajectoire robuste et précise;
- Il permet de maintenir cette précision même pendant la variation des paramètres du système, en adaptant le contrôleur à cette variation;
- Il permet l'identification et la convergence des paramètres du système vers leurs valeurs réelles.

Les 3 points précédents qui étaient confirmés par les tests expérimentaux n'ont pas pu être achevés avec le backstepping non-adaptatif, du deuxième chapitre, qui ne supporte pas les variations des paramètres du système. En présence de telles variations les résultats sont inacceptables.

Maintenant que le backstepping appliqué à un système électrohydraulique générique est étudié, analysé et optimisé avec ses différents aspects, il est nécessaire de l'employer dans une application particulière afin de percevoir l'étendue et l'utilité de cette approche dans l'industrie. En effet, le chapitre suivant (3ème article) traite la commande nonlinéaire d'une suspension active électrohydraulique. Cette technologie récente constitue un des sujets de recherche les plus actifs de l'industrie automobile. Dans cette étude, le backstepping à lui seul s'avère insuffisant pour achever la commande du système. L'idée principale porte sur le jumelage du backstepping avec une autre stratégie du même type (basée sur Lyapunov) qui est le forwarding. En fait, la dynamique de la suspension vient augmenter l'ordre et changer la structure du modèle mathématique par rapport à celui du système électrohydraulique seul. Ainsi, le backstepping sera utilisé pour commander une partie du système alors que le forwarding sera utilisé pour en commander l'autre.

CHAPITRE 4

INTERLACED BACKSTEPPING AND INTEGRATOR FORWARDING FOR NONLINEAR CONTROL OF AN ELECTROHYDRAULIC ACTIVE SUSPENSION

Claude Kaddissi, Jean-Pierre Kenné, and Maarouf Saad
École de Technologie Supérieure, 1100 Notre-Dame West street, Quebec H3C 1K3, Canada
Email: jean-pierre.kenne@etsmtl.ca

Abstract

Passengers' comfort in long road trips is of crucial importance; as a result, active suspension control became a vital subject in recent researches. This paper studies the control of an electrohydraulic active suspension, based on a combination of backstepping and integrator forwarding. Our goal is to control and reduce the car vertical motion and keep it to zero. The active suspension model is highly nonlinear and non-differentiable due to the hydraulic components, especially the servovalve and the hydraulic actuator which chambers volume varies during extension and retraction. Therefore, a powerful control strategy is required. In such cases, Lyapunov based control strategies are the most suitable, for offering a lot of maneuverability in building an analytical control signal. The mathematical model of an electrohydraulic active suspension can be classified among interlaced systems. This means that the state space model is a sequence of feedback and feedforward equations. Therefore, interlaced backstepping and integrator forwarding is an optimal control strategy to stabilize this class of systems, particularly electrohydraulic active suspension. Afterward, we will introduce and define this constructive control method and its basis. The foremost advantage carried on by this interlaced strategy is that it leaves no internal dynamic, as is the case of others. This is a great relief in control issues, since an unstable internal dynamic will destabilize the whole system whatever control method is being used. As it will be demonstrated, the interlaced backstepping and integrator forwarding is an outstanding control strategy to compensate the effect of chaotic roads on cars stability. The results are compared with a classic Proportional-Integral-Derivative regulator (PID) and a sliding mode controller,

to show that the proposed controller outperform a range of other existing ones for a range of perturbation signals.

Index Terms — Backstepping, Integrator Forwarding, Nonlinear control, Electrohydraulic Active suspension.

4.1 Introduction

Active suspension control is a very dynamic field in recent researches. This is because of the competence among car manufacturers to increase cars handling and to offer the best comfort to passengers. When designing a car suspension, there are two main objectives to be reached: On one hand, improve the car behavior in hard driving conditions and minimize the vertical motion of the car body, due to road imperfections, on the other. This consequently means reducing the force that is transmitted, through the suspension to the passengers. Electrohydraulic actuators are typically chosen for suspension control, this is because they are more powerful and less bulky as compared to D.C and A.C actuators. Moreover, they can grant the skyhook damping effect as explained by Yoshimura et al. (1997), which is the ideal design of a suspension. The only drawback of electrohydraulic systems is their nonlinear behavior. The latter is amplified when linear actuators are used and not motors. In fact, the volume of the inlet and outlet chambers is not constant because a linear actuator is not symmetric. However, the availability of the hydraulic components in all vehicles, such as the supply pump, the oil tank, the fluid hoses, is an ultimate reason which supports their use in active suspensions. There are several designs for the mathematical model and for the control strategy as well. In classic control, pole location was used by Leite and Peres (2002), where the actuator dynamic were neglected. In robust control, H_2 and H_∞ or a combination of both gave very satisfactory results with Abdellahi et al. (2000); except for the fact that these strategies deal with linear models, while at high frequencies some unmodeled nonlinearities could rise up. LPV based control is pretty powerful for nonlinear control systems. Gaspar et al. (2002) and Fialho and Balas (2002) applied it for active suspension control and obtained satisfactory results for a linearized model. On the other hand, singular perturbation method

with an LQG controller was adopted by Ando and Suzuki (1996), but here again the actuator dynamic was neglected hence reducing the control efficiency. Within nonlinear control strategies, a sliding mode controller was used by Sam et al. (2003) and compared with an LQG regulator. Noticeably, the sliding mode controller gave better results than the LQG one; however there was chattering involved by the switching control signal which would damage the hydraulic components. Another nonlinear controller that can be encountered, is the one based on the backstepping as Sirouspour and Salcudean (2000), where the controller gave very good results. Conversely when it was used in its direct adaptive form there was a steady error due to the velocity estimator. However, indirect adaptive backstepping used by Kaddissi et al. (2006), gave better results than the direct adaptive approach because it ensures the parameters convergence to their real physical values and not to some local optimum values. On the other hand, one should be aware that backstepping is used only with systems which mathematical model is in a feedback or low triangular form. It will be shown later that the mathematical model of an electrohydraulic active suspension is a concatenation of a feedback subsystem (lower triangular form) and a feedforward subsystem (upper triangular form), or simply, interlaced. Therefore, backstepping can be applied only to some part of the active suspension model and one should verify that the remaining part, which is called the internal dynamic of the system, is naturally stable. Lin and Kanellakopoulos (1997), used the backstepping for the control of an electrohydraulic active suspension., but the choice of the vertical motion of the car body as the control variable led to an unstable internal dynamic or better known as zero dynamic. This is why suspension travel had been chosen as the control variable to ensure stability.

This paper is an extension to our previous works (Kaddissi et al. 2007) and (2005). In the latter the control of an electrohydraulic active suspension was studied; it was based on the backstepping control strategy. The main focus in that work was to ensure a stable zero dynamic regardless of the control variable choice. This was achievable by adding some damping term to the tire model instead of being modeled only as a spring, which is the case of Lin and Kanellakopoulos (1997) where the tire was modeled as a set of springs in series. Physically, this is very reasonable, since the spring stands for the air in the tire and the

damper stands for the rubber material of which it is made. In this paper, figure 4.1 describes briefly the problem: x_r is the road perturbation and x_s is the vertical displacement of the car body that is transmitted to the passengers. The aim is to minimize the effect of x_r on x_s, to increase passengers' comfort and car handling. The latter is realized by establishing a control law that is consistent and that includes the dynamic of the whole system. This is achieved by combining the backstepping, described by Krstic et al. (1995) and the integrator forwarding described by Sepulchre et al. (1997). These constructive nonlinear control methods are extremely powerful and advantageous, because of the flexibility they offer in building a control signal based on the system dynamics, without canceling useful nonlinearities, as explained by Sepulchre et al. (1997). As it will be proved, this approach ensures ultimately bounded stability of the system and generates low amplitude, smooth control signal.

The rest of the paper is organized as follow: The motivation for this work is presented in section 2. In section 3, the mathematical model of the electrohydraulic active suspension is established and the class of interlaced systems is defined. In section 4, the constructive nonlinear control method based on backstepping and integrator forwarding is built up. Section 5 shows the simulation results and the effectiveness of the proposed approach in terms of minimizing and rejecting road perturbations and their effect on the car passengers. The results are compared with those obtained by a classic PID controller and those of a sliding mode controller, for a deterministic and a stochastic perturbation. While it might seem unfair to compare a nonlinear controller with a PID controller, we do make it, however, because the PID is the most popular and widespread controller used in industry. We therefore held it as a reference for the sake of comparison. Finally, section 6 contains some remarks and conclusions that bring this work to a close.

4.2 Motivation

The main issue is that, when it comes to passengers' comfort and cars handling, compromise and comfort must always be traded against other factors, such as performance. That is the reason why our prior works focused on enhancing active suspension control.

Previously, the emphasis was to improve the mathematical model by taking into account all the nonlinearities of the system on one hand, and choosing the most appropriate control strategy on the other. The latter topic is more critical. The choice of the backstepping as an optimal control strategy by Kaddissi et al. (2005) was based, in addition to what was mentioned in the introduction, on the fact that it relaxes the 'matching conditions', as explained through Khalil (2002), which are not respected in the active suspension model. This means that the perturbation signal or the uncertainties in the system model are not restricted to be in the state equation that contains the input of the system, as other control strategies require. Moreover, the ensuing control signal is analytical and free of derivatives, which reduces numerical errors and lightens the computations. In the current work, the goal is to have a closed loop dynamic which order is the same as the open loop system; in other words, the internal dynamic is absent. After analyzing the mathematical model of the electrohydraulic active suspension, it was clear that the internal dynamic results from its feedforward subsystem. With some necessary change of variables, the system can be rewritten in an interlaced form that is well defined through Sepulchre and Kokotovic (1997) and briefly elucidated in section 3. An archetypal characteristic of interlaced systems is that they are stabilized by sequences of backstepping and integrator forwarding. The main interest dwells in the fact that integrator forwarding was seldom tested on real physical systems; since most of physical systems have a feedback structure and those which have a feedforward structure are very rare. One can find in Kristic (2004) very good examples of stabilization studies for feedforward and interlaced systems, using integrator forwarding and backstepping; especially algorithms to reduce the calculations load. However, the examples refer to no physical systems and are purely mathematical. The present work constitutes an excellent opening to test the effectiveness of those approaches on a physical electrohydraulic active suspension.

In a first step, the next section elaborates the mathematical model of an electrohydraulic active suspension and defines the class of interlaced systems and shows the modifications brought to the active suspension model to fit in this category, in a further step.

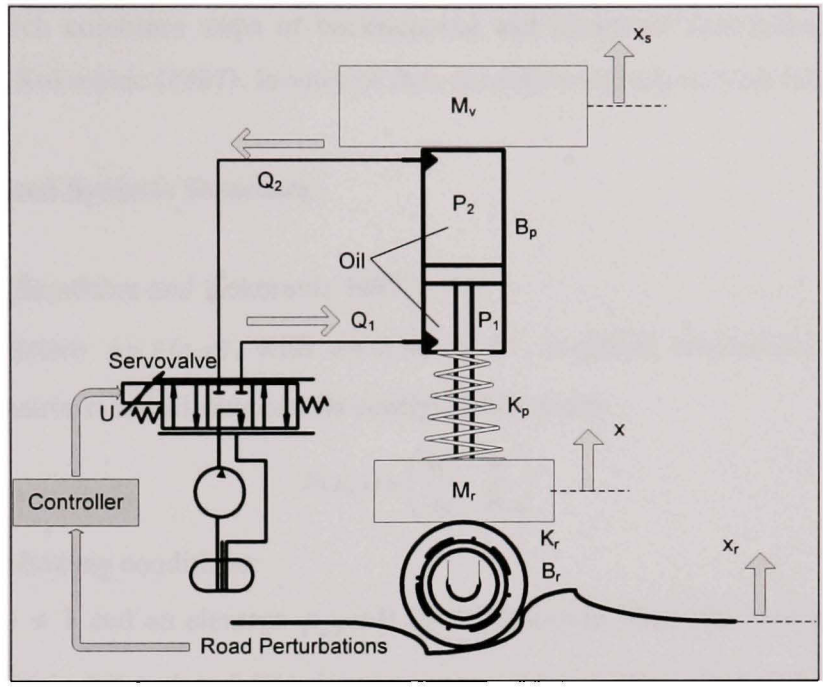

Figure 4.1 ***Quarter-car electrohydraulic active suspension.***

4.3 Interlaced Systems and System Modeling

Figure 4.1 shows an electrohydraulic active suspension of a quarter-car model. The suspension is composed of the hydraulic system that plays the active part of it, while the spring-damper system constitutes the classic passive suspension. The closed loop system works as follow: A sensor measures the tire vertical movement; the measured signal is transmitted to the controller. The latter, based on the control strategy that is being used, generates a control signal. The control signal is sent to the solenoid that controls the position of the servovalve spool. This will adjust the amount of oil flow to be sent to the actuator and consequently control the vertical motion, speed and acceleration of the car body. The actual controller is based on successions of backstepping and integrator forwarding steps. Therefore, to be able to control the electrohydraulic active suspension, its mathematical model must satisfy the conditions of an interlaced system. In fact, interlaced systems constitute a class of systems only characterized by their configuration matrix and a local stabilizability condition. All these systems are globally stabilizable by a recursive design

procedure, which combines steps of backstepping and integrator forwarding according to Sepulchre and Kokotovic (1997). In view of that, the following sub-section follows.

4.3.1 Interlaced Systems Structure

Definition 1: (Sepulchre and Kokotovic 1997)

A nonlinear system $\dot{x} = f(x,u)$, with $u \in R$, et $x \in R^n$, is called interlaced, if its Jacobian linearization matrix is stabilizable and its configuration matrix,

$$P(x,u) = \left(\frac{\partial f}{\partial x} \quad \frac{\partial f}{\partial u} \right) \tag{4.1}$$

Satisfies the following conditions:

- If $j > i + 1$ and an element $p_{i,j} \neq 0$ of the P matrix, then the element $p_{k,l} \equiv 0$ for every $k \geq l$, $k \leq j-1$ and $l \leq i$. (necessary condition to apply integrator forwarding);
- If an element $p_{i,j} \neq 0$ of the P matrix for some $j \leq i$, then $p_{i,i+1}$ is independent of the state variable x_{i+1} and $p_{i,i+1}(x) \neq 0$, for all x. (necessary condition to apply backstepping)

In the next sub-sections, we will develop the mathematical model of the electrohydraulic active suspension and test out if it verifies the previous definition.

4.3.2 Active Suspension Modeling

Figure 4.1 shows an electrohydraulic active suspension of a quarter-car model. The suspension is composed of the hydraulic system that plays the active part of it; while the spring-damper system constitutes the classic passive suspension.

Concerning the car dynamic, the mathematical model is classic and is obtained with Newton's second law. On the other hand, the hydraulic system model is obtained by applying the compressibility equations and using the servovalve dynamic. The electric control signal, generated by the designed controller actuates the servovalve spool to the right position

depending on the road perturbations. This in turn determines the action the actuator has to take in order to drive the vertical motion of the car body to zero.

4.3.3 Electrohydraulic System Model

The servovalve used in this application, is a double stage one with matched and symmetric orifices. Its dynamic equation, referring to LeQuoc et al. (1990), is be given by:

$$\tau_v \dot{A}_v + A_v = Ku \tag{4.2}$$

Where u is the control input, K is the servovalve constant, τ_v is its time constant and A_v is the orifice opening area. The flow rate from and to the servovalve, through the valve orifices, assuming small leakage, is given as:

$$Q_1 = Q_2 = C_d A_v \sqrt{\frac{P_S - P_L}{\rho}} \tag{4.3}$$

Where, P_L is the differential of pressure due to load, $P_L = P_1 - P_2$ in the positive direction of motion and $P_L = P_2 - P_1$ in the negative direction of motion. Finally, $P_S = P_1 + P_2$ is the source pressure, C_d is the flow discharge coefficient and ρ is the fluid oil density.

Since oil compressibility varies with pressure, it should be considered in the actuator dynamic along with oil leakage. Thus we give the compressibility equation:

$$\dot{P}_L = \frac{2V_0\beta}{V_0^2 - A^2(x_s - x)^2}\left[C_d A_v \sqrt{\frac{P_s - P_L.sigm(A_v)}{\rho}} - LP_L - A(\dot{x}_s - \dot{x})\right] \tag{4.4}$$

V_0 is the oil volume in one chamber of the actuator when the piston is at the center position. $V_0 - A(x_s - x)$ is the volume of the actuator chamber at every piston position. L is the flow leakage coefficient, β is the oil bulk modulus.

Note that in equation (4.3), as in Kaddissi et al. (2004), the sigmoid function '$sigm(A_v)$' is an approximation of the non-differentiable sign function '$sign(Av)$' that stands for the changing of the flow direction. The sigmoid function has the following properties:

$$sigm(A_v) = \frac{1 - e^{-aA_v}}{1 + e^{-aA_v}}; \quad a > 0 \tag{4.5}$$

This is a continuously differentiable function with

$$sigm(x) = \begin{cases} 1 \ if \ \ ax \to \infty \\ 0 \ if \ \ ax \to 0 \\ -1 \ if \ \ ax \to -\infty \end{cases} \tag{4.6}$$

and,

$$\frac{dsigm(x)}{dx} = \frac{2ae^{-ax}}{(1+e^{-ax})^2} \tag{4.7}$$

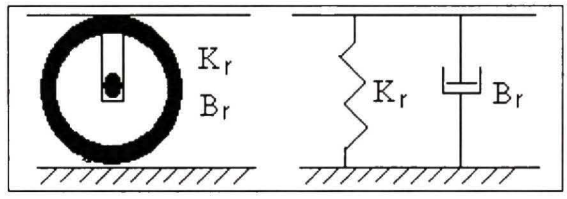

Figure 4.2 ***Tire modeling.***

Now, considering the hydraulic actuator equation of motion given by Newton's second law and referring to figures 3.1 and 3.2, we can write (refer to *Appendix A.3.1* for parameters definition):

$$\begin{aligned} \dot{x} = & \frac{K_p}{M_r}(x_s - x) + \frac{B_p}{M_r}(\dot{x}_s - \dot{x}) - \frac{K_r}{M_r}(x - x_r) \\ & - \frac{B_r}{M_r}(\dot{x} - \dot{x}_r) - \frac{A}{M_r}P_L \end{aligned} \tag{4.8}$$

4.3.4 Car Body Dynamic

The vertical acceleration of the car body is given by the following equation based on Newton's second law (refer to *Appendix A.3.1* for parameters definition):

$$\dot{x}_s = -\frac{K_p}{M_v}(x_s - x) - \frac{B_p}{M_v}(\dot{x}_s - \dot{x}) + \frac{A}{M_v}P_L \tag{4.9}$$

Note that the road fluctuation x_r, is considered as an external unknown perturbation.

4.3.5 Active Suspension Model

Finally, if we set

- $x_1 = x_s$: Vertical position of the car body, *m*
- $x_2 = \dot{x}_1$: Vertical speed of the car body, *m/s*
- $x_3 = x$: Vertical position of the car wheel, *m*
- $x_4 = \dot{x}_3$: Vertical speed of the car wheel, *m/s*
- $x_5 = P_L = P_1 - P_2$: Pressure differential of the hydraulic, *Pa*
- $x_6 = A_v$: Area of the servovalve orifice opening, m^2
- $u =$ Electric control signal, *Volts*

Then the previous six state variables define the electrohydraulic active suspension and the system can be described with a 6th order nonlinear state space model as follow:

$$\left.\begin{aligned}\dot{x}_1 &= x_2\\ \dot{x}_2 &= -a_0(x_1 - x_3) - b_0(x_2 - x_4) + a_1 x_5\end{aligned}\right\} \quad (4.10a)$$

$$\left.\begin{aligned}\dot{x}_3 &= x_4\\ \dot{x}_4 &= d_0(x_1 - x_3) + d_1(x_2 - x_4) - h_1(x_3 - x_r) - b_1(x_4 - \dot{x}_r) - c_1 x_5\\ \dot{x}_5 &= \frac{J_1}{f(.)}\left(C_d x_6 g(.) + A(x_4 - x_2) - L x_5\right)\\ \dot{x}_6 &= -\frac{1}{\tau}x_6 + \frac{k_v}{\tau}u\end{aligned}\right\} \quad (4.10b) \qquad (4.10)$$

Subsystem (4.10a) represents the dynamic of the car body and subsystem (4.10b) represents the electrohydraulic active suspension. Where, a_0, a_1, b_0, b_1, c_1, d_0, d_1, h_1, J_1, are appropriate constants given by:

$$\begin{aligned}&a_0 = \frac{K_p}{M_v},\ a_1 = \frac{A}{M_v}, b_0 = \frac{B_p}{M_v},\ b_1 = \frac{B_r}{M_r},\\ &c_1 = \frac{A}{M_r},\ d_0 = \frac{K_p}{M_r}, d_1 = \frac{B_p}{M_r}, h_1 = \frac{K_t}{M_u},\\ &J_1 = 2V_0\beta\end{aligned} \qquad (4.11)$$

And, $f(x_1, x_3), g(x_5, x_6)$, are appropriate functions given by:

$$f(x_1, x_3) = V_0^2 - A^2(x_3 - x_1)^2$$
$$g(x_5, x_6) = \sqrt{\frac{P_s - sigm(x_6)x_5}{\rho}} \tag{4.12}$$

It is obvious from the mathematical model in (4.10) and the defined functions in (4.12) that the active suspension model is highly nonlinear. This is why classic controllers fail to reach the desired objective, which is to minimize the vertical motion of the car body. In addition, they don't ensure global stability of the closed loop system. In the following section, the nonlinear proposed approach that is based on sequences of backstepping and integrator forwarding is employed to generate the control signal and simulation results will show its efficiency.

4.3.6 Verification of Definition 1 for Interlaced Systems

Let us check if the system model in (4.10) verifies definition 1 of sub-section 4.3.1.

- Firstly, the Jacobian linearization Matrix, J, of the non-perturbed system (4.10) can be easily calculated considering (x_1 = 0, x_2 = 0, x_3 = 0, x_4 = 0, x_5 = 0, x_6 = 0) as the equilibrium point:

$$J = \begin{pmatrix} 0 & 1 & 0 & 0 & 0 & 0 \\ -a_0 & -b_0 & a_0 & b_0 & a_1 & 0 \\ 0 & 0 & 0 & 1 & 0 & 0 \\ d_0 & d_1 & -d_0 - h_1 & -d_1 - b_1 & -c_1 & 0 \\ 0 & -\frac{J_1 A}{V_0^2} & 0 & \frac{J_1 A}{V_0^2} & -\frac{J_1 L}{V_0^2} & \frac{J_1 C_d}{V_0^2}\sqrt{\frac{P_s}{\rho}} \\ 0 & 0 & 0 & 0 & 0 & -\frac{1}{\tau} \end{pmatrix} \tag{4.13}$$

It is easy to verify that the eigenvalues of matrix J have negative real part, after replacing the constants with their values from Appendices *A3.1* and *A3.2*. This implies that the non-perturbed system is stable and the Jacobian linearization matrix of (4.10) is stabilizable.

- Secondly, we should calculate the configuration matrix P of the nonlinear system (4.10). It can be easily found that:

$$P=\begin{pmatrix} 0 & 1 & 0 & 0 & 0 & 0 & 0 \\ -a_0 & -b_0 & a_0 & b_0 & a_1 & 0 & 0 \\ 0 & 0 & 0 & 1 & 0 & 0 & 0 \\ d_0 & d_1 & -(d_0+h_1) & -(d_1+b_1) & -c_1 & 0 & 0 \\ \alpha & -\dfrac{J_1A}{f(.)} & \beta & \dfrac{J_1A}{f(.)} & \gamma & \dfrac{C_dJ_1g(.)}{f(.)} & 0 \\ 0 & 0 & 0 & 0 & 0 & -\dfrac{1}{\tau} & \dfrac{K_v}{\tau} \end{pmatrix} \tag{4.14}$$

With,

$$\alpha=\frac{2A^2J_1}{f(.)^2}\left(C_dg(.)x_6+A(x_4-x_2)-Lx_5\right)(x_1-x_3)$$

$$\beta=-\frac{2A^2J_1}{f(.)^2}\left(C_dg(.)x_6+A(x_4-x_2)-Lx_5\right)(x_1-x_3)$$

$$\gamma=\begin{cases}\dfrac{J_1}{f(.)}\left(-\dfrac{C_dx_6}{2\rho g(.)}-L\right) & \text{if } sign(x_6)>0 \\ \dfrac{J_1}{f(.)}\left(\dfrac{C_dx_6}{2\rho g(.)}-L\right) & \text{if } sign(x_6)<0\end{cases} \tag{4.15}$$

It is easy to notice that P does not verify condition I of definition 1. In fact, since $p_{2,4}=b_0\neq 0$ and $p_{2,5}=a_1\neq 0$, then we should have $p_{2,1}=0$, $p_{2,2}=0$, $p_{4,1}=0$ and $p_{4,2}=0$ which is not the case, because $p_{2,1}=-a_0\neq 0$, $p_{2,2}=-b_0\neq 0$, $p_{4,1}=d_0\neq 0$ and $p_{4,2}=d_1\neq 0$. The consequence of this conclusion is that when applying the integrator forwarding some state variables will be cancelled, while building the control law, before being stabilized. In other words, it is the equivalent of simplifying a zero and an unstable pole, from the transfer function of a linear system, before stabilizing the pole. The system will look stable mathematically because the unstable pole was simplified, however, it still exist. Consequently, the system doesn't belong to any of the classes studied by Kristic (2004), thus, we are unable to control it with sequences of backstepping and integrator forwarding. To remedy the problem, we propose the following change of variables:

$$\begin{aligned} &y_1=x_1;\ y_2=x_2;\ y_3=x_1-x_3=y_1-x_3;\ y_r=x_3-x_r \\ &y_4=x_2-x_4=y_2-x_4;\ y_5=x_5;\ y_6=x_6; \end{aligned} \tag{4.16}$$

Using this change of variables, the system model turns out to be,

$$\left.\begin{aligned}
\dot{y}_1 &= y_2 \\
\dot{y}_2 &= -a_0 y_3 - b_0 y_4 + a_1 y_5 \\
\dot{y}_3 &= y_4 \\
\dot{y}_4 &= -A_1 y_3 - A_2 y_4 + A_3 y_5 + h_1 y_r + b_1 \dot{y}_r \\
\dot{y}_5 &= \frac{J_1}{f(.)}\left(-A y_4 - L y_5 + C_d g(.) y_6\right) \\
\dot{y}_6 &= -\frac{1}{\tau} y_6 + \frac{k_v}{\tau} u
\end{aligned}\right\} \tag{4.17}$$

With,

$$\left.\begin{aligned}
A_1 &= a_0 + d_0 \\
A_2 &= b_0 + d_1 \\
A_3 &= a_1 + c_1
\end{aligned}\right\} \tag{4.18}$$

It is obvious that the Jacobian matrix is stabilizable, since the system dynamic is the same. Now, if we calculate the configuration matrix P_1 of system (4.17), we find:

$$P_1 = \begin{pmatrix}
0 & 1 & 0 & 0 & 0 & 0 & 0 \\
0 & 0 & -a_0 & -b_0 & a_1 & 0 & 0 \\
0 & 0 & 0 & 1 & 0 & 0 & 0 \\
0 & 0 & -a_0 + d_0 & -b_0 + d_1 & a_1 + c_1 & 0 & 0 \\
0 & 0 & \delta & -\frac{J_1 A}{f(.)} & \theta & \frac{C_d J_1 g(.)}{f(.)} & 0 \\
0 & 0 & 0 & 0 & 0 & -\frac{1}{\tau} & \frac{K_v}{\tau}
\end{pmatrix} \tag{4.19}$$

With,

$$\delta = \frac{2A^2 J_1}{f(.)^2}\left(C_d g(.) y_6 - A y_4 - L y_5\right) y_3$$

$$\theta = \begin{cases}
\dfrac{J_1}{f(.)}\left(-\dfrac{C_d y_6}{2\rho g(.)} - L\right) & \text{if } sign(y_6) > 0 \\
\dfrac{J_1}{f(.)}\left(\dfrac{C_d y_6}{2\rho g(.)} - L\right) & \text{if } sign(y_6) < 0
\end{cases} \tag{4.20}$$

Now, it is obvious that the configuration matrix P_1, verifies the conditions of the interlaced systems definition in sub-section 4.3.1. Thus, the new mathematical model structure (4.17), of the electrohydraulic active suspension, can be stabilized using sequences of backstepping and integrator forwarding.

4.4 Controller Design Based on Backstepping and Integrator Forwarding

In this section, the controller is designed based on sequences of backstepping and integrator forwarding as by Kristic (2004). A complete list of the intermediate variables and functions used to alleviate the expressions of the active suspension open and the closed loop model is given in Appendices *A3.3*, *A3.4*, *A3.5*. A detailed description, of the controller design and the proof of the following proposition, is given in Appendix *A3.6* as well. The choice of the control strategy is based on the following assessment: The subsystems of (4.17) that have a feedback structure are controlled using nonlinear backstepping and the subsystems that have a feedforward structure are controlled using integrator forwarding. Note, that according to the variables change in (4.16), y_r is currently the unknown perturbation, which is the relative motion between the tire and the road shape. Let us consider the following nonlinear model of the electrohydraulic active suspension (4.17), and define the following variables change:

$$\xi_1 = y_1 + \int_0^{\infty} (\xi_2 - A_9\xi_3 - A_{10}\xi_4)dt \tag{4.21}$$

$$\xi_2 = y_2 + \int_0^{\infty} (A_7\xi_3 - A_8\xi_4)dt \tag{4.22}$$

$$e_i = y_i - y_{id} \text{ , for } i = 3, 4, 5 \text{ and } 6 \tag{4.23}$$

$$Y_r = h_1 y_r + b_1 \dot{y}_r \tag{4.23'}$$

- ξ_i is a variable defined such that its counterpart is its initial value when no input is applied and when $y_r = 0$. (For instance, y_1 is the initial value of ξ_1 when $u = 0$ and $y_r = 0$, otherwise, ξ_1 does not exist, refer to Appendix *A3.6* for detailed explanation).
- z_i is the value of ξ_i when an input or a perturbation acts on the system, for $i = 1$ and 2. (For instance, z_1 is the value of ξ_1 when $u \neq 0$ and $y_r \neq 0$).
- y_{id} is the desired value of the state variable y_i, for $i = 3, 4, 5, 6$.

4.4.1 Proposition

- If there exist two stabilizing functions,

$$\begin{aligned} v_1 &= \Delta(z_1, z_2, e_4) \\ v_2 &= \Phi(z_1, z_2, e_4) \end{aligned} \tag{4.24}$$

Where Δ and Φ are functions designed using the integrator forwarding to stabilize y_1 and y_2 respectively. And,

- If there exist three stabilizing functions,

$$\begin{aligned} y_{4d} &= \Lambda(e_3) \\ y_{5d} &= \Theta(z_1, z_2, e_3, e_4) + v_2 + v_1 \\ Y_{6d} &= \Psi(z_1, z_2, e_3, e_4, e_5) \end{aligned} \tag{4.25}$$

Where Λ, Θ and Ψ are functions designed using the backstepping to stabilize y_3, y_4 and y_5 respectively. And,

- If there exist a bounded perturbation Y_r, with boundaries defined in (4.44), (4.58), (4.70), (4.77) and (4.86)

- Finally, knowing that $y_{3d} = 0$ since it represents the suspension travel and the goal is to keep it to zero.

Then, two options exist :

- Choosing the following positive definite Lyapunov function

$$V_6 = \frac{1}{2}z_1^2 + \frac{1}{2}z_2^2 + \frac{1}{2}e_3^2 + \frac{1}{2}e_4^2 + \frac{1}{2}e_5^2 + \frac{1}{2}e_6^2 \tag{4.26}$$

- Choosing the control input u as (refer to the final step of Appendix *A3.6*)

$$u = \Upsilon(z_1, z_2, e_3, e_4, e_5, e_6) \tag{4.27}$$

Where Υ is a function designed to stabilize the whole system (4.17). This will guarantee an ultimately bounded stability of the controlled system, since we will have,

$$\dot{V}_6 \begin{cases} < 0, & \forall \{z_1, z_2, e_3, e_4, e_5, e_6\} \neq 0 \\ = 0 & \text{for } z_1 = z_2 = e_3 = e_4 = e_5 = e_6 = 0 \end{cases} \tag{4.28}$$

In fact, if we rewrite the state space equations of system (4.17) in terms of the new variables, we will have the closed loop dynamic of the system, (refer to Appendix *A3.6*)

$$\left.\begin{aligned}
\dot{z}_1 &= -\frac{k_1}{k_2^2 A_{11}^2} z_1 - \frac{k_1}{k_2} z_2 - \frac{k_1 A_3}{k_2 A_{11}} e_4 - A_{150} Y_r \\
\dot{z}_2 &= -\frac{k_1}{k_2} z_1 - A_{19} z_2 - A_{20} e_4 + A_{11} e_5 + A_{10} Y_r \\
\dot{e}_3 &= -k_3 e_3 + e_4 \\
\dot{e}_4 &= -\frac{k_1 A_3}{k_2 A_{11}} z_1 - A_{21} z_2 - e_3 - A_{22} e_4 + A_3 e_5 + Y_r \\
\dot{e}_5 &= -A_{11} z_2 + A_3(.) e_4 - k_5 e_5 + e_6 + A_{160} Y_r \\
\dot{e}_6 &= -e_5 - k_6 e_6 + A_{170}(.) Y_r
\end{aligned}\right\} \qquad (4.29)$$

By examining the system (4.29), it is easy to verify the effect of the different tuning parameters k_1, k_2, k_3, k_4, k_5 and k_6 on how it accelerate or slow down the convergence of each state variable. Moreover, as one can see, the resulting closed loop system is a 6th order system, like the open loop system, which means there is no internal dynamic, unlike the case where solely backstepping is used as with Jung-Shan and Kanellakopoulos *(1997)* and Kaddissi Kenné et al. *(2005)*. This results in a greater stability. (Refer to Appendix *A3.3*)

4.5 Tests and Simulation

This section presents and analyzes the simulation results obtained from the backstepping - integrator forwarding controller versus those obtained by a classic PID controller and a sliding mode controller. The goal is to evaluate the transient reaction and stability of a car body equipped with an electrohydraulic active suspension that is controlled with the previous designed controller.

4.5.1 The Controllers Design

- Refer to Appendix *A3.6* for a complete description of the backstepping - integrator forwarding controller;
- The gains of the PID controller were optimized using the 'Nonlinear Control Design' outport of the 'NCD Blockset' library of Matlab–Simulink. The maximum allowed

value for y_1 was 3 *cm* and the maximum allowed value for the control signal u was 2 Volts. Their values are given in Appendix *A3.3*;

- The sliding mode controller is based on the following sliding surface:

$$S = C_1 y_1 + C_2 \dot{y}_1 + C_3 \ddot{y}_1 + C_4 \dddot{y}_1 \tag{4.30}$$

The sliding surface is a function of the controlled variable y1 which is the vertical motion of the car body and its derivatives. The sliding surface is chosen in a way that its derivative $\dot{S}$ encloses the control signal u. This is why in the expression of S there is no need to go further than the third order derivative of y_1. The tuning parameters C_1, C_2, C_3 and C_4 were chosen by identifying the characteristic polynomial of (4.30) with a third degree polynomial having a 3 multiplicity stable pole equal to – 50. Their values are given in Appendix *A3.3*.

4.5.2 Simulation Results

The road disturbances used for this simulation consist of two succeeding bumps of 10 cm height that last 0.6 *sec* and 0.25 *sec* respectively for the first test; and a random perturbation of bumps and potholes with a maximum peak of 25 *cm* for the second test, as plotted in figure 4.3 (a) and (b) respectively. Figure 4.4 compares the vertical motion of the car body for the backstepping - integrator forwarding controller (a), the PID controller (b) and the sliding mode controller (c) in case of 10 *cm* height bumps. As we can see in (a), the peaks are 0.4 cm for a bump that lasts 0.6 sec and 0.95 *cm* for a bump that lasts 0.25 *sec*. It is obvious and expected that this controller outperform the PID controller (b) where the peaks are 3.7 *cm* for a bump that lasts 0.6 *sec* and 5.8 *cm* for a bump that lasts 0.25 *sec*.

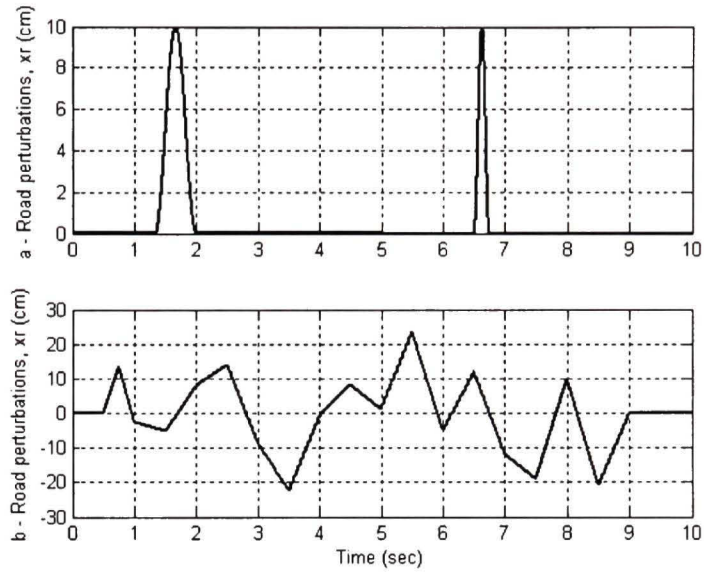

Figure 4.3 ***a – 10 cm bumps, x_r (cm). b – Random perturbation, x_r (cm).***

The performances of the sliding mode controller (c) are very close to those of the backstepping - integrator forwarding controller (a), with slightly lower amplitude of the car vertical motion in the case of the backstepping - integrator forwarding controller and a slightly better transient state in the case of the sliding mode controller. Figure 4.5 compares the vertical motion of the car body for the backstepping - integrator forwarding controller (a), the PID controller (b) and the sliding mode controller (c) in case of random perturbations. As we can see, the maximum peak is 0.7 *cm* in (a) and 7 *cm* in (b); here again the resulting performance of the controllers is expected. On the other hand, the performances of the sliding mode controller (c) are quite different this time from those of the backstepping - integrator forwarding controller (a). Much higher amplitudes of the car vertical motion are observed with the sliding mode controller than with the backstepping - integrator forwarding controller; however, the variations are smoother with the sliding mode controller. Further more, the oscillations that are apparent in the backstepping - integrator forwarding are extremely small to be sensed by the passengers, hence the latter controller is more efficient in presence of random perturbations and chaotic roads.

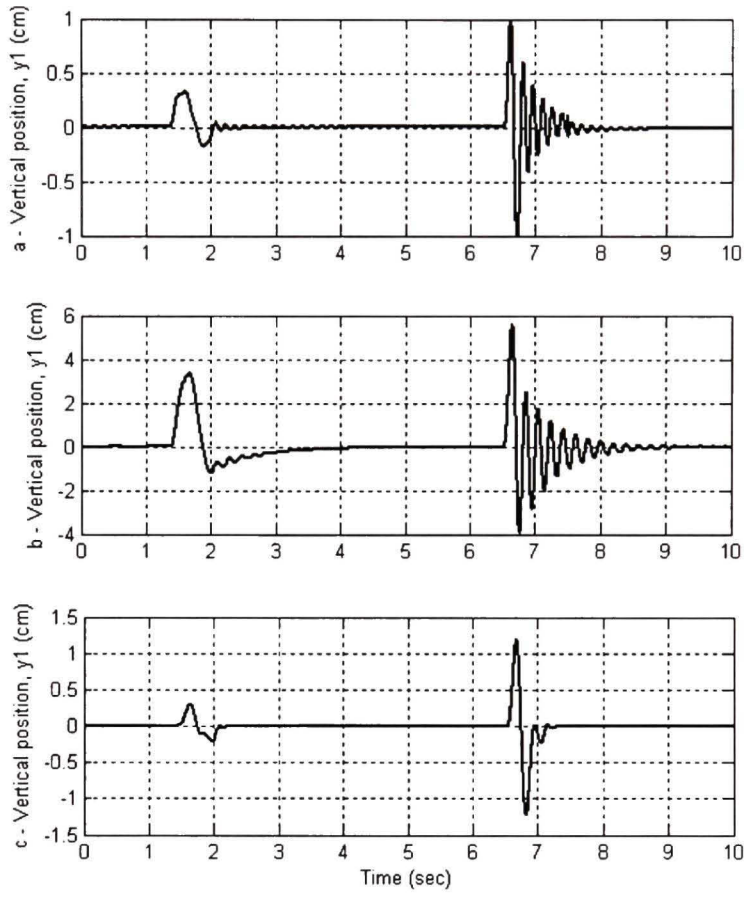

Figure 4.4 10 cm bumps, a - Car vertical motion, y_1 (cm), when using the backstepping - integrator forwarding nonlinear controller. b - Car vertical motion, y_1 (cm), when using the PID Controller. c - Car vertical motion, y_1 (cm), when using the sliding mode controller.

Another essential comparison is to be made for the control signals generated by these different controllers. Figures 3.6 puts side by side the control signals of the three controllers, in case of 10 *cm* height bumps. We can see that the control signal of the backstepping – integrator forwarding controller (a) is lower in amplitude and smoother than the PID controller (b) and the sliding mode controller (c). On the other side, figure 7 evaluates the control signals of the three controllers, in case of a random perturbation. Here again, we can see that the control signal of the backstepping – integrator forwarding controller (a) is obviously lower in amplitude and smoother than the PID controller (b) and the sliding mode controller (c). In fact, a lot of oscillations appear in the PID control signal and the chattering effect is very present in the sliding mode control signal. Those phenomena make the valve

spool shift from one position to another at a high frequency, which can damage the servovalve itself. Moreover, this chattering will have larger amplitude in real-time control, because the sampling time will be most probably larger. In a few words, the backstepping – integrator forwarding controller that was designed in this paper allowed us to fully control the electrohydraulic active suspension without leaving any internal dynamics and thus leading to a very adequate stability and satisfactory passengers comfort.

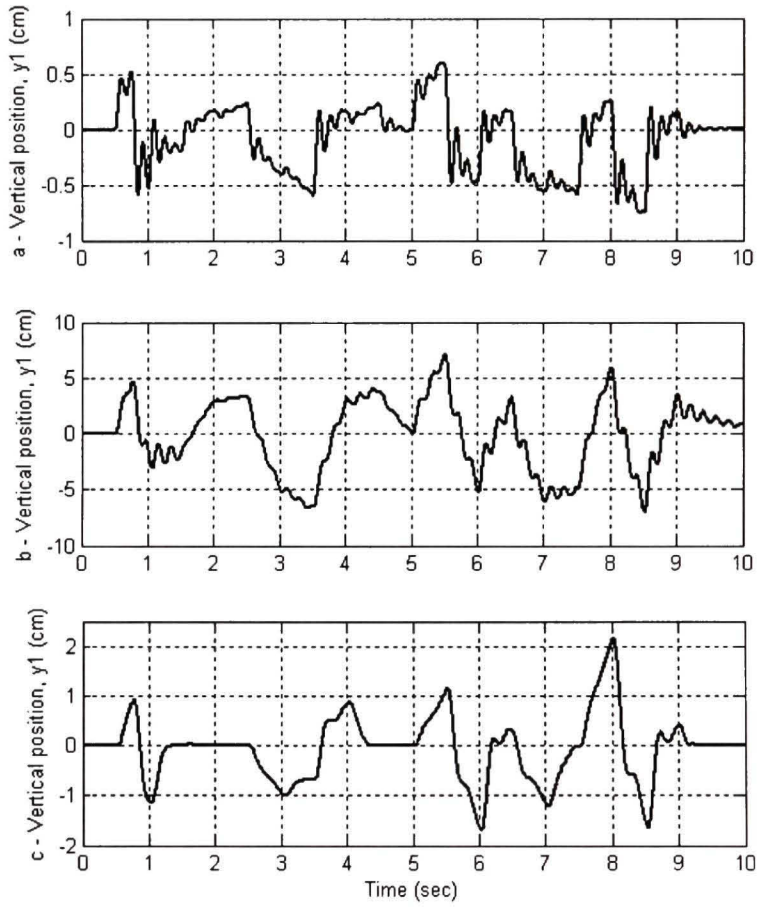

Figure 4.5 ***Random perturbations, a - Car vertical motion, y_1 (cm), when using the backstepping - integrator forwarding nonlinear controller. b - Car vertical motion, y_1 (cm), when using the PID Controller. c - Car vertical motion, y_1 (cm), when using the sliding mode Controller.***

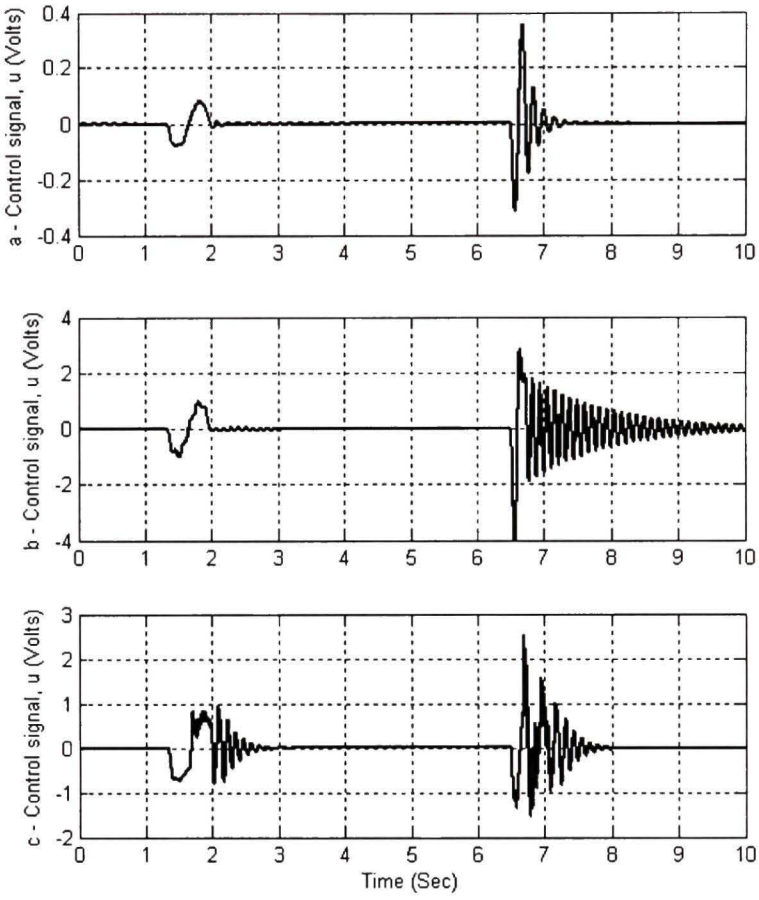

Figure 4.6 ***10 cm bumps, a - control signal, u (Volts) when using the backstepping - integrator forwarding nonlinear controller. b - Control signal, u (Volts) when using the PID controller. c - Control signal, u (Volts) when using the sliding mode controller.***

4.6 Conclusion

In this paper, we presented a nonlinear control strategy of an electrohydraulic active suspension. Giving that the mathematical model of the electrohydraulic active suspension is neither feedback nor feedforward, we made a change of variables that allows the system to be classified as an interlaced system. Consequently, the ensuing controller is based on a combination of backstepping and integrator forwarding. We can see how the designed controller succeeded in stabilizing the vertical motion of the car body and reducing the perturbation transmitted to the passengers as well. Two simulation tests were made. The first

one was for two succeeding 10 *cm* bumps that last 0.6 *sec* and 0.25 *sec* respectively, the second one was for a random perturbation signal with a maximum value of 25 *cm*. The use of this control strategy permitted us to achieve a full control over the hydraulic active suspension, without any remaining internal dynamic as in many other control approaches. The results were compared with those obtained by employing a classic PID controller and a sliding mode controller. The PID obviously led to less efficient results; however the sliding mode controller while giving interesting results in minimizing the car vertical motion, generated a high amplitude control signal involving chattering. This can eventually damage the hydraulic components especially the servovalve. Our further work relies on implementing this control strategy on an industrial active suspension to achieve a real-time control.

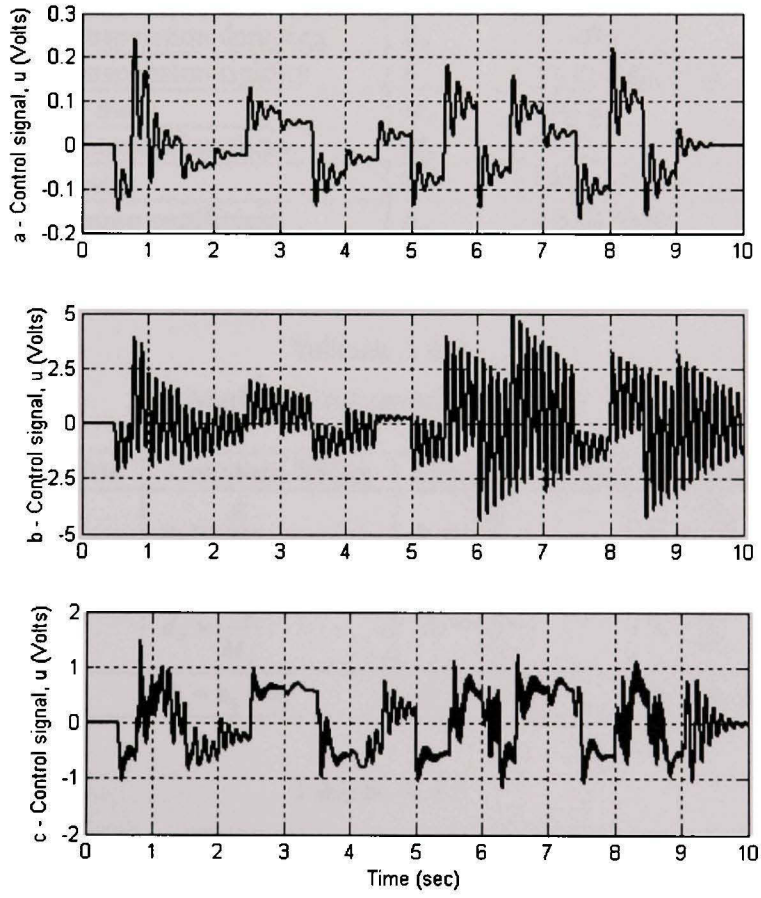

Figure 4.7 ***Random perturbations, a - control signal, u (Volts) when using the backstepping - integrator forwarding nonlinear controller. b - Control signal, u (Volts) when using PID controller. c - Control signal, u (Volts) when using sliding mode controller.***

Appendix

Tableau A 4.1

Active suspension properties

Property Name	Symbol	Value & Unit
Servovalve time constant	τ	3.18×10^{-3} *sec*
Servovalve amplifier gain	K	0.0397 cm^2/V
Flow discharge coefficient	C_d	0.63
Fluid bulk modulus	β	7995 daN/cm^2
Actuator chamber volume	V_0	135.4 cm^3
Supply pressure	P_S	103.42 daN/cm^2
Fluid mass density	ρ	0.867 g/cm^3
Leakage coefficient	L	0.09047 $cm^5/daN.s$
Actuator piston area	A	3.35 cm^2
Passive suspension damping	B_p	1 *daNs/cm*
Passive suspension rigidity	K_p	*16.812 daN/cm*
Car body mass	M_v	*290 Kg*
Tire and suspension mass	M_r	59 *Kg*
Tire stiffness	K_r	190 *daN/cm*
Tire damping coefficient	B_r	0.5 *daNs/m*
Exponential Constant	a	2000

Tableau A 4.2

Mathematical model constants

Constant Value	Constant Value	Constant Value	Constant Value
$a_0 = \frac{K_p}{M_v}$	$a_1 = \frac{A}{M_v}$	$b_0 = \frac{B_p}{M_v}$	$b_1 = \frac{B_r}{M_r}$
$c_1 = \frac{A}{M_r}$	$d_0 = \frac{K_p}{M_r}$	$d_1 = \frac{B_p}{M_r}$	$h_1 = \frac{K_t}{M_u}$
$J_1 = 2V_0\beta$	$A_1 = a_0 + d_0$	$A_2 = b_0 + d_1$	$A_3 = a_1 + c_1$

Tableau A 4.3

Controllers tuning parameters

Tuning parameter	Value	Comments
k_1	50	Large enough to ensure condition (70)

Tuning parameter	Value	Comments
k_2	100	$k_2 > k_1$ so that the car vertical speed converges faster than the position and large enough to ensure condition (58)
k_3	10	---
k_4	33	$k_4 > k_3$ so that the suspension vertical speed converges faster than the position and large enough to ensure condition (44)
k_5	106	Large enough to ensure condition (77)
k_6	1070	Large enough to ensure condition (86)
K_p	10	NCD toolbox - Simulink
K_i	2	NCD toolbox - Simulink
K_d	0.01	NCD toolbox - Simulink
C_1	125000	By identification to $(s + 50)^3$
C_2	7500	By identification to $(s + 50)^3$
C_3	150	By identification to $(s + 50)^3$
C_4	1	By identification to $(s + 50)^3$

Tableau A 4.4

Intermediate constants for controller design

Constant Value	Constant Value
$A_4 = -A_1 + k_3 A_2 - k_3^2$	$A_{50} = A_2 - k_3$
$A_5 = A_4 + 1$	$A_6 = k_4 - A_{50}$
$A_7 = -a_0 + b_0 k_3 - a_1 A_5 / A_3$	$A_8 = b_0 + a_1 A_6 / A_3$
$Den = 1 + k_3 k_4$	$A_9 = (A_8 + k_4 A_7)/Den$
$A2_0 = (A_7 - k_3 A_8)/Den$	$A2_1 = A2/A_3 + A2_0 A_3$
$A_{12} = k_4 + k_2 A_3^2$	$DEN = A_{11} \begin{Bmatrix} -1 + k_2 k_3 A_3^2 \\ -k_3 A_{12} \end{Bmatrix}$
$A_{13} = \begin{Bmatrix} 1 + k_3 A_{12} \\ +k_2 k_3 A_3 A_{11} A_{10} \\ +k_2 A_3 A_{11} A_9 \end{Bmatrix} \Big/ (k_2 A_{11} DEN)$	$A_{14} = \begin{Bmatrix} A_{11} A_{10} + A_3 \\ -A_{11} A_9 A_{12} \\ +k_2 A_3^2 A_{11} A_9 \end{Bmatrix} \Big/ DEN$
$A_{15} = \begin{Bmatrix} -k_3 A_3 - A_{11} A_9 \\ -k_3 A_{11} A_{10} \end{Bmatrix} \Big/ DEN$	$A_{16} = k_1 A_{11} + k_2 A_{11}$
$A_{17} = (1 + A_4) / A_3$	$A_{18} = (k_4 - A_{50}) / A_3 + k_2 A_3 + k_1 A_3$

Constant Value	Constant Value
$A_{19} = k_2 A_{11}^2 + k_1 A_{11}^2$	$A_{20} = k_2 A_{11} A_3 + k_1 A_{11} A_3$
$A_{21} = k_1 A_3 A_{11} + k_2 A_3 A_{11}$	$A_{22} = A_{12} + k_1 A_3^2$
$A_{23} = k_1^2 /(k_2^2 A_{11}^3) + k_1 A_{16} / k_2 + k_1 A_3 A_{18} /(k_2 A_{11})$	$A_{24} = k_1^2 /(k_2^2 A_{11}) + A_{18} A_{21} + A_{16} A_{19}$
$A_{25} = k_3 A_{17} + A_{18}$	$A_{26} = k_1^2 A_3 /(k_1^2 A_{11}^2) + A_{16} A_{20} - A_{17} + A_{18} A_{22}$
$A_{29} = J_1 A k_3 + J_1 L A_{17}$	$A_{30} = - J_1 A + J_1 L A_{18}$
$A_{150} = A_{10} A_{13} + A_{15}$	$A_{160} = -k_1 A_{150} /(k_2 A_{11}) + A_{18} + A_{16} A_{10}$

Tableau A 4.5

Intermediate functions for controller design

Function Value	Function Value
$A_{27}(.) = -A_{23} + \frac{J_1 L k_1}{f(.) k_2 A_{11}}$	$A_{28}(.) = -A_{24} + \frac{J_1 L A_{16}}{f(.)}$
$A_{29}(.) - A_{25} + \frac{J_1 A k_3}{f(.)} + \frac{J_1 L A_{17}}{f(.)}$	$A_{30}(.) = -A_{26} - \frac{J_1 A}{f(.)} + \frac{J_1 L A_{18}}{f(.)}$
$A_{31}(.) = A_{11} + A_{28}(.)$	$A_{32}(.) = A_3 + A_{30}(.)$
$A_{33}(.) = \frac{J_1 L}{f(.)} - k_5$	$w(.) = \frac{dsigm(y_6)}{dy_6} = \frac{2ae^{-ay_6}}{(1+e^{-ay_6})^2}$
$f_p(.) = \frac{df(.)}{dt} = -2A^2 y_3 y_4$	$V(.) = \frac{sgm(y_6)\dot{y}_5 y_6}{2\rho g(.) f(.)} - \frac{w(.) y_5 y_6^2}{2\rho\tau g(.) f(.)} - \frac{f_p(.) g(.)}{f(.)^2} y_6 - \frac{g(.) y_6}{f(.)\tau}$
$Z(.) = J_1 C_d \left\{ \begin{matrix} \frac{K_v g(.)}{f(.)\tau} \\ -\frac{K_v y_5 y_6 w(.)}{2\rho\tau g(.) f(.)} \end{matrix} \right\}$	$\dot{A}_{27}(.) = -\frac{J_1 L k_1}{k_2 A_{11}} \frac{f_p(.)}{f^2(.)}$
$\dot{A}_{29}(.) = -\left\{ \begin{matrix} J_1 A k_3 \\ +J_1 L A_{17} \end{matrix} \right\} \frac{f_p(.)}{f^2(.)}$	$\dot{A}_{31}(.) = -J_1 L A_{16} \frac{f_p(.)}{f^2(.)}$

Function Value	Function Value
$\dot{A}_{32}(.) = (J_1 A - J_1 L A_{18}) \dfrac{f_p(.)}{f^2(.)}$	$A_{34}(.) = \dfrac{k_1 A_{27}(.)}{k_2^2 A_{11}^2} - \dot{A}_{27}(.) - \dfrac{k_1 A_3 A_{32}(.)}{k_2 A_{11}} + A_{33}(.) A_{27}(.) - \dfrac{k_1 A_{31}(.)}{k_2}$
$A_{35}(.) = \dfrac{k_1 A_{27}(.)}{k_2} - A_{31}(.) A_{19} + A_{21} A_{32}(.) + A_{28} A_{33(.)} - \dot{A}_{31}(.)$	$A_{36}(.) = -k_3 A_{29}(.) + A_{32}(.) + A_{29}(.) A_{33}(.) - \dot{A}_{29}(.)$
$A_{37}(.) = \dfrac{k_1 A_3 A_{27}(.)}{k_2 A_{11}} - A_{29}(.) + A_{20} A_{31}(.) + A_{22} A_{32}(.) + A_{30}(.) A_{33}(.) - \dot{A}_{32}(.)$	$A_{38}(.) = -A_{11} A_{31}(.) - A_3 A_{32}(.) - \dfrac{J_1 L A_{33}(.)}{f(.)} - \dfrac{J_1 L f_p(.)}{f^2(.)}$
$A_{39}(.) = \dfrac{J_1 C_d g(.) A_{33}(.)}{f(.)}$	$A_{170}(.) = A_{150} A_{27}(.) - A_{32}(.) - A_{10} A_{31}(.) - A_{160} A_{33}(.)$
$Y_r = h_1 y_r + b_1 \dot{y}_r$	

A 4.6 Backstepping - integrator forwarding controller

Consider the following subsystem of (4.17) with y_5 as input,

$$\left.\begin{aligned} \dot{y}_1 &= y_2 \\ \dot{y}_2 &= -a_0 y_3 - b_0 y_4 + a_1 y_5 \\ \dot{y}_3 &= y_4 \\ \dot{y}_4 &= -A_1 y_3 - A_2 y_4 + A_3 y_5 + h_1 y_r + b_1 \dot{y}_r \end{aligned}\right\} \tag{4.31}$$

In fact, it is easy to find that,

$$P_{12} = \begin{pmatrix} 0 & 1 & 0 & 0 & 0 \\ 0 & 0 & -a_0 & -b_0 & a_1 \\ 0 & 0 & 0 & 1 & 0 \\ 0 & 0 & -A_1 & -A_2 & A_3 \end{pmatrix} \tag{4.32}$$

The previous matrix is of the form,

$$P = \begin{pmatrix} 0 & * & 0 & 0 & 0 \\ 0 & 0 & * & * & * \\ 0 & 0 & 0 & * & 0 \\ 0 & 0 & * & * & * \end{pmatrix} \tag{4.33}$$

As it can be seen through Sepulchre and Kokotovic (1997), a system which configuration matrix is like the one in (4.33), is stabilized with two steps of backstepping, for (y_3, y_4), followed by two steps of integrator forwarding, for (y_1, y_2).

Let us apply the backstepping to the subsystem composed of ($\dot{y}_3$, $\dot{y}_4$) :

$$\left.\begin{aligned} \dot{y}_3 &= y_4 \\ \dot{y}_4 &= -A_1 y_3 - A_2 y_4 + A_3 y_5 + h_1 y_r + b_1 \dot{y}_r \end{aligned}\right\} \tag{4.34}$$

Step 1: Define the error variable $e_3 = y_3 - 0 = y_3$, since the goal is that y_3 (the suspension travel) converges to zero and define the candidate Lyapunov function for the state $\dot{y}_3 = y_4$,

$$V_3 = \frac{1}{2} e_3^2 \tag{4.35}$$

Then,

$$\dot{V}_3 = e_3 \dot{e}_3 = e_3 y_4 \tag{4.36}$$

If we consider y_4 as the virtual input of $\dot{y}_3$, then its desired value that will achieve stabilization is,

$$y_{4d} = -k_3 e_3 \tag{4.37}$$

This will give,

$$\dot{V}_3 = -k_3 e_3^2 < 0 \tag{4.38}$$

Step 2: Define the error variable $e_4 = y_4 - y_{4d}$ and the candidate Lyapunov function,

$$V_4 = V_3 + \frac{1}{2} e_4^2 \tag{4.39}$$

for the state $\dot{y}_4 = -A_1 y_3 - A_2 y_4 + A_3 y_5 + h_1 y_r + b_1 \dot{y}_r$ of subsystem (4.17).

First, this allows writing,

$$\dot{e}_3 = \dot{y}_3 = y_4 = e_4 + y_{4d} = -k_3 e_3 + e_4 \tag{4.40}$$

Then,

$$\dot{V}_4 = -k_3 e_3^2 + e_4 (e_3 + A_4 e_3 - A_{50} e_4 + A_3 y_5 + Y_r) \tag{4.41}$$

If we consider y_5 as the virtual input of $\dot{y}_4$, then its desired value that will achieve stabilization is,

$$y_{5d} = \frac{1}{A_3}[A_{50}e_4 - (A_4 + 1)e_3 - k_4 e_4] \tag{4.42}$$

This will give,

$$\begin{aligned} \dot{V}_4 &= -k_3 e_3^2 - k_4 e_4^2 + e_4 Y_r \\ &= -k_3 e_3^2 - \frac{k_4}{2} e_4^2 - \frac{k_4}{2}\left(e_4 - \frac{Y_r}{k_4}\right)^2 + \frac{Y_r^2}{2k_4} \end{aligned} \tag{4.43}$$

Equation (4.43) is negative if,

$$Y_r < \frac{e_4}{2} k_4 \tag{4.44}$$

In order to be able to apply integrator forwarding to the subsystem $(\dot{y}_1, \dot{y}_2)$, we have to augment the input y_{5d} of subsystem (4.31). Hence, equation (4.42) becomes,

$$y_{5d} = \frac{1}{A_3}[A_{50}e_4 - (A_4 + 1)e_3 - k_4 e_4] + v_2 \tag{4.45}$$

This allows writing,

$$\begin{aligned} \dot{e}_4 &= \dot{y}_4 + k_3 \dot{e}_3 \\ &= -A_1 y_3 - A_2 y_4 + A_3 y_{5d} + h_1 y_r + b_1 \dot{y}_r - k_3^2 e_3 + k_3 e_4 \\ &= -e_3 - k_4 e_4 + A_3 v_2 + Y_r \end{aligned} \tag{4.46}$$

And,

$$\begin{aligned} \dot{y}_2 &= -a_0 y_3 - b_0 y_4 + a_1 y_{5d} \\ &= (-a_0 + b_0 k_3 - \frac{a_1 A_5}{A_3}) e_3 - (b_0 + \frac{a_1 A_6}{A_3}) e_4 + \frac{a_1}{A_3} v_2 \end{aligned} \tag{4.47}$$

Substituting (4.46) and (4.47) in subsystem (4.31), leads to the new subsystem,

$$\left.\begin{aligned} \dot{y}_1 &= y_2 \\ \dot{y}_2 &= A_7 e_3 - A_8 e_4 + \frac{a_1}{A_3} v_2 \\ \dot{e}_3 &= -k_3 e_3 + e_4 \\ \dot{e}_4 &= -e_3 - k_4 e_4 + A_3 v_2 + Y_r \end{aligned}\right\} \tag{4.48}$$

Step 3: Let us consider the non-perturbed subsystem of (4.48) formed by $\{\dot{y}_2, \dot{e}_3, \dot{e}_4\}$ and make the following change of variables (Sepulchre et al. 1997),

$$\left.\begin{aligned}\dot{\xi}_2 &= A_7\xi_3 - A_8\xi_4 \quad \xi_2(0) = y_2\\ \dot{\xi}_3 &= -k_3\xi_3 + \xi_4 \quad \xi_3(0) = e_3\\ \dot{\xi}_4 &= -\xi_3 - k_4\xi_4 \quad \xi_4(0) = e_4\end{aligned}\right\} \tag{4.49}$$

In other words, (y_2, e_3, e_4) become the initial values of the new variables (ξ_2, ξ_3, ξ_4). The latter variables change allows us to write,

$$\xi_2 = y_2 + \int_0^\infty (A_7\xi_3 - A_8\xi_4)dt \tag{4.50}$$

Solving the differential equations (4.49) and integrating (4.50), gives the following solution:

$$\xi_2 = y_2 + A_9e_3 + A_{10}e_4 \tag{4.51}$$

And,

$$\begin{aligned}\dot{z}_2 &= \dot{y}_2 + A_9\dot{e}_3 + A_{10}\dot{e}_4\\ &= A_7e_3 - A_8e_4 + \frac{a_1}{A_3}v_2 + A_9(-k_3e_3 + e_4)\\ &\quad + A_{10}(-e_3 - k_4e_4 + A_3v_2 + Y_r)\\ &= \left(\frac{a_1}{A_3} + A_3A_{10}\right)v_2 + A_{10}Y_r\end{aligned} \tag{4.52}$$

Therefore (4.48) becomes,

$$\left.\begin{aligned}\dot{z}_2 &= A_{11}v_2 + A_{10}Y_r\\ \dot{e}_3 &= -k_3e_3 + e_4\\ \dot{e}_4 &= -e_3 - k_4e_4 + A_3v_2 + Y_r\end{aligned}\right\} \tag{4.53}$$

As one can see, the added input v_2 will be used to stabilize the subsystem (4.53), particularly $\dot{z}_2$. Therefore, consider the following candidate Lyapunov function,

$$V_2 = V_4 + \frac{1}{2}(z_2)^2 \tag{4.54}$$

Then,

$$\dot{V}_2 = \dot{V}_4 + v_2(A_{11}z_2 + A_3e_4) + A_{10}z_2Y_r \tag{4.55}$$

The value of v_2 that will ensure the stabilization of $\dot{z}_2$ is,

$$v_2 = -k_2(A_{11}z_2 + A_3e_4) \tag{4.56}$$

This will give,

$$\dot{V}_2 = \dot{V}_4 - k_2(A_3e_4 + A_{11}z_2)^2 + A_{10}z_2Y_r \tag{4.57}$$

Equation (4.57) is negative if,

$$Y_r < \frac{(A_3e_4 + A_{11}z_2)^2}{A_{10}z_2}k_2 \tag{4.58}$$

Step 4: In order to stabilize $\dot{y}_1$; the control v_2 should be augmented. Hence, the augmented input becomes,

$$v_2 = -k_2(A_{11}z_2 + A_3e_4) + v_1 \tag{4.59}$$

Therefore, subsystem (4.48) combined with (4.51), (4.53) and (4.59) becomes,

$$\left.\begin{aligned} \dot{y}_1 &= y_2 = z_2 - A_9e_3 - A_{10}e_4 \\ \dot{z}_2 &= -k_2A_{11}^2z_2 - k_2A_{11}A_3e_4 + A_{11}v_1 + A_{10}Y_r \\ \dot{e}_3 &= -k_3e_3 + e_4 \\ \dot{e}_4 &= -k_2A_3A_{11}z_2 - e_3 - A_{12}e_4 + A_3v_1 + Y_r \end{aligned}\right\} \tag{4.60}$$

Let us consider the non-perturbed subsystem of (4.60) and make the following change of variables,

$$\left.\begin{aligned} \dot{\xi}_1 &= \xi_2 - A_9\xi_3 - A_{10}\xi_4 & \xi_1(0) &= y_1 \\ \dot{\xi}_2 &= -k_2A_{11}^2\xi_2 - k_2A_{11}A_3\xi_4 & \xi_2(0) &= z_2 \\ \dot{\xi}_3 &= -k_3\xi_3 + \xi_4 & \xi_3(0) &= e_3 \\ \dot{\xi}_4 &= -k_2A_3A_{11}\xi_2 - \xi_3 - A_{12}\xi_4 & \xi_4(0) &= e_4 \end{aligned}\right\} \tag{4.61}$$

In other words, $(y_1,\ \xi_2,\ e_3 \text{ and } e_4)$ become the initial values of the new variables $(\xi_1,\ \xi_2,\ \xi_3 \text{ and } \xi_4)$. The latter variables change allows us to write,

$$\xi_1 = y_1 + \int_0^\infty (\xi_2 - A_9\xi_3 - A_{10}\xi_4)dt \tag{4.62}$$

Solving the differential equations (4.61) and integrating (4.62), gives the following solution,

$$\xi_1 = y_1 - A_{13}z_2 - A_{14}e_3 - A_{15}e_4 \tag{4.63}$$

And,

$$\begin{aligned} \dot{z}_1 &= \dot{y}_1 - A_{13}\dot{z}_2 - A_{14}\dot{e}_3 - A_{15}\dot{e}_4 \\ &= z_2 - A_9e_3 - A_{10}e_4 - A_{13}\left(-k_2A_{11}^2z_2 - k_2A_{11}A_3e_4 + A_{11}v_1 + A_{10}Y_r\right) \\ &\quad - A_{14}\left(-k_3e_3 + e_4\right) - A_{15}\left(-k_2A_3A_{11}z_2 - e_3 - A_{12}e_4 + A_3v_1 + Y_r\right) \\ &= \frac{1}{k_2A_{11}}v_1 - (A_{10}A_{13} + A_{15})Y_r \end{aligned} \tag{4.64}$$

Therefore (4.60) becomes,

$$\left.\begin{aligned} \dot{z}_1 &= \frac{1}{k_2 A_{11}} v_1 - A_{150} Y_r \\ \dot{z}_2 &= -k_2 A_{11}^2 z_2 - k_2 A_{11} A_3 e_4 + A_{11} v_1 + A_{10} Y_r \\ \dot{e}_3 &= -k_3 e_3 + e_4 \\ \dot{e}_4 &= -k_2 A_3 A_{11} z_2 - e_3 - A_{12} e_4 + A_3 v_1 + Y_r \end{aligned}\right\} \tag{4.65}$$

As one can see, the added input v_1 will be used to stabilize the subsystem (4.65), particularly $\dot{z}_1$. Consequently, consider the following candidate Lyapunov function,

$$V_1 = V_2 + \frac{1}{2}\left(z_1\right)^2 \tag{4.66}$$

Then,

$$\dot{V}_1 = \dot{V}_2 + v_1\left(\frac{1}{k_2 A_{11}} z_1 + A_{11} z_2 + A_3 e_4\right) - A_{150} z_1 Y_r \tag{4.67}$$

The value of v_1 that will ensure the stabilization of $\dot{z}_1$ is,

$$v_1 = -k_1\left(\frac{1}{k_2 A_{11}} z_1 + A_{11} z_2 + A_3 e_4\right) \tag{4.68}$$

This will give,

$$\dot{V}_1 = \dot{V}_2 - k_1\left(\frac{1}{k_2 A_{11}} z_1 + A_{11} z_2 + A_3 e_4\right)^2 - A_{150} z_1 Y_r \tag{4.69}$$

Equation (4.69) is negative if,

$$Y_r < -\frac{\left(\frac{1}{k_2 A_{11}} z_1 + A_{11} z_2 + A_3 e_4\right)^2}{A_{150} z_1} k_1 \tag{4.70}$$

Let us now apply the backstepping to stabilize the rest of the system. In the previous steps, y_5 was considered as the virtual input of subsystem (4.31). Its desired value that will yield subsystem (4.31) to stabilization is found by replacing v_2 and v_1 with their expressions in equation (4.45),

$$y_{5d} = -\frac{k_1}{k_2 A_{11}} z_1 - A_{16} z_2 - A_{17} e_3 - A_{18} e_4 \tag{4.71}$$

Step 5: Since y_{5d} is not the real input of the system we will define the error variable $e_5 = y_5 - y_{5d}$ and the candidate Lyapunov function,

$$V_5 = V_1 + \frac{1}{2}\left(e_5^2\right) \tag{4.72}$$

for the state $\dot{y}_5 = \frac{J_1}{f(.)}\left(-Ay_4 - Ly_5 + C_d g(.) y_6\right)$, of subsystem (4.17).

First, this allows writing

$$\begin{aligned}
\dot{e}_5 &= \dot{y}_5 + \frac{k_1}{k_2 A_{11}}\dot{z}_1 + A_{16}\dot{z}_2 + A_{17}\dot{e}_3 + A_{18}\dot{e}_4 \\
&= \frac{J_1}{f(.)}\left(-Ay_4 - Ly_5 + C_d g(.) y_6\right) + \frac{k_1}{k_2 A_{11}}\left(-\frac{k_1}{k_2^2 A_{11}^2} z_1 - \frac{k_1}{k_2} z_2 - \frac{k_1 A_3}{k_2 A_{11}} e_4 - A_{150} Y_r\right) \\
&+ A_{16}\left(-\frac{k_1}{k_2} z_1 - A_{19} z_2 - A_{20} e_4 + A_{10} Y_r\right) + A_{17}\left(-k_3 e_3 + e_4\right) \\
&+ A_{18}\left(-\frac{k_1 A_3}{k_2 A_{11}} z_1 - A_{21} z_2 - e_3 - A_{22} e_4 + Y_r\right) \\
&= \left(-A_{23} + \frac{J_1 L k_1}{f(.) k_2 A_{11}}\right) z_1 + \left(-A_{24} + \frac{J_1 L A_{16}}{f(.)}\right) z_2 + \left(-A_{25} + \frac{J_1 A k_3}{f(.)} + \frac{J_1 L A_{17}}{f(.)}\right) e_3 \\
&+ \left(-A_{26} - \frac{J_1 A}{f(.)} + \frac{J_1 L A_{18}}{f(.)}\right) e_4 - \frac{J_1 L}{f(.)} e_5 + \frac{J_1 C_d g(.)}{f(.)} y_6 + A_{160}(.) Y_r
\end{aligned} \tag{4.73}$$

Then,

$$\begin{aligned}
\dot{V}_5 &= \dot{V}_1 \\
&+ e_5\left(A_{27}(.) z_1 + (A_{11} + A_{28}(.)) z_2 + A_{29}(.) e_3 + (A_3 + A_{30}(.)) e_4 - \frac{J_1 L}{f(.)} e_5 + Y_6 + A_{160}(.) Y_r\right)
\end{aligned} \tag{4.75}$$

If we consider Y_6 as the virtual input of $\dot{y}_5$, then its desired value that will achieve stabilization is,

$$Y_{6d} = -A_{27}(.) z_1 - (A_{11} + A_{28}(.)) z_2 - A_{29}(.) e_3 - (A_3 + A_{30}(.)) e_4 + \left(\frac{J_1 L}{f(.)} - k_5\right) e_5 \tag{4.75}$$

This will give,

$$\dot{V}_5 = \dot{V}_1 - k_5 e_5^2 + A_{160}(.) Y_r \tag{4.76}$$

Equation (4.76) is negative if,

$$Y_r < \frac{e_5^2}{A_{160}(.)} k_5 \tag{4.77}$$

Step 6: Consider now the new error variable $e_6 = Y_6 - Y_{6d}$ and the candidate Lyapunov function,

$$V_6 = V_5 + \frac{1}{2}e_6^2 \tag{4.78}$$

for the state $\dot{y}_6 = -\frac{1}{\tau}y_6 + \frac{k_v}{\tau}u$ of subsystem (4.17).

Firstly, substituting (4.75) and e_6 in (4.72), allows writing,

$$\dot{e}_5 \quad = -A_{11}z_2 + A_3(.)e_4 - k_5e_5 + e_6 + A_{160}Y_r \tag{4.79}$$

Secondly,

$$\dot{e}_6 = \dot{Y}_6 - \dot{Y}_{6d}\,. \tag{4.80}$$

- Calculation of $\dot{Y}_6$

$$\begin{aligned}
\dot{Y}_6 &= J_1C_d\left(\frac{\dot{g}(.)f(.) - \dot{f}(.)g(.)}{f(.)^2}y_6 + \frac{g(.)}{f(.)}\dot{y}_6\right) \\
&= J_1C_d\left(\frac{sgm(y_6)\dot{y}_5y_6}{2\rho g(.)f(.)} - \frac{w(.)y_5y_6^2}{2\rho\tau g(.)f(.)} - \frac{f_p(.)g(.)}{f(.)^2}y_6 - \frac{g(.)y_6}{f(.)\tau}\right) \\
&+ J_1C_d\left(\frac{K_vg(.)}{f(.)\tau} - \frac{K_vy_5y_6w(.)}{2\rho\tau g(.)f(.)}\right)u \\
&= V(.) + Z(.)u
\end{aligned} \tag{4.80'}$$

- Calculation of $\dot{Y}_{6d}$

$$\begin{aligned}
\dot{Y}_{6d} &= -A_{27}(.)\dot{z}_1 - A_{31}(.)\dot{z}_2 - A_{29}(.)\dot{e}_3 - A_{32}(.)\dot{e}_4 + \frac{J_1L}{f(.)}\dot{e}_5 - k_5\dot{e}_5 - \dot{A}_{27}(.)z_1 - \dot{A}_{31}(.)z_2 \\
&- \dot{A}_{29}(.)e_3 - \dot{A}_{32}(.)e_4 + \frac{J_1Lf_p(.)}{f^2(.)}e_5 \\
&= \left(\frac{k_1A_{27}(.)}{k_2^2A_{11}^2} - \frac{k_1A_{31}(.)}{k_2} - \frac{k_1A_3A_{32}(.)}{k_2A_{11}} + A_{33}(.)A_{27}(.) - \dot{A}_{27}(.)\right)z_1 \\
&+ \left(\frac{k_1A_{27}(.)}{k_2} - A_{31}(.)A_{19} + A_{21}A_{32}(.) + A_{28}A_{33(.)} - \dot{A}_{31}(.)\right)z_2 \\
&+ \left(-k_3A_{29}(.) + A_{29}(.)A_{33}(.) + A_{32}(.) - \dot{A}_{29}(.)\right)e_3 \\
&+ \left(\frac{k_1A_3A_{27}(.)}{k_2A_{11}} - A_{29}(.) + A_{20}A_{31}(.) + A_{22}A_{32}(.) + A_{30}(.)A_{33}(.) - \dot{A}_{32}(.)\right)e_4 \\
&+ \left(-A_{11}A_{31}(.) - A_3A_{32}(.) - \frac{J_1LA_{33}(.)}{f(.)} - \frac{J_1Lf_p(.)}{f^2(.)}\right)e_5 + \underbrace{\left(\frac{J_1C_dg(.)A_{33}(.)}{f(.)}\right)}_{A_{39}(.)}e_6 \\
&+ \left(A_{150}A_{27}(.) - A_{10}A_{31}(.) - A_{32}(.) - A_{160}A_{33}(.)\right)Y_r
\end{aligned} \tag{4.80''}$$

And consequently,

$$\dot{e}_6 = V(.) + Z(.)u - A_{34}(.)z_1 - A_{35}(.)z_2 - A_{36}(.)e_3 - A_{37}(.)e_4 - A_{38}(.)e_5 - A_{39}(.)e_6 - A_{170}(.)Y_r \tag{4.82}$$

Finally,

$$\dot{V}_6 = \dot{V}_5 + e_6 \begin{Bmatrix} V(.) - A_{34}(.)z_1 - A_{35}(.)z_2 - A_{36}(.)e_3 - A_{37}(.)e_4 \\ -A_{38}(.)e_5 + e_5 - A_{39}(.)e_6 + Z(.)u - A_{170}(.)Y_r \end{Bmatrix} .. \tag{4.83}$$

The value of the real input u that will ensure the stabilization of the entire electrohydraulic active suspension is,

$$u = \frac{1}{Z(.)} \begin{Bmatrix} -V(.) + A_{34}(.)z_1 + A_{35}(.)z_2 + A_{36}(.)e_3 \\ +A_{37}(.)e_4 + (A_{38}(.) - 1)e_5 + A_{39}(.)e_6 - k_6 e_6 \end{Bmatrix} .. \tag{4.84}$$

This will give,

$$\dot{V}_6 = \dot{V}_5 - k_6 e_6^2 + A_{170}(.)Y_r \tag{4.85}$$

Equation (4.85) is negative if,

$$Y_r < \frac{e_6^2}{A_{170}(.)} k_6 \tag{4.86}$$

Substituting u in (4.82) with its expression in (4.84), allows writing,

$$\dot{e}_6 \quad = -e_5 - k_6 e_6 + A_{170}(.)Y_r \tag{4.87}$$

The previous steps finally yield to the closed loop system dynamic given by,

$$\left.\begin{aligned} \dot{z}_1 &= -\frac{k_1}{k_2^2 A_{11}^2} z_1 - \frac{k_1}{k_2} z_2 - \frac{k_1 A_3}{k_2 A_{11}} e_4 - A_{150} Y_r \\ \dot{z}_2 &= -\frac{k_1}{k_2} z_1 - A_{19} z_2 - A_{20} e_4 + A_{11} e_5 + A_{10} Y_r \\ \dot{e}_3 &= -k_3 e_3 + e_4 \\ \dot{e}_4 &= -\frac{k_1 A_3}{k_2 A_{11}} z_1 - A_{21} z_2 - e_3 - A_{22} e_4 + A_3 e_5 + Y_r \\ \dot{e}_5 &= -A_{11} z_2 + A_3(.)e_4 - k_5 e_5 + e_6 + A_{160} Y_r \\ \dot{e}_6 &= -e_5 - k_6 e_6 + A_{170}(.)Y_r \end{aligned}\right\} \tag{4.88}$$

References

Abdellahi, E., D. Mehdi, and M. Saad (2000). On the design of active suspension system by H and mixed H2 / H: an LMI approach. 2000 Americal Control Conference, Jun 28-Jun 30 2000, Chicago, IL, USA, Institute of Electrical and Electronics Engineers Inc., Piscataway, NJ, USA.

Ando, Y. and M. Suzuki (1996). "Control of active suspension systems using the singular perturbation method." Control Engineering Practice 4(3): 287-293.

Fialho, I. and G. J. Balas (2002). "Road adaptive active suspension design using linear parameter-varying gain-scheduling." Control Systems Technology, IEEE Transactions on 10(1): 43-54.

Gaspar, P., I. Szaszi, and J. Bokor (2002). Nonlinear Active Suspension Modelling Using Linear Parameter Varying Approach. Proceedings of the 10th Mediterranean Conference on Control and Automation - MED2002, Lisbon, Portugal.

Jung-Shan, L. and I. Kanellakopoulos (1997). "Nonlinear design of active suspensions." Control Systems Magazine, IEEE 17(3): 45-59.

Kaddissi, C., J.-P. Kenné, and M. Saad (2005). Drive by wire control of an electro-hydraulic active suspension a backstepping approach. Control Applications, 2005. CCA 2005. Proceedings of 2005 IEEE Conference on.

Kaddissi, C., J.-P. Kenné, and M. Saad (2006). Indirect Adaptive Control of an Electro-Hydraulic Servo System Based on Nonlinear Backstepping. International Symposium on Industrial Electronics. ISIE 2006, Montreal, Quebec.

Kaddissi, C., J.-P. Kenné, and M. Saad (2007). "Identification and Real-Time Control of an Electro-Hydraulic Servo System Based on Nonlinear Backstepping." IEEE/ASME Transactions on Mechatronics 12(1).

Khalil, H. K. (2002). Nonlinear systems. New Jersey, Upper Saddle River, N.J: Prentice Hall, c2002.

Kristic, M. (2004). "Feedback Linearizability and Explicit Integrator Forwarding Controllers for Classes of Feedforward Systems." IEEE Transactions on Automatic Control 49(10): 1668-1682.

Krstic, M., I. Kanellakopoulos, and P. V. Kokotovic,. (1995). Nonlinear and adaptive control design, New York, N.Y. J. Wiley and Sons, c1995.

Leite, V. J. S. and P. L. D. Peres (2002). Robust pole location for an active suspension quarter-car model through parameter dependent control. Proceedings of the 2002 IEEE International Conference on Control Applications, Sep 18-20 2002, Glasgow, United Kingdom, Institute of Electrical and Electronics Engineers Inc.

LeQuoc, S., R. M. H. Cheng, and K.H. Leung, (1990). "Tuning an electrohydraulic servovalve to obtain a high amplitude ratio and a low resonance peak." Journal of Fluid Control 20(3Mar): 30-49.

Lin, J.-S. and I. Kanellakopoulos (1997). "Nonlinear design of active suspensions." IEEE Control Systems Magazine 17(3): 45-59.

Sam, Y. M., J. H. S. Osman, and M. R. A. Ghani (2003). Active suspension control: Performance comparison using proportional integral sliding mode and linear quadratic regulator methods. Proceedings of 2003 IEEE Conference on Control Applications, Istanbul, Turkey, Institute of Electrical and Electronics Engineers Inc.

Sepulchre, R., M. Jankovic, and P. V. Kokotovic (1997). Constructive Nonlinear Control. New York, Springer-Verlag.

Sepulchre, R., M. Jankovic, and P. V. Kokotovic. (1997). "Integrator Forwarding: A New Recursive Nonlinear Robust Design." Automatica 33(5): 979-984.

Sepulchre, R. and P. V. Kokotovic (1997). Interlaced Systems and Recursive Designs for Global Stabilization. 4th European Control Conference ECC, Brussels.

Sirouspour, M. R. and S. E. Salcudean (2000). On the nonlinear control of hydraulic servo-systems. ICRA 2000: IEEE International Conference on Robotics and Automation,

Apr 24-Apr 28 2000, San Francisco, CA, USA, Institute of Electrical and Electronics Engineers Inc., Piscataway, NJ, USA.

Yoshimura, T., Y. Isari, Q. Li and J. Hino (1997). "Active suspension of motor coaches using skyhook damper and fuzzy logic control." Control Engineering Practice 5(2): 175-184.

CONCLUSION GÉNÉRALE

Dans ce travail, une étude complète a été réalisée sur la modélisation, l'identification et le contrôle d'un système électrohydraulique générique. En outre, une étude dans le domaine de l'industrie automobile, qui porte sur la modélisation et la commande d'une suspension active électrohydraulique, a été faite. Les travaux ont été réalisés en trois phases principales.

Dans un premier temps, un modèle mathématique qui tient compte de toute la dynamique d'un système électrohydraulique, à part quelques hypothèses simplificatrices pour diminuer la complexité des équations, a été développé. En plus, une identification hors ligne du système a été effectuée. Il était possible d'utiliser l'algorithme des moindres carrés récursifs en réécrivant le modèle mathématique du système sous une forme LP. Concernant la commande, le backstepping nonlinéaire a été employé pour contrôler le suivi de la position angulaire du moteur hydraulique. À ce niveau, l'accent a été mis sur le choix de la fonction de Lyapunov. Cette dernière était choisie de telle sorte que les paramètres du contrôleur apparaissent dans la matrice de la dynamique de l'erreur, non seulement dans la diagonale principale, mais aussi dans les autres diagonales; offrant ainsi une plus grande flexibilité pour contrôler la convergence de l'erreur vers zéro. Pour compléter cette phase, un contrôleur PID a été implanté dans le but de comparer l'état transitoire, les erreurs de suivi de trajectoire et l'effet de la variation de la charge.

Dans une deuxième étape, un contrôleur basé sur le backstepping adaptatif indirect a été conçu et implanté, en temps réel, pour le même système électrohydraulique générique. En effet, il est bien connu que les paramètres des systèmes électrohydrauliques sont soumis à des variations, en fonction de la charge et de la pression du système; en particulier le coefficient de frottement qui est affecté par les deux. Pour cette raison, dans cette thèse, nous avons considéré de faire varier la charge agissant sur le moteur hydraulique, afin d'augmenter la pression du système et de voir la variation de ses paramètres en conséquence. Les résultats ont été comparés à ceux obtenus avec un contrôleur backstepping non-adaptatif, similaire à celui employé dans la première phase de cette thèse. Nous avons remarqué alors que, lors de

la variation des paramètres, le contrôleur adaptatif était en mesure de suivre le signal de référence désiré avec un léger comportement transitoire suite à la variation des paramètres. Par contre, le contrôleur non-adaptatif était incapable d'assurer le suivi de trajectoire lorsque les paramètres du système se sont mis à varier et s'est retrouvé dans un état instable. En ce qui concerne la conception du contrôleur, nous avons adopté la même stratégie de choix des paramètres de réglage que celle décrite dans le paragraphe précédent. Cette mesure vise à accélérer la convergence des états à leurs trajectoires désirées et à réduire l'amplitude et la saturation du signal de commande. Suite à cette étude, il est devenu évident que les contrôleurs adaptatifs sont la meilleure option pour la commande des systèmes hydrauliques, étant donné que les paramètres de tels systèmes sont susceptibles de varier en fonction des conditions d'opération. La commande adaptative indirecte est particulièrement recommandée parce qu'elle aboutit aux valeurs réelle et physique des paramètres du système.

Dans une troisième étape, nous avons développé une stratégie de contrôle nonlinéaire pour une suspension active électrohydraulique. Étant donné que le modèle mathématique de la suspension active électrohydraulique est ni triangulaire inférieur, ni triangulaire supérieur mais plutôt entre les deux; il n'était pas possible d'utiliser ni le backstepping ni le forwarding pour la commande. C'est pourquoi, nous avons fait un changement de variables qui permet au système d'être classé dans la catégorie des systèmes entrelacés. Par conséquent, il est devenu possible de le commander par une combinaison entrelacée de backstepping et de forwarding. Le contrôleur que nous avons conçu a réussi à stabiliser le mouvement vertical de la carrosserie de la voiture face aux perturbations de la route et de réduire les agitations transmises aux passagers. Deux essais de simulation ont été faits: le premier en utilisant une perturbation déterministe du trajet formée par deux bosses successives, le second en utilisant une perturbation aléatoire avec des amplitudes variables. L'utilisation de cette stratégie de commande a permis d'aboutir à un contrôle complet de la suspension active électrohydraulique, sans laisser aucune dynamique interne, contrairement à beaucoup d'autres approches de contrôle. Les résultats ont été comparés avec ceux obtenus par l'emploi d'un contrôleur PID classique et un contrôleur par mode de glissement. Le PID évidemment a conduit à des résultats moins efficaces, alors que le mode de glissement, tout en donnant des

résultats intéressants dans la réduction du mouvement vertical de la voiture, a généré un signal de contrôle à forte amplitude impliquant des oscillations à hautes fréquences. Ceci peut éventuellement endommager les composants hydrauliques en particulier la servovalve. Les résultats mentionnés précédemment sont très encourageants, surtout que la commande basée sur le backstepping et le forwarding entrelacés, pour le contrôle nonlinéaire, est un sujet très actif dans les recherches récentes et la compréhension en profondeur de l'approche pourrait contribuer à l'amélioration de son application pratique.

En résumé, le backstepping ou le forwarding ne sont pas de nouvelles approches de commande en elles-mêmes. Toutefois, elles sont souvent employées inefficacement. L'amélioration que nous avons faite dans la façon de les employer dans la commande des systèmes électrohydrauliques, en bien gérant les nonlinéarités et en ajustant les paramètres de réglage du contrôleur ainsi que dans la commande d'une suspension active électrohydraulique en combinant les deux approches pour améliorer sa performance, a contribué à la valorisation de leur intérêt et leur utilité.

RECOMMANDATIONS

Pour conclure cette thèse après avoir analysé tous les résultats obtenus; l'auteur aimerait mettre le point sur quelques recommandations qui seront utiles aux personnes qui travaillerons sur le même sujet. Les recommandations sont divisées en deux parties : celles qui concernent le banc d'essai au laboratoire LITP de l'ÉTS et celles qui concernent la commande des systèmes électrohydraulique en général.

En premier lieu, concernant le banc d'essai, plusieurs améliorations peuvent êtres apportées :

- Installer un encodeur sur le moteur hydraulique afin d'avoir une mesure plus précise de sa position angulaire. Dans notre cas, la position était calculée en intégrant le signal du tachymètre, ce qui n'est pas assez précis, surtout que le signal du tachymètre engendre des bruits de mesure;
- Installer une servovalve avec LVDT serait très recommandé afin d'avoir une mesure précise de la position de son tiroir. Présentement le seul moyen de connaître la position du tiroir de la servovalve est à partir du débit, de la pression différentielle et de la masse volumique de l'huile qui n'est pas toujours connue;
- Mettre à niveau le banc d'essai en installant des vérins hydrauliques. Présentement, seulement un moteur hydraulique est installé. L'installation de vérins permettrait de faire des tests plus variés en temps réel.

En second lieu, les points suivants donneront, si traités, une valeur ajoutée au travail que nous avons déjà achevé :

- Concernant le backstepping adaptatif, nous avons remarqué que certains paramètres varient plus que d'autres. Il serait intéressant d'établir la loi de variation de ces derniers en fonction de la température et de la pression. L'installation d'un thermomètre permettra d'avoir l'instrumentation complète pour faire ce travail;
- Lorsque le banc d'essai sera équipé de vérins hydrauliques, il serait intéressant d'implanter en temps réel les résultats du chapitre quatre, concernant la commande d'une suspension active électrohydraulique. Les équipements propres à la suspension

(ressort, pneus et châssis) pourront être simulés en parallèle, créant ainsi un environnement complexe.

ANNEXE A

A : Développement complet du backstepping avec la nouvelle technique d'introduction des paramètres de contrôle.

Dans ce qui suit, nous allons détailler toutes les étapes de développement du backstepping avec la nouvelle technique qui consiste à introduire les paramètres de contrôle non seulement dans la trajectoire désirée, mais aussi dans la fonction de Lyapunov.

Ensuite, nous allons montrer que cette nouvelle technique permet d'accélérer énormément la convergence des erreurs vers zéro et d'améliorer considérablement le régime transitoire en boucle fermée.

Soit le modèle mathématique suivant du système électrohydraulique :

$$\begin{cases} \dot{x}_1 = x_2 \\ \dot{x}_2 = w_a x_3 - w_b x_2 - w_c \\ \dot{x}_3 = p_a C_d x_4 g(.) - p_b x_3 - p_c x_2 \\ \dot{x}_4 = -r_a x_4 + r_b u \\ y = x_1 ... Sortie \end{cases} \tag{A.1}$$

Où :

$$sigm(x_4) = \frac{1-e^{-ax_4}}{1+e^{-ax_4}} \; ; \; g(.) = \sqrt{\frac{P_s - x_3 sigm(x_4)}{\rho}}$$

$$r_a = \frac{1}{\tau_v} \quad , \quad r_b = \frac{K}{\tau_v} \quad , \quad p_a = \frac{2\beta}{V} \; , \; p_b = \frac{2\beta C_L}{V} \; ,$$

$$p_c = \frac{2\beta D_m}{V} \; , \; w_a = \frac{D_m}{J} \; , \; w_b = \frac{B}{J} \quad , \quad w_c = \frac{T_L}{J}$$

Soit $e_i = x_i - x_{id}$ l'erreur entre une variable d'état et sa valeur désirée.

Étape 1 : Considérons la fonction de Lyapunov suivante :

$$V_1 = \frac{1}{2\rho_1} e_1^2 \text{ Alors, } \dot{V}_1 = \frac{e_1}{\rho_1}(\dot{x}_1 - \dot{x}_{1d}) = \frac{e_1}{\rho_1}(x_2 - \dot{x}_{1d}) \tag{A.2}$$

En prenant, $x_{2d} = \dot{x}_{1d} - \rho_1 e_1$ et en remplaçant $x_2 = e_2 + x_{2d}$, nous aurons :

$$\dot{V}_1 = -e_1^2 + \frac{e_1 e_2}{\rho_1} \text{ et } \dot{e}_1 = \dot{x}_1 - \dot{x}_{1d} = -\rho_1 e_1 + e_2$$

- Calcul de $\dot{e}_2$:

$$\begin{aligned}\dot{e}_2 &= \dot{x}_2 - \dot{x}_{2d} \\ &= w_a x_3 - w_b x_2 - w_c + \rho_1 \dot{e}_1 - \ddot{x}_{1d} \\ &= w_a x_3 - w_b (e_2 - \rho_1 e_1 + \dot{x}_{1d}) - w_c + \rho_1 (-\rho_1 e_1 + e_2) - \ddot{x}_{1d} \\ &= w_a x_3 + (w_b - \rho_1)\rho_1 e_1 + (\rho_1 - w_b) e_2 - w_b \dot{x}_{1d} - \ddot{x}_{1d} - w_c\end{aligned} \tag{A.3}$$

Étape 2 : Considérons maintenant la fonction de Lyapunov suivante :

$V_2 = \frac{1}{2\rho_1} e_1^2 + \frac{1}{2\rho_2} e_2^2$ Alors,

$$\begin{aligned}\dot{V}_2 &= \dot{V}_1 + \frac{e_2}{\rho_2}\dot{e}_2 \\ &= -e_1^2 + \frac{e_1 e_2}{\rho_1} + e_2\left[\frac{w_a}{\rho_2} x_3 + \frac{(w_b - \rho_1)\rho_1}{\rho_2} e_1 + \frac{(\rho_1 - w_b)}{\rho_2} e_2 - \frac{w_b}{\rho_2}\dot{x}_{1d} - \frac{\ddot{x}_{1d}}{\rho_2} - \frac{w_c}{\rho_2}\right] \\ &= -e_1^2 + e_2\left[\frac{w_a}{\rho_2} x_3 + \left(\frac{1}{\rho_1} + \frac{(w_b - \rho_1)\rho_1}{\rho_2}\right) e_1 + \frac{(\rho_1 - w_b)}{\rho_2} e_2 - \frac{w_b}{\rho_2}\dot{x}_{1d} - \frac{\ddot{x}_{1d}}{\rho_2} - \frac{w_c}{\rho_2}\right]\end{aligned} \tag{A.4}$$

En prenant,

$$\begin{aligned}x_{3d} &= -\underbrace{\left(\frac{\rho_2}{\rho_1 w_a} + \frac{(w_b - \rho_1)\rho_1}{w_a}\right)}_{a_1} e_1 - \underbrace{\frac{(\rho_1 - w_b + \rho_2)}{w_a}}_{a_2} e_2 + \frac{w_b}{w_a}\dot{x}_{1d} + \frac{\ddot{x}_{1d}}{w_a} + \frac{w_c}{w_a} \\ &= -a_1 e_1 - a_2 e_2 + \frac{w_b}{w_a}\dot{x}_{1d} + \frac{\ddot{x}_{1d}}{w_a} + \frac{w_c}{w_a}\end{aligned} \tag{A.5}$$

Et en remplaçant $x_3 = e_3 + x_{3d}$

Nous aurons, $\dot{V}_2 = -e_1^2 - e_2^2 + \frac{w_a}{\rho_1} e_2 e_3$ et,

$$\begin{aligned}\dot{e}_2 &= w_a\left(e_3 - a_1 e_1 - a_2 e_2 + \frac{w_b}{w_a}\dot{x}_{1d} + \frac{\ddot{x}_{1d}}{w_a} + \frac{w_c}{w_a}\right) \\ &\quad + (w_b - \rho_1)\rho_1 e_1 + (\rho_1 - w_b) e_2 - w_b \dot{x}_{1d} - \ddot{x}_{1d} - w_c \\ &= -\frac{\rho_2}{\rho_1} e_1 - \rho_2 e_2 + w_a e_3\end{aligned} \tag{A.6}$$

- Calcul de $\dot{e}_3$:

Nous savons que : $e_3 = x_3 - x_{3d} = x_3 + a_1 e_1 + a_2 e_2 - \frac{w_b}{w_a}\dot{x}_{1d} - \frac{\ddot{x}_{1d}}{w_a} - \frac{w_c}{w_a}$ (A.7)

Alors :

$$\begin{aligned}
\dot{e}_3 &= \dot{x}_3 - \dot{x}_{3d} \\
&= \left(p_a C_d x_4 g(.) - p_b x_3 - p_c x_2\right) + a_1\dot{e}_1 + a_2\dot{e}_2 - \frac{w_b}{w_a}\ddot{x}_{1d} - \frac{\dddot{x}_{1d}}{w_a} \\
&= \left[p_a C_d x_4 g(.) - p_b\left(e_3 - a_1 e_1 - a_2 e_2 + \frac{w_b}{w_a}\dot{x}_{1d} + \frac{\ddot{x}_{1d}}{w_a} + \frac{w_c}{w_a}\right) - p_c\left(e_2 - \rho_1 e_1 + \dot{x}_{1d}\right)\right] \\
&\quad + a_1\left(-\rho_1 e_1 + e_2\right) + a_2\left(-\frac{\rho_2}{\rho_1}e_1 - \rho_2 e_2 + w_a e_3\right) - \frac{w_b}{w_a}\ddot{x}_{1d} - \frac{\dddot{x}_{1d}}{w_a} \\
&= p_a C_d x_4 g(.) + \underbrace{\left(p_b a_1 + p_c\rho_1 - a_1\rho_1 - \frac{\rho_2}{\rho_1}a_2\right)}_{b_1} e_1 + \underbrace{\left(p_b a_2 - p_c + a_1 - a_2\rho_2\right)}_{b_2} e_2 \\
&\quad + \underbrace{(w_a a_2 - p_b)}_{b_3} e_3 - \underbrace{\left(\frac{p_b w_b}{w_a} + p_c\right)}_{b_4}\dot{x}_{1d} - \underbrace{\left(\frac{p_b}{w_a} + \frac{w_b}{w_a}\right)}_{b_5}\ddot{x}_{1d} - \frac{\dddot{x}_{1d}}{w_a} - p_b\frac{w_c}{w_a} \\
&= p_a C_d x_4 g(.) + b_1 e_1 + b_2 e_2 + b_3 e_3 - b_4\dot{x}_{1d} - b_5\ddot{x}_{1d} - \frac{\dddot{x}_{1d}}{w_a} - p_b\frac{w_c}{w_a}
\end{aligned} \tag{A.8}$$

Étape 3 : Considérons à cette étape la fonction de Lyapunov suivante :

$V_3 = \frac{1}{2\rho_1}e_1^2 + \frac{1}{2\rho_2}e_2^2 + \frac{1}{2\rho_3}e_3^2$ Alors,

$$\begin{aligned}
\dot{V}_3 &= \dot{V}_2 + \frac{e_3}{\rho_3}\dot{e}_3 \\
&= -e_1^2 - e_2^2 + e_3\left\{\begin{array}{l} \frac{p_a C_d x_4 g(.)}{\rho_3} + \frac{b_1}{\rho_3}e_1 + (\frac{b_2}{\rho_3} + \frac{w_a}{\rho_2})e_2 + \frac{b_3}{\rho_3}e_3 - \frac{b_4}{\rho_3}\dot{x}_{1d} - \frac{b_5}{\rho_3}\ddot{x}_{1d} \\ -\frac{\dddot{x}_{1d}}{\rho_3 w_a} - \frac{p_b w_c}{\rho_3 w_a}\end{array}\right\}
\end{aligned} \tag{A.9}$$

En prenant,

$$x_{4d} = \frac{1}{p_a C_d g(.)}\left[-b_1 e_1 - (b_2 + \frac{\rho_3 w_a}{\rho_2})e_2 - (b_3 + \rho_3)e_3 + b_4\dot{x}_{1d} + b_5\ddot{x}_{1d} + \frac{\dddot{x}_{1d}}{w_a} + \frac{p_b w_c}{w_a}\right] \tag{A.10}$$

Et en remplaçant $x_4 = e_4 + x_{4d}$

Nous aurons, $\dot{V}_3 = -e_1^2 - e_2^2 - e_3^2 + \frac{p_a C_d g(.)}{\rho_3} e_3 e_4$ et,

$$\dot{e}_3 = p_a C_d \left[e_4 \frac{1}{p_a C_d g(.)} \left\{ \begin{array}{l} -b_1 e_1 - (b_2 + \frac{\rho_3 w_a}{\rho_2}) e_2 - b_3 e_3 + b_4 \dot{x}_{1d} + b_5 \ddot{x}_{1d} \\ + \frac{\dddot{x}_{1d}}{w_a} + \frac{p_b w_c}{w_a} - \rho_3 e_3 \end{array} \right\} \right] g(.)$$

$$+ b_1 e_1 + b_2 e_2 + b_3 e_3 - b_4 \dot{x}_{1d} - b_5 \ddot{x}_{1d} - \frac{\dddot{x}_{1d}}{w_a} - p_b \frac{w_c}{w_a} \qquad \text{(A.11)}$$

$$= -\frac{\rho_3}{\rho_2} w_a e_2 - \rho_3 e_3 + p_a C_d g(.) e_4$$

Remarque : La fonction x_{4d} dépend de $g(.)$, qui à son tour dépend de x_4. Ceci risque d'induire une confusion, étant donné que la variable stabilisée dépend d'elle-même. En effet, ce qui précède n'est pas tout à fait vrai, parce que $g(.)$ dépend du signe de x_4 et non pas de la valeur de x_4.

Posons :

$$h(.) = -b_1 e_1 - \underbrace{\left(b_2 + \frac{\rho_3 w_a}{\rho_2} \right)}_{c_1} e_2 - \underbrace{(b_3 + \rho_3)}_{c_2} e_3 + b_4 \dot{x}_{1d} + b_5 \ddot{x}_{1d} + \frac{\dddot{x}_{1d}}{w_a} + \frac{p_b w_c}{w_a}$$

$$= -b_1 e_1 - c_1 e_2 - c_2 e_3 + b_4 \dot{x}_{1d} + b_5 \ddot{x}_{1d} + \frac{\dddot{x}_{1d}}{w_a} + \frac{p_b w_c}{w_a} \qquad \text{(A.12)}$$

Alors : $x_{4d} = \frac{1}{p_a C_d g(.)} h(.)$

- Calcul de $\dot{e}_4$:

Nous savons que $e_4 = x_4 - \frac{1}{p_a C_d g(.)} h(.)$, alors :

$$\dot{e}_4 = \dot{x}_4 - \frac{1}{p_a C_d g(.)} \dot{h}(.) - h(.) \frac{d}{dt} \left(\frac{1}{p_a C_d g(.)} \right) \qquad \text{(A.13)}$$

1. Calcul de $\dot{x}_4$:

$$\dot{x}_4 = -r_a x_4 + r_b u$$

2. Calcul de $\dot{h}(.)$:

$$\begin{aligned}
\dot{h}(.) &= -b_1\dot{e}_1 - c_1\dot{e}_2 - c_2\dot{e}_3 + b_4\ddot{x}_{1d} + b_5\dddot{x}_{1d} + \frac{x_{4d}^{(4)}}{w_a} \\
&= -b_1\left(-\rho_1 e_1 + e_2\right) - c_1\left(-\frac{\rho_2}{\rho_1}e_1 - \rho_2 e_2 + w_a e_3\right) - c_2\left(-\frac{\rho_3}{\rho_2}w_a e_2 - \rho_3 e_3 + p_a C_d g(.)e_4\right) \\
&\quad + b_4\ddot{x}_{1d} + b_5\dddot{x}_{1d} + \frac{x_{4d}^{(4)}}{w_a} \\
&= \underbrace{\left(b_1\rho_1 + c_1\frac{\rho_2}{\rho_1}\right)}_{d_1}e_1 + \underbrace{\left(-b_1 + c_1\rho_2 + c_2\frac{\rho_3}{\rho_2}w_a\right)}_{d_2}e_2 + \underbrace{\left(-c_1 w_a + c_2\rho_3\right)}_{d_3}e_3 \\
&\quad + c_2 p_a C_d g(.)e_4 + b_4\ddot{x}_{1d} + b_5\dddot{x}_{1d} + \frac{x_{4d}^{(4)}}{w_a} \\
&= d_1 e_1 + d_2 e_2 + d_3 e_3 - c_2 p_a C_d g(.)e_4 + b_4\ddot{x}_{1d} + b_5\dddot{x}_{1d} + \frac{x_{4d}^{(4)}}{w_a}
\end{aligned} \tag{A.14}$$

Posons :

$$J(.) = \dot{h}(.) = d_1 e_1 + d_2 e_2 + d_3 e_3 - c_2 p_a C_d g(.)e_4 + b_4\ddot{x}_{1d} + b_5\dddot{x}_{1d} + \frac{x_{4d}^{(4)}}{w_a} \tag{A.15}$$

3. Calcul de $\dfrac{d}{dt}\left(\dfrac{1}{p_a C_d g(.)}\right)$:

$$\begin{aligned}
\frac{d}{dt}\left(\frac{1}{p_a C_d g(.)}\right) &= \frac{1}{2p_a C_d g(.)^3}\left[\dot{x}_3 sigm(x_4) + \underbrace{\left(\frac{2ae^{-ax_4}}{(1+e^{-ax_4})^2}\right)}_{f(.)}x_3\dot{x}_4\right] \\
&= \frac{1}{2p_a C_d g(.)^3}\left[\dot{x}_3 sigm(x_4) + \underbrace{\left(\frac{2ae^{-ax_4}}{(1+e^{-ax_4})^2}\right)}_{f(.)}x_3\left(-r_a x_4 + r_b u\right)\right] \\
&= \frac{1}{2\rho p_a C_d g(.)^3}\left[\dot{x}_3 sigm(x_4) - r_a f(.)x_3 x_4\right] + \frac{r_b f(.)h(.)x_3}{2\rho p_a C_d g(.)^3}u
\end{aligned} \tag{A.16}$$

Revenons au calcul de $\dot{e}_4$:

$$\dot{e}_4 = -r_a x_4 + r_b u - \frac{1}{p_a C_d g(.)} J(.) - \left\{ \begin{array}{l} \frac{1}{2\rho p_a C_d g(.)^3}\left[\dot{x}_3 sigm(x_4) - r_a f(.) x_3 x_4\right] \\ + \frac{r_b f(.) h(.) x_3}{2\rho p_a C_d g(.)^3} u \end{array} \right\} h(.)$$

$$= -r_a x_4 - \frac{1}{p_a C_d g(.)} J(.) - \frac{1}{2\rho p_a C_d g(.)^3}\left[\dot{x}_3 sigm(x_4) - r_a f(.) x_3 x_4\right] h(.) \qquad \text{(A.17)}$$

$$+ r_b \left(1 - \frac{r_b f(.) h(.) x_3}{2\rho p_a C_d g(.)^3}\right) u$$

Étape 4 : Considérons finalement la fonction de Lyapunov globale suivante

$V_4 = \frac{1}{2\rho_1} e_1^2 + \frac{1}{2\rho_2} e_2^2 + \frac{1}{2\rho_3} e_3^2 + \frac{1}{2\rho_4} e_4^2$ Alors,

$$\dot{V}_4 = \dot{V}_3 + \frac{e_4}{\rho_4} \dot{e}_4$$

$$= -e_1^2 - e_2^2 - e_3^2 + e_4 \left[\begin{array}{l} -\frac{r_a}{\rho_4} x_4 - \frac{J(.)}{\rho_4 p_a C_d g(.)} + \frac{p_a C_d g(.) e_3}{\rho_3} \\ -\frac{1}{2 p_a C_d \rho_4 \rho . g(.)^3}\left(\dot{x}_3 sgm(x_4) - r_a x_3 x_4 f(.)\right) h(.) \\ \frac{r_b}{\rho_4}\left(1 - \frac{x_3 f(.) h(.)}{2 p_a C_d \rho . g(.)^3}\right) u \end{array} \right] \qquad \text{(A.18)}$$

Si nous choisissons la loi de commande suivante :

$$u = \frac{\left[-\frac{\rho_4}{\rho_3} p_a C_d g(.) e_3 + r_a x_4 + \frac{J(.)}{p_a C_d g(.)} + \frac{1}{2 p_a C_d \rho . g(.)^3}\left(\dot{x}_3 sgm(x_4) - r_a x_3 x_4 f(.)\right) h(.) - \rho_4 e_4 \right]}{r_b \left(1 - \frac{x_3 f(.) h(.)}{2 p_a C_d \rho . g(.)^3}\right)} \qquad \text{(A.19)}$$

Nous aurons, $\dot{V}_4 = -e_1^2 - e_2^2 - e_3^2 - e_4^2 < 0$ et,

$$\dot{e}_4 = -\frac{\rho_4}{\rho_3} p_a C_d g(.) e_3 - \rho_4 e_4 \qquad \text{(A.20)}$$

L'équation de $\dot{V}_4$ montre que la dynamique de l'erreur et globalement asymptotiquement stable.

Dynamique de l'erreur :

Si nous récapitulons les équations de la dynamique de l'erreur, nous aurons :

$$\begin{cases} \dot{e}_1 = -\rho_1 e_1 + e_2 \\ \dot{e}_2 = -\dfrac{\rho_2}{\rho_1} e_1 - \rho_2 e_2 + w_a e_3 \\ \dot{e}_3 = -\dfrac{\rho_3}{\rho_2} w_a e_2 - \rho_3 e_3 + p_a C_d g(.) e_4 \\ \dot{e}_4 = -\dfrac{\rho_4}{\rho_3} p_a C_d g(.) e_3 - \rho_4 e_4 \end{cases} \tag{A.21}$$

Ou bien sous forme matricielle :

$$\begin{pmatrix} \dot{e}_1 \\ \dot{e}_2 \\ \dot{e}_3 \\ \dot{e}_4 \end{pmatrix} = \underbrace{\begin{pmatrix} -\rho_1 & 1 & 0 & 0 \\ -\dfrac{\rho_2}{\rho_1} & -\rho_2 & w_a & 0 \\ 0 & -\dfrac{\rho_3}{\rho_2} w_a & -\rho_3 & p_a C_d g(.) \\ 0 & 0 & -\dfrac{\rho_4}{\rho_3} p_a C_d g(.) & -\rho_4 \end{pmatrix}}_{A_1} \begin{pmatrix} e_1 \\ e_2 \\ e_3 \\ e_4 \end{pmatrix} \tag{A.22}$$

Comme nous le remarquons, les paramètres de contrôle apparaissent non seulement sur la diagonale principale de la matrice A_1; mais aussi sur la première sous-diagonale.

Donc, un bon choix des paramètres, serait de façon à rendre les termes de la première sous-diagonale :

$$-\frac{\rho_2}{\rho_1},\ -\frac{\rho_3}{\rho_2} w_a,\ -\frac{\rho_4}{\rho_3} p_a C_d g(.)$$

Très faible par rapport aux termes de la diagonale principale qui sont les paramètres de contrôle ρ_1, ρ_2, ρ_3 et ρ_4. De cette manière la matrice A_1 tend à se comporter comme une matrice triangulaire supérieure dont les valeurs propres sont $-\rho_1, -\rho_2, -\rho_3$ et $-\rho_4$. En procédant ainsi, nous garantissons que seulement les termes de la diagonale $-\rho_1, -\rho_2, -\rho_3$ et $-\rho_4$ affectent la convergence des erreurs vers zéro.

ANNEXE B

B : Développement du backstepping adaptatif indirect.

Le backstepping adaptatif indirect, du point de vue développement mathématique, est réalisé de la même manière que le backstepping non-adaptif. La seule différence est que les paramètres du système, qui étaient supposés connus dans le cas non-adaptatif, sont maintenant inconnus. Par conséquent, ces paramètres sont identifiés continuellement à chaque pas de calcul pendant le processus de contrôle; et leur valeur est injectée dans la structure du contrôleur.

Nous supposons ici que la variation des paramètres du système électrohydraulique est faible et surtout lente. En d'autres termes, les paramètres du système sont supposés constants sur l'intervalle de calcul; par suite il n'est pas nécessaire de calculer leur dérivée temporelle vu que cette dernière est presque nulle.

L'algorithme d'identification utilisé est celui des moindres carrés récursifs (MCR) à trace constante pour les systèmes à paramètres variables.

En ce référant au chapitre 3, le système à identifier est le suivant :

$$\begin{pmatrix} \dot{x}_2 \\ \dot{x}_3 \end{pmatrix} = \begin{pmatrix} x_3 & 0 \\ -x_2 & 0 \\ -1 & 0 \\ 0 & x_4 g(.) \\ 0 & -x_3 \\ 0 & -x_2 \end{pmatrix}^T \times \begin{pmatrix} w_a \\ w_b \\ w_c \\ p_a \\ p_b \\ p_c \end{pmatrix} \tag{B.1}$$

Étant donné que le système est linéaire par rapport à ses paramètres nous pouvons employer l'algorithme des moindres carrés récursifs. Pour cela nous avons posé :

$$\begin{cases} y(t) = \begin{pmatrix} \dot{x}_2 \\ \dot{x}_3 \end{pmatrix} \\ \varphi(t) = \begin{pmatrix} x_3 & -x_2 & -1 & 0 & 0 & 0 \\ 0 & 0 & 0 & x_4 g(.) & -x_3 & -x_2 \end{pmatrix} \\ \theta(t)^T = \begin{pmatrix} w_a & w_b & w_c & p_a & p_b & p_c \end{pmatrix} \end{cases} \tag{B.2}$$

$y(t)$ est le vecteur d'observation, $\varphi(t)$ est la matrice des régresseurs et $\theta(t)$ est le vecteur des paramètres inconnus à identifier.

Donc, nous pouvons écrire :

$$y(t) = \varphi(t)\theta(t) \tag{B.3}$$

Nous définissons maintenant l'erreur $\varepsilon(t)$ de $y(t)$, l'erreur quadratique $V(\theta)$ de $y(t)$ et la matrice $P(t)$ suivantes :

$$\varepsilon(t) = y(t) - \varphi(t)\theta(t)$$

$$V(\theta) = \int_0^t e^{\alpha(t-s)} \left(y(s) - \varphi(s)\theta(s) \right)^2 ds \quad ; \; 0 < \alpha < 1 \tag{B.4}$$

$$P(t) = \left(\int_0^t \varphi(s)\varphi(s)^T ds \right)^{-1}$$

Les paramètres sont identifiés de manière à minimiser l'erreur quadratique $V(\theta)$. Alors, l'algorithme d'identification est implanté en temps réel de la manière suivante :

1. Nous posons un instant t_0;
   a. Lorsque $t < t_0$ l'erreur $\varepsilon(t)$ est surtout due à l'erreur d'estimation et par suite les variations de $\theta(t)$ peuvent être négligées;
   b. À partir de $t > t_0$ l'erreur $\varepsilon(t)$ provient surtout de la variation du vrai vecteur $\theta(t)$ et non de l'erreur d'estimation.
2. Par conséquent, pour un système lentement variant comme le nôtre, nous commençons par appliquer l'algorithme MCR régulier, en supposant que le système est invariant;
3. À partir de l'instant t_0 où la trace de $P(t_0)$ devient suffisamment faible, nous appliquons l'algorithme MCR à trace constante. Typiquement, la trace de $P(t_0)$ est considérée faible si elle est inférieure à N×c, N étant le nombre des paramètres à estimer (5 dans notre cas)

et c une constante comprise entre 0 et 4;

En définitive, l'algorithme MCR pour les systèmes variants devient le suivant :

1. Initialement, nous introduisons la constante c et nous donnons à t_0 une très grande valeur;
2. La matrice $P(t\text{-}1)$ et les vecteurs $\varphi(t)$ et $\hat{\theta}(t)$, obtenus durant l'étape t, sont stockés dans la mémoire;
3. À l'instant t, nous lisons les valeurs de $y(t)$ et de $u(t)$ (la loi de commande);
4. Durant l'étape $t + 1$, c'est-à-dire entre t et $t + 1$, nous effectuons successivement les opérations suivantes:
   a. $\hat{y}(t) = \varphi(t)\hat{\theta}(t)$;
   b. $\varepsilon(t) = y(t) - \hat{y}(t)$;
   c. Si $t > t_0$, nous passons à f;
   d. $P(t) = P(t-1) - \dfrac{P(t-1).\varphi^T(t).\varphi(t).P(t-1)}{1/\lambda(t) + \varphi(t).P(t-1).\varphi^T(t)}$, avec $\lambda(0) = k$, k constante arbitraire;
   e. Si la trace de $P(t) \leq N \times c$, nous posons $t_0 = t$ et $tr = \text{trace}[P(t)]$. Nous passons à h;
   f. $\lambda(t) = 1 - \dfrac{\left\|P(t-1).\varphi(t)\right\|^2}{k + \varphi^T(t).P(t-1).\varphi(t).tr}$;
   g. $P(t) = \dfrac{1}{\lambda(t)}\left[P(t-1) - \dfrac{P(t-1).\varphi(t).\varphi^T(t).P(t-1)}{k + \varphi^T(t).P(t-1).\varphi(t)}\right]$;
   h. $\hat{\theta}(t+1) = \hat{\theta}(t) + \alpha_t.P(t).\varphi(t).\varepsilon(t)$;
   i. $\varphi^T(t+1) = [-y(t), \varphi_1(t), \ldots, \varphi_{(n-1)}(t), u(t), \varphi_{(n+1)}(t), \ldots, \varphi_{(n+m-1)}(t)]$.

ANNEXE C

C : Développement complet de la commande entrelacée pour une suspension active électrohydraulique

Par convenance, le 'backstepping' et le 'integrator forwarding' sont introduits dans la littérature comme étant des stratégies de commande pour les systèmes qui consistent en un sous système z-nonlinéaire et un sous-système formé par une chaîne d'intégrateurs. Cependant, ces deux stratégies s'appliquent à des classes plus larges de système.

En effet, le backstepping s'applique à des systèmes qui ont la structure 'feedback' ou triangulaire inférieure suivante :

$$\begin{cases} \dot{z} = f(z) + \psi(z, \xi_1)\xi_1 \\ \dot{\xi}_1 = a_1(\xi_1, \xi_2) \\ \dot{\xi}_2 = a_2(\xi_1, \xi_2, \xi_3) \\ \vdots \\ \dot{\xi}_n = a_n(\xi_1, \xi_2, \xi_3, ..., \xi_n, u) \end{cases} \tag{C.1}$$

D'un autre côté le 'integrator forwarding' s'applique à des systèmes qui ont la structure 'feedforward' ou triangulaire supérieure suivante :

$$\begin{cases} \dot{\xi}_1 = f_1(\xi_1) + \psi_1(\xi_1, \xi_2, \xi_3, ..., \xi_n, z, u) \\ \dot{\xi}_2 = f_2(\xi_2) + \psi_2(\xi_2, \xi_3, ..., \xi_n, z, u) \\ \vdots \\ \dot{\xi}_{n-1} = f_{n-1}(\xi_{n-1}) + \psi_{n-1}(\xi_{n-1}, \xi_n, z, u) \\ \dot{z} = f(z) + \psi(z, \xi_n)\xi_n \\ \dot{\xi}_n = u \end{cases} \tag{C.2}$$

La combinaison de ces deux stratégies de commande s'applique pour des systèmes dont la structure est un mélange des deux structures précédentes, avec quelques conditions à vérifier. Tel est le cas de la suspension active électrohydraulique.

Soit alors le modèle ci-dessous, d'une suspension active électrohydraulique, tel que développé dans le chapitre 4 :

$$\begin{cases} \dot{x}_1 = x_2 \\ \dot{x}_2 = -a_0(x_1 - x_3) - b_0(x_2 - x_4) + a_1 x_5 \\ \dot{x}_3 = x_4 \\ \dot{x}_4 = d_0(x_1 - x_3) + d_1(x_2 - x_4) - h_1(x_3 - x_r) - b_1(x_4 - \dot{x}_r) - c_1 x_5 \\ \dot{x}_5 = \dfrac{J_1}{f(.)}\left(C_d x_6 g(.) + A(x_4 - x_2) - L x_5\right) \\ \dot{x}_6 = -\dfrac{1}{\tau} x_6 + \dfrac{k_v}{\tau} u \end{cases} \quad \text{(C.3)}$$

Avec :

$$g(.) = \sqrt{\frac{P_s - sigm(x_6).x_5}{\rho}} \ ;$$

$$sigm(x_6) = \frac{1 - e^{-ax_6}}{1 + e^{-ax_6}} \ ;$$

$$f(.) = V_0^2 - A^2(x_1 - x_3)^2$$

Posons : $x = \begin{bmatrix} x_1 & x_2 & x_3 & x_4 & x_5 & x_6 \end{bmatrix}^T$

Et,

$$F(x,u) = \begin{pmatrix} x_2 \\ -a_0(x_1 - x_3) - b_0(x_2 - x_4) + a_1 x_5 \\ x_4 \\ d_0(x_1 - x_3) + d_1(x_2 - x_4) - h_1(x_3 - x_r) - b_1(x_4 - \dot{x}_r) - c_1 x_5 \\ \dfrac{J_1}{f(.)}\left(C_d x_6 g(.) + A(x_4 - x_2) - L x_5\right) \\ -\dfrac{1}{\tau} x_6 + \dfrac{k_v}{\tau} u \end{pmatrix} \quad \text{(C.4)}$$

Alors : $\dot{x} = F(x,u)$

La matrice de configuration $P(x,u) = \begin{pmatrix} \dfrac{\partial F}{\partial x} & \dfrac{\partial F}{\partial u} \end{pmatrix}$ de ce système est:

$$P=\begin{pmatrix} 0 & 1 & 0 & 0 & 0 & 0 & 0 \\ -a_0 & -b_0 & a_0 & b_0 & a_1 & 0 & 0 \\ 0 & 0 & 0 & 1 & 0 & 0 & 0 \\ d_0 & d_1 & -(d_0+h_1) & -(d_1+b_1) & -c_1 & 0 & 0 \\ \alpha & -\dfrac{J_1 A}{f(.)} & \beta & \dfrac{J_1 A}{f(.)} & \gamma & \dfrac{C_d J_1 g(.)}{f(.)} & 0 \\ 0 & 0 & 0 & 0 & 0 & -\dfrac{1}{\tau} & \dfrac{K_v}{\tau} \end{pmatrix} \tag{C.5}$$

Avec,

$$\begin{aligned} \alpha &= \frac{\partial}{\partial x_1}\left(\frac{J_1}{f(.)}\left(C_d x_6 g(.)+A(x_4-x_2)-Lx_5\right)\right) \\ &= \frac{\partial}{\partial x_1}\left(\frac{J_1}{\left[V_0^2-A^2(x_1-x_3)^2\right]}\left(C_d x_6 g(.)+A(x_4-x_2)-Lx_5\right)\right) \\ &= \frac{2A^2 J_1(x_1-x_3)}{\left[V_0^2-A^2(x_1-x_3)^2\right]^2}\left(C_d x_6 g(.)+A(x_4-x_2)-Lx_5\right) \\ &= \frac{2A^2 J_1}{f(.)^2}\left(C_d x_6 g(.)+A(x_4-x_2)-Lx_5\right)(x_1-x_3) \end{aligned} \tag{C.6}$$

$$\begin{aligned} \beta &= \frac{\partial}{\partial x_3}\left(\frac{J_1}{f(.)}\left(C_d x_6 g(.)+A(x_4-x_2)-Lx_5\right)\right) \\ &= \frac{\partial}{\partial x_3}\left(\frac{J_1}{\left[V_0^2-A^2(x_1-x_3)^2\right]}\left(C_d x_6 g(.)+A(x_4-x_2)-Lx_5\right)\right) \\ &= \frac{-2A^2 J_1(x_1-x_3)}{\left[V_0^2-A^2(x_1-x_3)^2\right]^2}\left(C_d x_6 g(.)+A(x_4-x_2)-Lx_5\right) \\ &= -\frac{2A^2 J_1}{f(.)^2}\left(C_d x_6 g(.)+A(x_4-x_2)-Lx_5\right)(x_1-x_3) \end{aligned} \tag{C.7}$$

$$\gamma = \frac{\partial}{\partial x_5}\left(\frac{J_1}{f(.)}\left(C_d x_6 g(.) + A(x_4 - x_2) - L x_5\right)\right) \qquad \text{si } sigm(x_6) > 0$$

$$= \frac{\partial}{\partial x_5}\left(\frac{J_1}{f(.)}\left(C_d x_6 \sqrt{\frac{P_s - x_5}{\rho}} + A(x_4 - x_2) - L x_5\right)\right)$$

$$= \frac{J_1}{f(.)}\left(C_d x_6 \frac{-1}{2\rho\sqrt{\frac{P_s - x_5}{\rho}}} - L\right) \qquad \text{(C.8)}$$

$$= -\frac{J_1}{f(.)}\left(\frac{C_d x_6}{2\rho g(.)} + L\right)$$

$$\gamma = \frac{\partial}{\partial x_5}\left(\frac{J_1}{f(.)}\left(C_d x_6 g(.) + A(x_4 - x_2) - L x_5\right)\right) \qquad \text{si } sigm(x_6) < 0$$

$$= \frac{\partial}{\partial x_5}\left(\frac{J_1}{f(.)}\left(C_d x_6 \sqrt{\frac{P_s + x_5}{\rho}} + A(x_4 - x_2) - L x_5\right)\right)$$

$$= \frac{J_1}{f(.)}\left(C_d x_6 \frac{1}{2\rho\sqrt{\frac{P_s + x_5}{\rho}}} - L\right) \qquad \text{(C.9)}$$

$$= \frac{J_1}{f(.)}\left(\frac{C_d x_6}{2\rho g(.)} - L\right)$$

Nous rappelons que la fonction sigmoïde [$sigm(x_6)$] n'est qu'une approximation continue de la fonction discontinue $sign(x_6)$.

Comme nous l'avons expliqué dans le chapitre 4, la première condition pour que le système soit entrelacé n'est pas vérifiée par la matrice *P*.

C'est pourquoi nous allons faire un changement de variables qui permettra à cette condition d'être vérifiée.

Changement de variables

Posons :

$$y_1 = x_1;\ y_2 = x_2;\ y_3 = x_1 - x_3 = y_1 - x_3;\ y_4 = x_2 - x_4 = y_2 - x_4;\ y_5 = x_5;\ y_6 = x_6 \quad \text{(C.10)}$$

Alors le nouveau système devient:

$$\begin{cases} \dot{y}_1 = y_2 \\ \dot{y}_2 = -a_0 y_3 - b_0 y_4 + a_1 y_5 \\ \dot{y}_3 = y_4 \\ \dot{y}_4 = \dot{x}_2 - \dot{x}_4 \\ \quad = [-a_0(x_1 - x_3) - b_0(x_2 - x_4) + a_1 x_5] - \begin{Bmatrix} d_0(x_1 - x_3) + d_1(x_2 - x_4) \\ -h_1(x_3 - x_r) - b_1(x_4 - \dot{x}_r) - c_1 x_5 \end{Bmatrix} \\ \quad = -(a_0 + d_0) y_3 - (b_0 + d_1) y_4 + (a_1 + c_1) y_5 + h_1(y_1 - y_3 - x_r) + b_1(y_2 - y_4 - \dot{x}_r) \\ \dot{y}_5 = \dfrac{J_1}{f(.)}(-A y_4 - L y_5 + C_d g(.) y_6) \\ \dot{y}_6 = -\dfrac{1}{\tau} y_6 + \dfrac{k_v}{\tau} u \end{cases} \quad \text{(C.11)}$$

Rappelons que : $x_3 - x_r = y_1 - y_3 - x_r$ est le déplacement vertical du pneu par rapport à la route. Ce déplacement est dû à l'élasticité du pneu et peut être supposé très faible. C'est pourquoi nous allons considérer après ce nouveau changement de variable que la perturbation est $x_3 - x_r = y_r$.

Le nouveau modèle mathématique devient alors :

$$\begin{cases} \dot{y}_1 = y_2 \\ \dot{y}_2 = -a_0 y_3 - b_0 y_4 + a_1 y_5 \\ \dot{y}_3 = y_4 \\ \dot{y}_4 = -\overbrace{(a_0 + d_0)}^{A_1} y_3 - \overbrace{(b_0 + d_1)}^{A_2} y_4 + \overbrace{(a_1 + c_1)}^{A_3} y_5 + h_1 y_r + b_1 \dot{y}_r \\ \dot{y}_5 = \dfrac{J_1}{f(.)}(-A y_4 - L y_5 + C_d g(.) y_6) \\ \dot{y}_6 = -\dfrac{1}{\tau} y_6 + \dfrac{k_v}{\tau} u \end{cases} \quad \text{(C.12)}$$

Avec,

$$g(.)=\sqrt{\frac{P_s-sigm(y_6).y_5}{\rho}}\ ;$$

$$sigm(x_6)=\frac{1-e^{-ay_6}}{1+e^{-ay_6}}\ ;$$

$$f(.)=V_0^2-A^2y_3^2$$

Posons :

$$y=\begin{bmatrix}y_1 & y_2 & y_3 & y_4 & y_5 & y_6\end{bmatrix}^T \tag{C.13}$$

Et,

$$F(y,u)=\begin{pmatrix} y_2 \\ -a_0y_3-b_0y_4+a_1y_5 \\ y_4 \\ -A_1y_3-A_2y_4+A_3y_5+h_1y_r+b_1\dot{y}_r \\ \frac{J_1}{f(.)}\left(-Ay_4-Ly_5+C_dg(.)y_6\right) \\ -\frac{1}{\tau}y_6+\frac{k_v}{\tau}u \end{pmatrix} \tag{C.14}$$

Alors :

$$\dot{y}=F(y,u)$$

La nouvelle matrice de configuration $P(y,u)=\begin{pmatrix}\frac{\partial F}{\partial y} & \frac{\partial F}{\partial u}\end{pmatrix}$ de ce nouveau système est:

$$P=\begin{pmatrix} 0 & 1 & 0 & 0 & 0 & 0 & 0 \\ 0 & 0 & -a_0 & -b_0 & a_1 & 0 & 0 \\ 0 & 0 & 0 & 1 & 0 & 0 & 0 \\ 0 & 0 & -A_1 & -A_2 & A_3 & 0 & 0 \\ 0 & 0 & \delta & -\frac{J_1A}{f(.)} & \theta & \frac{C_dJ_1g(.)}{f(.)} & 0 \\ 0 & 0 & 0 & 0 & 0 & -\frac{1}{\tau} & \frac{K_v}{\tau} \end{pmatrix} \tag{C.15}$$

Avec,

$$\begin{aligned}\delta &= \frac{\partial}{\partial y_3}\left(\frac{J_1}{f(.)}\left(C_d y_6 g(.) - A y_4 - L y_5\right)\right)\\ &= \frac{\partial}{\partial y_3}\left(\frac{J_1}{\left[V_0^2 - A^2 y_3^2\right]}\left(C_d y_6 g(.) - A y_4 - L y_5\right)\right)\\ &= \frac{2A^2 J_1 y_3}{\left[V_0^2 - A^2 y_3^2\right]^2}\left(C_d y_6 g(.) - A y_4 - L y_5\right)\\ &= \frac{2A^2 J_1}{f(.)^2}\left(C_d y_6 g(.) - A y_4 - L y_5\right) y_3\end{aligned} \tag{C.16}$$

$$\begin{aligned}\theta &= \frac{\partial}{\partial y_5}\left(\frac{J_1}{f(.)}\left(C_d y_6 g(.) - A y_4 - L y_5\right)\right) \qquad \text{si } sigm(y_6) > 0\\ &= \frac{\partial}{\partial y_5}\left(\frac{J_1}{f(.)}\left(C_d y_6 \sqrt{\frac{P_s - y_5}{\rho}} - A y_4 - L y_5\right)\right)\\ &= \frac{J_1}{f(.)}\left(C_d y_6 \frac{-1}{2\rho\sqrt{\frac{P_s - y_5}{\rho}}} - L\right)\\ &= -\frac{J_1}{f(.)}\left(\frac{C_d y_6}{2\rho g(.)} + L\right)\end{aligned} \tag{C.17}$$

$$\begin{aligned}\theta &= \frac{\partial}{\partial y_5}\left(\frac{J_1}{f(.)}\left(C_d y_6 g(.) - A y_4 - L y_5\right)\right) \qquad \text{si } sigm(y_6) < 0\\ &= \frac{\partial}{\partial y_5}\left(\frac{J_1}{f(.)}\left(C_d y_6 \sqrt{\frac{P_s + y_5}{\rho}} - A y_4 - L y_5\right)\right)\\ &= \frac{J_1}{f(.)}\left(C_d y_6 \frac{1}{2\rho\sqrt{\frac{P_s - y_5}{\rho}}} - L\right)\\ &= \frac{J_1}{f(.)}\left(\frac{C_d y_6}{2\rho g(.)} + L\right)\end{aligned} \tag{C.18}$$

Nous remarquons, que cette nouvelle matrice P vérifie la première condition pour pouvoir classer le système comme entrelacé et procéder à sa stabilisation par une série d'étapes de 'backstepping' et de 'integrator forwarding'.

Soit alors, le modèle final de la suspension active électrohydraulique :

$$\begin{cases} \dot{y}_1 = y_2 \\ \dot{y}_2 = -a_0 y_3 - b_0 y_4 + a_1 y_5 \\ \dot{y}_3 = y_4 \\ \dot{y}_4 = -A_1 y_3 - A_2 y_4 + A_3 y_5 + h_1 y_r + b_1 \dot{y}_r \\ \dot{y}_5 = \dfrac{J_1}{f(.)}\left(-A y_4 - L y_5 + C_d g(.) y_6\right) \\ \dot{y}_6 = -\dfrac{1}{\tau} y_6 + \dfrac{k_v}{\tau} u \end{cases} \tag{C.19}$$

Il est évident que le sous-système $(\dot{y}_5, \dot{y}_6)$ a une structure 'feedback'. Par contre, le sous système $(\dot{y}_1, \dot{y}_2, \dot{y}_3, \dot{y}_4)$ a une structure entrelacée, avec y_5 comme entrée :

$$\begin{cases} \dot{y}_1 = y_2 \\ \dot{y}_2 = -a_0 y_3 - b_0 y_4 + a_1 y_5 \\ \dot{y}_3 = y_4 \\ \dot{y}_4 = -A_1 y_3 - A_2 y_4 + A_3 y_5 + h_1 y_r + b_1 \dot{y}_r \end{cases} \tag{C.20}$$

Posons :

$$y^* = \begin{bmatrix} y_1 & y_2 & y_3 & y_4 \end{bmatrix}^T$$

Et,

$$F^*(y^*, y_5) = \begin{pmatrix} y_2 \\ -a_0 y_3 - b_0 y_4 + a_1 y_5 \\ y_4 \\ -A_1 y_3 - A_2 y_4 + A_3 y_5 + h_1 y_r + b_1 \dot{y}_r \end{pmatrix} \tag{C.21}$$

Alors : $\dot{y}^* = F^*(y^*, y_5)$

Pour savoir la séquence de stabilisation de ce sous système, il faut calculer sa matrice de configuration $P^*(y^*, y_5) = \begin{pmatrix} \dfrac{\partial F^*}{\partial y^*} & \dfrac{\partial F^*}{\partial y_5} \end{pmatrix}$:

$$P^* = \begin{pmatrix} 0 & 1 & 0 & 0 & 0 \\ 0 & 0 & -a_0 & -b_0 & a_1 \\ 0 & 0 & 0 & 1 & 0 \\ 0 & 0 & -A_1 & -A_2 & -A_3 \end{pmatrix} \tag{C.22}$$

Selon P^* le sous-système $(\dot{y}_1, \dot{y}_2, \dot{y}_3, \dot{y}_4)$ doit être stabilisé au début par deux étapes de 'backstepping' pour $(\dot{y}_3, \dot{y}_4)$ suivies de deux étapes de 'integrator forwarding' pour $(\dot{y}_1, \dot{y}_2)$.

Backstepping

$$\begin{cases} \dot{y}_3 = y_4 \\ \dot{y}_4 = -A_1 y_3 - A_2 y_4 + A_3 y_5 + h_1 y_r + b_1 \dot{y}_r \end{cases} \tag{C.23}$$

Étape 1 : Posons $e_3 = y_3$ et $e_4 = y_4 - y_{4d}$ et considérons la fonction de Lyapunov suivante : $V_3 = \frac{1}{2} e_3^2$,

Alors, $\dot{V}_3 = e_3 \dot{e}_3 = e_3 y_4$

Donc, la valeur désirée de y_4 qui stabilise y_3 est $y_{4d} = -k_3 e_3$. Ce qui donne $\dot{V}_3 = -k_3 e_3^2 < 0$.

Posons maintenant $e_4 = y_4 - y_{4d} = y_4 + k_3 e_3$.

Alors $\dot{e}_3 = y_4 = -k_3 e_3 + e_4$

Et,

$$\begin{aligned} \dot{e}_4 &= \dot{y}_4 + k_3 \dot{e}_3 \\ &= \left(-A_1 y_3 - A_2 y_4 + A_3 y_5 + h_1 y_r + b_1 \dot{y}_r\right) - k_3^2 e_3 + k_3 e_4 \\ &= \underbrace{(-A_1 + k_3 A_2 - k_3^2)}_{A_4} e_3 - \underbrace{(A_2 - k_3)}_{A_{50}} e_4 + A_3 y_5 + \underbrace{h_1 y_r + b_1 \dot{y}_r}_{Y_r} \end{aligned} \tag{C.24}$$

Étape 2 : Considérons maintenant la fonction de Lyapunov,

$$V_4 = V_3 + \frac{1}{2} e_4^2 = \frac{1}{2} e_3^2 + \frac{1}{2} e_4^2 \tag{C.25}$$

Alors,

$$\begin{aligned} \dot{V}_4 &= e_3(-k_3 e_3 + e_4) + e_4(A_4 e_3 - A_{50} e_4 + A_3 y_5 + Y_r) \\ &= -k_3 e_3^2 + e_4(e_3 + A_4 e_3 - A_{50} e_4 + A_3 y_5 + Y_r) \end{aligned} \tag{C.26}$$

Donc, si nous choisissons l'entrée y_5 du sous-système (C.20) de la manière suivante :

$$y_{5d} = \frac{1}{A_3}[A_{50}e_4 - (A_4 + 1)e_3 - k_4 e_4] \tag{C.27}$$

Nous aurons,

$$\begin{aligned} \dot{V}_4 &= -k_3 e_3^2 - k_4 e_4^2 + e_4 Y_r \qquad \text{développement en carré parfait} \Rightarrow \\ &= -k_3 e_3^2 - \frac{k_4}{2} e_4^2 - \frac{k_4}{2}\left(e_4 - \frac{Y_r}{k_4}\right)^2 + \frac{Y_r^2}{2k_4} \end{aligned} \tag{C.28}$$

$\dot{V}_4$ est négative pour des valeurs assez grandes de k_3 et k_4 ou plus précisément si :

$$-\frac{k_4}{2}\left(e_4 - \frac{Y_r}{k_4}\right)^2 + \frac{Y_r^2}{2k_4} \le 0 \Rightarrow$$

$$-\left(e_4 - \frac{Y_r}{k_4}\right)^2 \le -\frac{Y_r^2}{k_4^2} \Rightarrow$$

$$\left(e_4 - \frac{Y_r}{k_4}\right)^2 \ge \frac{Y_r^2}{k_4^2} \Rightarrow$$

$$e_4 - \frac{Y_r}{k_4} \ge \frac{Y_r}{k_4} \Rightarrow$$

$$Y_r \le \frac{e_4}{2k_4}. \tag{C.29}$$

Étant donné que e_4 est majorée par y_4 la condition précédente peut être écrite de la façon suivante :

$$Y_r < \frac{\max(y_4)}{2k_4} \tag{C.30}$$

En plus, en remplaçant y_5 par y_{5d} dans $\dot{e}_4$ et $\dot{y}_2$ nous aurons :

$$\dot{e}_4 = -e_3 - k_4 e_4 + Y_r \tag{C.31}$$

Et,

$$\begin{aligned} \dot{y}_2 &= -a_0 y_3 - b_0 y_4 + \frac{a_1}{A_3}[A_{50}e_4 - (A_4 + 1)e_3 - k_4 e_4] \\ &= -a_0 e_3 - b_0(-k_3 e_3 + e_4) + \frac{a_1}{A_3}[-\underbrace{(A_4 + 1)}_{A_5} e_3 - \underbrace{(k_4 - A_{50})}_{A_6} e_4] \end{aligned} \tag{C.32}$$

Ce qui donne après regroupement,

$$\dot{y}_2 = \underbrace{(-a_0 + b_0 k_3 - \frac{a_1 A_5}{A_3})}_{A_7} e_3 - \underbrace{(b_0 + \frac{a_1 A_6}{A_3})}_{A_8} e_4 \tag{C.33}$$

Le sous-système (C.20) après deux étapes de 'backstepping' devient :

$$\begin{cases} \dot{y}_1 = y_2 \\ \dot{y}_2 = A_7 e_3 - A_8 e_4 \\ \dot{e}_3 = -k_3 e_3 + e_4 \\ \dot{e}_4 = -e_3 - k_4 e_4 + Y_r \end{cases} \tag{C.34}$$

Integrator Forwarding

Nous allons commencer par appliquer le 'integrator forwarding' à $\{\dot{y}_2, \dot{e}_3, \dot{e}_4\}$. Pour cela l'entrée y_{5d} du sous-système doit être augmentée d'une commande v_2 :

$$y_{5d} = \frac{1}{A_3}[A_{50} e_4 - (A_4 + 1) e_3 - k_4 e_4] + v_2 \tag{C.35}$$

Par suite, le nouveau sous-système (C.20) devient :

$$\begin{cases} \dot{y}_1 = y_2 \\ \dot{y}_2 = A_7 e_3 - A_8 e_4 + \frac{a_1}{A_3} v_2 \\ \dot{e}_3 = -k_3 e_3 + e_4 \\ \dot{e}_4 = -e_3 - k_4 e_4 + A_3 v_2 + Y_r \end{cases} \tag{C.36}$$

Posons, $\{\xi_2, \xi_3, \xi_4\}$ les valeurs respectives de $\{y_2, e_3, e_4\}$ lorsque $v_2 = 0$ et $Y_r = 0$. Alors :

$$\begin{aligned} \dot{\xi}_2 &= A_7 \xi_3 - A_8 \xi_4 \quad \text{avec} \quad \xi_2(0) = y_2 \\ \dot{\xi}_3 &= -k_3 \xi_3 + \xi_4 \quad \text{avec} \quad \xi_3(0) = e_3 \\ \dot{\xi}_4 &= -\xi_3 - k_4 \xi_4 \quad \text{avec} \quad \xi_4(0) = e_4 \end{aligned} \tag{C.37}$$

Donc, les états y_2, e_3, e_4 deviennent les conditions initiales des nouvelles variables ξ_2, ξ_3, ξ_4.

Si nous résolvons le sous-système (C.37) pour ξ_2 en intégrant, nous obtenons :

$$\xi_2 = y_2 + \int_0^\infty (A_7 \xi_3 - A_8 \xi_4) dt \tag{C.38}$$

$$\xi_2 = y_2 + \underbrace{\left(\frac{A_8 + k_4 A_7}{1 + k_3 k_4}\right)}_{A_9} e_3 + \underbrace{\left(\frac{A_7 - k_3 A_8}{1 + k_3 k_4}\right)}_{A_{10}} e_4 \tag{C.39}$$

Soit z_2 la valeur de ξ_2 lorsque $v_2 \neq 0$ et $Y_r \neq 0$. Alors,

$$\begin{aligned} \dot{z}_2 &= \dot{y}_2 + A_9 \dot{e}_3 + A_{10} \dot{e}_4 \\ &= A_7 e_3 - A_8 e_4 + \frac{a_1}{A_3} v_2 + A_9(-k_3 e_3 + e_4) + A_{10}(-e_3 - k_4 e_4 + A_3 v_2 + Y_r) \\ &= \underbrace{\left(\frac{a_1}{A_3} + A_3 A_{10}\right)}_{A_{11}} v_2 + A_{10} Y_r \end{aligned} \tag{C.40}$$

Le sous-système (C.37) devient alors,

$$\begin{cases} \dot{z}_2 = A_{11} v_2 + A_{10} Y_r \\ \dot{e}_3 = -k_3 e_3 + e_4 \\ \dot{e}_4 = -e_3 - k_4 e_4 + A_3 v_2 + Y_r \end{cases} \tag{C.41}$$

Étape 3 : Considérons maintenant la fonction de Lyapunov,

$V_2 = V_4 + \frac{1}{2} z_2^2 = \frac{1}{2} e_3^2 + \frac{1}{2} e_4^2 + \frac{1}{2} z_2^2$ alors,

$$\begin{aligned} \dot{V}_2 &= e_3(-k_3 e_3 + e_4) + e_4(-e_3 - k_4 e_4 + A_3 v_2 + Y_r) + z_2(A_{11} v_2 + A_{10} Y_r) \\ &= -k_3 e_3^2 - k_4 e_4^2 + v_2(A_{11} z_2 + A_3 e_4) + e_4 Y_r + A_{10} z_2 Y_r \end{aligned} \tag{C.42}$$

Donc, la valeur de v_2 qui stabilise le sous-système (C.41) est :

$$v_2 = -k_2(A_{11} z_2 + A_3 e_4) \tag{C.43}$$

Ce qui donne : $\dot{V}_2 = -k_3 e_3^2 - k_4 e_4^2 - k_2(A_{11} z_2 + A_3 e_4)^2 + e_4 Y_r + A_{10} z_2 Y_r$ (C.44)

$\dot{V}_2$ est négative pour des valeurs assez grandes de k_2, k_3 et k_4 ou plus précisément si :

$$\begin{aligned} &-k_2(A_{11} z_2 + A_3 e_4)^2 + A_{10} z_2 Y_r \leq 0 \Rightarrow \\ &-k_2(A_{11} z_2 + A_3 e_4)^2 \leq -A_{10} z_2 Y_r \Rightarrow \\ &k_2(A_{11} z_2 + A_3 e_4)^2 \geq A_{10} z_2 Y_r \Rightarrow \\ &(A_{11} z_2 + A_3 e_4)^2 \geq \frac{A_{10} z_2}{k_2} Y_r \Rightarrow \\ &Y_r \leq \frac{(A_{11} z_2 + A_3 e_4)^2}{A_{10} z_2} k_2 \end{aligned} \tag{C.45}$$

Rappelons que z_2 et e_4 ont le même ordre de grandeur. En effet, $\max(z_2) = \max(y_2)$ où y_2 est la vitesse du mouvement vertical du corps du véhicule. D'un autre côté, $\max(e_4) = \max(y_4)$. Donc nous pouvons dire que $z_2 \simeq e_4$.

$$\text{Donc, } Y_r \leq \frac{(A_{11} + A_3)^2 k_2}{A_{10}} \max(y_2) \tag{C.46}$$

En plus, nous aurons en remplaçant v_2 par son expression dans $\dot{z}_2$ et $\dot{e}_4$,

$$\dot{z}_2 = -k_2 A_{11}^2 z_2 - k_2 A_{11} A_3 e_4 + A_{10} Y_r \tag{C.47}$$

Et,

$$\dot{e}_4 = -k_2 A_3 A_{11} z_2 - e_3 - \underbrace{(k_4 + k_2 A_3^2)}_{A_{12}} e_4 + Y_r$$

Le sous-système (C.41) après une étape de 'integrator forwarding' devient :

$$\begin{cases} \dot{y}_1 = y_2 = z_2 - A_9 e_3 - A_{10} e_4 \\ \dot{z}_2 = -k_2 A_{11}^2 z_2 - k_2 A_{11} A_3 e_4 + A_{10} Y_r \\ \dot{e}_3 = -k_3 e_3 + e_4 \\ \dot{e}_4 = -k_2 A_3 A_{11} z_2 - e_3 - A_{12} e_4 + Y_r \end{cases} \tag{C.48}$$

Maintenant, pour appliquer le 'integrator forwarding' à $\{\dot{y}_1, \dot{z}_2, \dot{e}_3, \dot{e}_4\}$, l'entrée v_2 doit être augmentée d'une commande v_1, donc :

$$v_2 = -k_2 (A_{11} z_2 + A_3 e_4) + v_1 \tag{C.50}$$

Le sous-système (C.48) devient,

$$\begin{cases} \dot{y}_1 = z_2 - A_9 e_3 - A_{10} e_4 \\ \dot{z}_2 = -k_2 A_{11}^2 z_2 - k_2 A_{11} A_3 e_4 + A_{11} v_1 + A_{10} Y_r \\ \dot{e}_3 = -k_3 e_3 + e_4 \\ \dot{e}_4 = -k_2 A_3 A_{11} z_2 - e_3 - A_{12} e_4 + A_3 v_1 + Y_r \end{cases} \tag{C.51}$$

Posons, $\{\xi_1, \xi_2, \xi_3, \xi_4\}$ les valeurs respectives de $\{y_1, z_2, e_3, e_4\}$ lorsque $v_1 = 0$ et $Y_r = 0$. Alors :

$$\begin{aligned} \dot{\xi}_1 &= \xi_2 - A_9 \xi_3 - A_{10} \xi_4 && \text{avec } \xi_1(0) = y_1 \\ \dot{\xi}_2 &= -k_2 A_{11}^2 \xi_2 - k_2 A_{11} A_3 \xi_4 && \text{avec } \xi_2(0) = z_2 \\ \dot{\xi}_3 &= -k_3 \xi_3 + \xi_4 && \text{avec } \xi_3(0) = e_3 \\ \dot{\xi}_4 &= -k_2 A_3 A_{11} \xi_2 - \xi_3 - A_{12} \xi_4 && \text{avec } \xi_4(0) = e_4 \end{aligned} \tag{C52}$$

Donc, les états $\{y_1,\ z_2,\ e_3,\ e_4\}$ deviennent les conditions initiales des nouvelles variables $\{\xi_1, \xi_2, \xi_3, \xi_4\}$.

Si nous résolvons le sous-système (C.52) pour ξ_1 en intégrant, nous obtenons :

$$\xi_1 = y_1 + \int_0^\infty (\xi_2 - A_9\xi_3 - A_{10}\xi_4)dt$$

$$\begin{aligned}\xi_1 = y_1 &- \underbrace{\left(\frac{1+k_2k_3A_3A_{10}A_{11}+k_3A_{12}+k_2A_3A_9A_{11}}{k_2A_{11}^2(-1+k_2k_3A_3^2-k_3A_{12})}\right)}_{A_{13}} z_2 - \underbrace{\left(\frac{A_{10}A_{11}+A_3-A_9A_{11}A_{12}+k_2A_3^2A_9A_{11}}{A_{11}(-1+k_2k_3A_3^2-k_3A_{12})}\right)}_{A_{14}} e_3 \\ &- \underbrace{\left(\frac{k_3A_3-A_9A_{11}-k_3A_{10}A_{11}}{k_2A_{11}^2(-1+k_2k_3A_3^2-k_3A_{12})}\right)}_{A_{15}} e_4\end{aligned} \tag{C.53}$$

Soit z_1 la valeur de ξ_1 lorsque $v_1 \neq 0$ et $Y_r \neq 0$. Alors,

$$\begin{aligned}\dot{z}_1 &= \dot{y}_1 - A_{13}\dot{z}_2 - A_{14}\dot{e}_3 - A_{15}\dot{e}_4 \\ &= \left(z_2 - A_9e_3 - A_{10}e_4\right) - A_{13}\left(-k_2A_{11}^2z_2 - k_2A_{11}A_3e_4 + A_{11}v_1 + A_{10}Y_r\right) - A_{14}\left(-k_3e_3 + e_4\right) \\ &\quad - A_{15}\left(-k_2A_3A_{11}z_2 - e_3 - A_{12}e_4 + A_3v_1 + Y_r\right) \\ &= \frac{1}{k_2A_{11}}v_1 - \underbrace{(A_{10}A_{13}+A_{15})}_{A_{150}}Y_r\end{aligned} \tag{C.54}$$

Donc, le sous-système (C.51) devient,

$$\begin{cases}\dot{z}_1 = \dfrac{1}{k_2A_{11}}v_1 - A_{150}Y_r \\ \dot{z}_2 = -k_2A_{11}^2z_2 - k_2A_{11}A_3e_4 + A_{11}v_1 + A_{10}Y_r \\ \dot{e}_3 = -k_3e_3 + e_4 \\ \dot{e}_4 = -k_2A_3A_{11}Az_2 - e_3 - A_{12}e_4 + A_3v_1 + Y_r\end{cases} \tag{C.55}$$

Étape 4 : Considérons maintenant la fonction de Lyapunov,

$V_1 = V_2 + \frac{1}{2}z_1^2 = \frac{1}{2}e_3^2 + \frac{1}{2}e_4^2 + \frac{1}{2}z_2^2 + \frac{1}{2}z_1^2$ alors,

$$\begin{aligned}\dot{V}_1 &= e_3\left(-k_3e_3 + e_4\right) + e_4\left(-k_2A_3A_{11}z_2 - e_3 - A_{12}e_4 + A_3v_1 + Y_r\right) \\ &\quad + z_2\left(-k_2A_{11}^2z_2 - k_2A_{11}A_3e_4 + A_{11}v_1 + A_{10}Y_r\right) + z_1\left(\frac{1}{k_2A_{11}}v_1 - A_{150}Y_r\right)\end{aligned} \tag{C.56}$$

$$\dot{V}_1 = -k_3 e_3^2 - k_4 e_4^2 - k_2 \left(A_{11} z_2 + A_3 e_4 \right)^2 + v_1 \left(\frac{1}{k_2 A_{11}} z_1 + A_{11} z_2 + A_3 e_4 \right) + \left(A_{10} z_2 + e_4 - A_{150} z_1 \right) Y_r \quad \text{(C.57)}$$

Donc, la valeur de v_1 qui stabilise le sous-système (C.55) est,

$$v_1 = -k_1 \left(\frac{1}{k_2 A_{11}} z_1 + A_{11} z_2 + A_3 e_4 \right) \quad \text{(C.58)}$$

Ce qui donne :

$$\dot{V}_1 = -k_3 e_3^2 - k_4 e_4^2 - k_2 \left(A_{11} z_2 + A_3 e_4 \right)^2 - k_1 \left(\frac{1}{k_2 A_{11}} z_1 + A_{11} z_2 + A_3 e_4 \right)^2 + \left(A_{10} z_2 + e_4 - A_{150} z_1 \right) Y_r \quad \text{(C.59)}$$

$\dot{V}_1$ est négative pour des valeurs assez grandes de k_1, k_2, k_3 et k_4. En plus, nous aurons en remplaçant v_1 par son expression dans $\dot{z}_2$ et $\dot{e}_4$:

$$\dot{z}_2 = -\frac{k_1}{k_2} z_1 - \underbrace{\left(k_2 A_{11}^2 + k_1 A_{11}^2 \right)}_{A_{19}} z_2 - \underbrace{\left(k_2 A_{11} A_3 + k_1 A_{11} A_3 \right)}_{A_{20}} e_4 + A_{10} Y_r \quad \text{(C.60)}$$

Et,

$$\dot{e}_4 = -\frac{k_1 A_3}{k_2 A_{11}} z_1 - \underbrace{\left(k_2 A_3 A_{11} + k_1 A_3 A_{11} \right)}_{A_{21}} z_2 - e_3 - \underbrace{\left(A_{12} + k_1 A_3^2 \right)}_{A_{22}} e_4 + Y_r \quad \text{(C.61)}$$

Le sous-système (C.55) devient alors,

$$\begin{cases} \dot{z}_1 = -\dfrac{k_1}{k_2^2 A_{11}^2} z_1 - \dfrac{k_1}{k_2} z_2 - \dfrac{k_1 A_3}{k_2 A_{11}} e_4 - A_{150} Y_r \\ \dot{z}_2 = -\dfrac{k_1}{k_2} z_1 - A_{19} z_2 - A_{20} e_4 + A_{10} Y_r \\ \dot{e}_3 = -k_3 e_3 + e_4 \\ \dot{e}_4 = -\dfrac{k_1 A_3}{k_2 A_{11}} z_1 - A_{21} z_2 - e_3 - A_{22} e_4 + Y_r \end{cases} \quad \text{(C.62)}$$

Pour compléter, en remplaçant v_2 et v_1 dans l'expression de l'entrée y_{5d} du sous-système de départ, nous obtenons :

$$y_{5d} = -\frac{k_1}{k_2 A_{11}} z_1 - \underbrace{\left(k_1 A_{11} + k_2 A_{11} \right)}_{A_{16}} z_2 - \underbrace{\left(\frac{1 + A_4}{A_3} \right)}_{A_{17}} e_3 - \underbrace{\left(\frac{A_6}{A_3} + k_2 A_3 + k_1 A_3 \right)}_{A_{18}} e_4 \quad \text{(C.63)}$$

Étape 5 : En effet, y_{5d} n'est pas la vraie entrée du système. Ce n'est que la pression différentielle due à la charge, entre les ports de l'actionneur hydraulique. Pour cela nous allons définir la variable

$$e_5 = y_5 - y_{5d} = y_5 + \frac{k_1}{k_2 A_{11}} z_1 + A_{16} z_2 + A_{17} e_3 + A_{18} e_4 \tag{C.64}$$

Appliquons maintenant le 'backstepping' pour stabiliser le reste du système, comme nous l'avons expliqué au début.

$$\begin{aligned}
\dot{e}_5 &= \dot{y}_5 + \frac{k_1}{k_2 A_{11}} \dot{z}_1 + A_{16} \dot{z}_2 + A_{17} \dot{e}_3 + A_{18} \dot{e}_4 \\
&= \frac{J_1}{f(.)} \left(-A y_4 - L y_5 + C_d g(.) y_6 \right) + \frac{k_1}{k_2 A_{11}} \left(-\frac{k_1}{k_2^2 A_{11}^2} z_1 - \frac{k_1}{k_2} z_2 - \frac{k_1 A_3}{k_2 A_{11}} e_4 - A_{150} Y_r \right) \\
&\quad + A_{16} \left(-\frac{k_1}{k_2} z_1 - A_{19} z_2 - A_{20} e_4 + A_{10} Y_r \right) + A_{17} \left(-k_3 e_3 + e_4 \right) \\
&\quad + A_{18} \left(-\frac{k_1 A_3}{k_2 A_{11}} z_1 - A_{21} z_2 - e_3 - A_{22} e_4 + Y_r \right)
\end{aligned} \tag{C.65}$$

Ce qui donne après un premier regroupement,

$$\begin{aligned}
\dot{e}_5 &= \underbrace{-\left(\frac{k_1^2}{k_2^3 A_{11}^3} + \frac{k_1 A_{16}}{k_2} + \frac{k_1 A_3 A_{18}}{k_2 A_{11}} \right)}_{A_{23}} z_1 \underbrace{-\left(\frac{k_1^2}{k_2^2 A_{11}} + A_{18} A_{21} + A_{16} A_{19} \right)}_{A_{24}} z_2 \underbrace{-\left(k_3 A_{17} + A_{18} \right)}_{A_{25}} e_3 \\
&\quad \underbrace{-\left(\frac{k_1^2 A_3}{k_2^2 A_{11}^2} + A_{16} A_{20} - A_{17} + A_{18} A_{22} \right)}_{A_{26}} e_4 + \frac{J_1 C_d g(.)}{f(.)} y_6 - \frac{J_1 A}{f(.)} (e_4 - k_3 e_3) \\
&\quad - \frac{J_1 L}{f(.)} \left(e_5 - \frac{k_1}{k_2 A_{11}} z_1 - A_{16} z_2 - A_{17} e_3 - A_{18} e_4 \right) + \underbrace{\left(-\frac{k_1 A_{150}}{k_2 A_{11}} + A_{16} A_{10} + A_{18} \right)}_{A_{160}(.)} Y_r
\end{aligned} \tag{C.66}$$

Et finalement,

$$\begin{aligned}
\dot{e}_5 &= \underbrace{\left(-A_{23} + \frac{J_1 L k_1}{f(.) k_2 A_{11}} \right)}_{A_{27}(.)} z_1 + \underbrace{\left(-A_{24} + \frac{J_1 L A_{16}}{f(.)} \right)}_{A_{28}(.)} z_2 + \underbrace{\left(-A_{25} + \frac{J_1 A k_3}{f(.)} + \frac{J_1 L A_{17}}{f(.)} \right)}_{A_{29}(.)} e_3 \\
&\quad + \underbrace{\left(-A_{26} - \frac{J_1 A}{f(.)} + \frac{J_1 L A_{18}}{f(.)} \right)}_{A_{30}(.)} e_4 - \frac{J_1 L}{f(.)} e_5 + \frac{J_1 C_d g(.)}{f(.)} y_6 + A_{160}(.) Y_r
\end{aligned} \tag{C.67}$$

Le système de départ (C.3) devient maintenant,

$$\begin{cases} \dot{z}_1 = -\dfrac{k_1}{k_2^2 A_{11}^2} z_1 - \dfrac{k_1}{k_2} z_2 - \dfrac{k_1 A_3}{k_2 A_{11}} e_4 - A_{150} Y_r \\ \dot{z}_2 = -\dfrac{k_1}{k_2} z_1 - A_{19} z_2 - A_{20} e_4 + A_{11} e_5 + A_{10} Y_r \\ \dot{e}_3 = -k_3 e_3 + e_4 \\ \dot{e}_4 = -\dfrac{k_1 A_3}{k_2 A_{11}} z_1 - A_{21} z_2 - e_3 - A_{22} e_4 + A_3 e_5 + Y_r \\ \dot{e}_5 = A_{27}(.) z_1 + A_{28}(.) z_2 + A_{29}(.) e_3 + A_{30}(.) e_4 - \dfrac{J_1 L}{f(.)} e_5 + \dfrac{J_1 C_d g(.)}{f(.)} y_6 + A_{160}(.) Y_r \\ \dot{y}_6 = -\dfrac{1}{\tau} y_6 + \dfrac{K_v}{\tau} u \end{cases} \tag{C.68}$$

Considérons maintenant la fonction de Lyapunov,

$$V_5 = V_1 + \frac{1}{2} e_5^2 = \frac{1}{2} e_3^2 + \frac{1}{2} e_4^2 + \frac{1}{2} z_2^2 + \frac{1}{2} z_1^2 + \frac{1}{2} e_5^2 \tag{C.69}$$

Alors,

$$\dot{V}_5 = \dot{V}_1 + e_5 \dot{e}_5 = \underbrace{(.....)}_{<0 \text{ depuis l'étape 4}} + e_5 \left\{ \begin{array}{l} A_{11} z_2 + A_3 e_4 + A_{27}(.) z_1 + A_{28}(.) z_2 + A_{29}(.) e_3 \\ + A_{30}(.) e_4 - \dfrac{J_1 L}{f(.)} e_5 + \underbrace{\dfrac{J_1 C_d g(.)}{f(.)} y_6}_{Y_6} + A_{160}(.) Y_r \end{array} \right\} \tag{C.70}$$

Donc, si nous choisissons Y_6 de la manière suivante :

$$\begin{aligned} Y_{6d} &= -A_{27}(.) z_1 - A_{11} z_2 - A_{28}(.) z_2 - A_{29}(.) e_3 - A_3 e_4 - A_{30}(.) e_4 + \frac{J_1 L}{f(.)} e_5 - k_5 e_5 \\ &= -A_{27}(.) z_1 - \underbrace{\left(A_{11} + A_{28}(.)\right)}_{A_{31}(.)} z_2 - A_{29}(.) e_3 - \underbrace{\left(A_3 + A_{30}(.)\right)}_{A_{32}(.)} e_4 + \underbrace{\left(\frac{J_1 L}{f(.)} - k_5 \right)}_{A_{33}(.)} e_5 \end{aligned} \tag{C.71}$$

Nous aurons, $\dot{V}_5 = \dot{V}_1 - k_5 e_5^2 + A_{160}(.) Y_r$ (C.72)

Il est simple de vérifier que $\dot{V}_5$ est négative pour de valeurs assez grandes de k_1, k_2, k_3, k_4, k_5

ou plus précisément si : $Y_r \le \dfrac{k_5}{A_{160}(.)} e_5^2$ (C.73)

Comme e_5 est majorée par $y_5 = x_5$ alors $Y_r \le \dfrac{k_5}{A_{160}(.)} \max(x_5^2)$ (C.74)

Étape 6 : Définissons maintenant la nouvelle variable,

$$e_6 = Y_6 - Y_{6d} = Y_6 + A_{27}(.)z_1 + A_{31}(.)z_2 + A_{29}(.)e_3 + A_{32}(.)e_4 - A_{33}(.)e_5 \tag{C.75}$$

En remplaçant $Y_6 = e_6 + Y_{6d}$ dans $\dot{e}_5$ nous obtenons,

$$\dot{e}_5 = -A_{11}z_2 + A_3(.)e_4 - k_5e_5 + e_6 + A_{160}Y_r \tag{C.76}$$

Calcul de $\dot{e}_6$

$$\dot{e}_6 = \dot{Y}_6 - \dot{Y}_{6d} \tag{C.77}$$

$$1.\ \dot{Y}_6 = J_1C_d\left(\frac{\dot{g}(.)f(.) - \dot{f}(.)g(.)}{f(.)^2}y_6 + \frac{g(.)}{f(.)}\dot{y}_6\right) \tag{C.78}$$

- $$\dot{g}(.) = -\frac{1}{2g(.)}\left[-\frac{1}{\rho}sigm(y_6)\dot{y}_5 + \dot{\overbrace{sigm(y_6)}}\,y_5\right] \tag{C.79}$$

Or,

$$\dot{\overbrace{sigm(y_6)}} = \frac{dsigm(y_6)}{dt} = \frac{2ae^{-ay_6}}{(1+e^{-ay_6})^2}\dot{y}_6 = \underbrace{\left(\frac{2ae^{-ay_6}}{(1+e^{-ay_6})^2}\right)}_{w(.)}\left(-\frac{1}{\tau}y_6 + \frac{K_v}{\tau}u\right) \tag{C.80}$$

Donc,

$$\dot{g}(.) = \frac{sigm(y_6)\dot{y}_5}{2\rho g(.)} - \frac{w(.)y_5y_6}{2\rho\tau g(.)} - \frac{K_v y_5 w(.)}{2\rho\tau g(.)}u \tag{C.81}$$

- $$\dot{f}(.) = f_p(.) = -2A^2y_3\dot{y}_3 = -2A^2y_3y_4 \tag{C.82}$$
- $$\frac{g(.)}{f(.)}\dot{y}_6 = \frac{g(.)}{f(.)}\left(-\frac{1}{\tau}y_6 + \frac{K_v}{\tau}u\right) = -\frac{g(.)y_6}{f(.)\tau} + \frac{K_v g(.)}{f(.)\tau}u \tag{C.83}$$

Ce qui donne en regroupant les termes qui contiennent la commande u,

$$\dot{Y}_6 = \underbrace{J_1C_d\left(\frac{sgm(y_6)\dot{y}_5y_6}{2\rho g(.)f(.)} - \frac{w(.)y_5y_6^2}{2\rho\tau g(.)f(.)} - \frac{f_p(.)g(.)}{f(.)^2}y_6 - \frac{g(.)y_6}{f(.)\tau}\right)}_{V(.)} + \underbrace{J_1C_d\left(\frac{K_v g(.)}{f(.)\tau} - \frac{K_v y_5y_6w(.)}{2\rho\tau g(.)f(.)}\right)}_{Z(.)}u \tag{C.84}$$

$$= V(.) + Z(.)u$$

$$2.\ \dot{Y}_{6d} = -A_{27}(.)\dot{z}_1 - A_{31}(.)\dot{z}_2 - A_{29}(.)\dot{e}_3 - A_{32}(.)\dot{e}_4 + A_{33}(.)\dot{e}_5$$

$$-\dot{A}_{27}(.)z_1 - \dot{A}_{31}(.)z_2 - \dot{A}_{29}(.)e_3 - \dot{A}_{32}(.)e_4 + \frac{J_1Lf_p(.)}{f^2(.)}e_5 \tag{C.85}$$

$$\begin{aligned}\dot{Y}_{6d} = &-A_{27}(.)\left(-\frac{k_1}{k_2^2 A_{11}^2} z_1 - \frac{k_1}{k_2} z_2 - \frac{k_1 A_3}{k_2 A_{11}} e_4 - A_{150} Y_r\right) \\ &- A_{31}(.)\left(-\frac{k_1}{k_2} z_1 - A_{19} z_2 - A_{20} e_4 + A_{11} e_5 + A_{10} Y_r\right) - A_{29}(.)\left(-k_3 e_3 + e_4\right) \\ &- A_{32}(.)\left(-\frac{k_1 A_3}{k_2 A_{11}} z_1 - A_{21} z_2 - e_3 - A_{22} e_4 + A_3 e_5 + Y_r\right) \\ &- A_{33}(.)\left(-A_{11} z_2 + A_3(.) e_4 - k_5 e_5 + e_6 + A_{160} Y_r\right) \\ &- \dot{A}_{27}(.) z_1 - \dot{A}_{31}(.) z_2 - \dot{A}_{29}(.) e_3 - \dot{A}_{32}(.) e_4 + \frac{J_1 L f_p(.)}{f^2(.)} e_5\end{aligned} \tag{C.86}$$

Avec,

$$\begin{aligned}\dot{A}_{27}(.) &= \frac{\partial}{\partial t} A_{27}(.) = -\frac{J_1 L k_1}{k_2 A_{11}} \frac{f_p(.)}{f^2(.)} \\ \dot{A}_{31}(.) &= \frac{\partial}{\partial t} A_{31}(.) = \frac{\partial}{\partial t} A_{28}(.) = -J_1 L A_{16} \frac{f_p(.)}{f^2(.)} \\ \dot{A}_{29}(.) &= \frac{\partial}{\partial t} A_{29}(.) = -\left(J_1 A k_3 + J_1 L A_{17}\right) \frac{f_p(.)}{f^2(.)} \\ \dot{A}_{32}(.) &= \frac{\partial}{\partial t} A_{32}(.) = \frac{\partial}{\partial t} A_{30}(.) = \left(J_1 A - J_1 L A_{18}\right) \frac{f_p(.)}{f^2(.)}\end{aligned} \tag{C.87}$$

Finalement,

$$\begin{aligned}\dot{Y}_{6d} = &\underbrace{\left(\frac{k_1 A_{27}(.)}{k_2^2 A_{11}^2} - \frac{k_1 A_{31}(.)}{k_2} - \frac{k_1 A_3 A_{32}(.)}{k_2 A_{11}} + A_{33}(.) A_{27}(.) - \dot{A}_{27}(.)\right)}_{A_{34}(.)} z_1 \\ &+ \underbrace{\left(\frac{k_1 A_{27}(.)}{k_2} - A_{31}(.) A_{19} + A_{21} A_{32}(.) + A_{28} A_{33(.)} - \dot{A}_{31}(.)\right)}_{A_{35}(.)} z_2 \\ &+ \underbrace{\left(-k_3 A_{29}(.) + A_{32}(.) + A_{29}(.) A_{33}(.) - \dot{A}_{29}(.)\right)}_{A_{36}(.)} e_3 \\ &+ \underbrace{\left(\frac{k_1 A_3 A_{27}(.)}{k_2 A_{11}} - A_{29}(.) + A_{20} A_{31}(.) + A_{22} A_{32}(.) + A_{30}(.) A_{33}(.) - \dot{A}_{32}(.)\right)}_{A_{37}(.)} e_4 \\ &+ \underbrace{\left(-A_{11} A_{31}(.) - A_3 A_{32}(.) - \frac{J_1 L A_{33}(.)}{f(.)} - \frac{J_1 L f_p(.)}{f^2(.)}\right)}_{A_{38}(.)} e_5 + \underbrace{\left(\frac{J_1 C_d g(.) A_{33}(.)}{f(.)}\right)}_{A_{39}(.)} e_6 \\ &+ \underbrace{\left(A_{150} A_{27}(.) - A_{10} A_{31}(.) - A_{32}(.) - A_{160} A_{33}(.)\right)}_{A_{170}(.)} Y_r\end{aligned} \tag{C.88}$$

Alors,

$$\dot{e}_6 = V(.) + Z(.)u - A_{34}(.)z_1 - A_{35}(.)z_2 - A_{36}(.)e_3 - A_{37}(.)e_4 - A_{38}(.)e_5 - A_{39}(.)e_6 - A_{170}(.)Y_r \quad \text{(C.89)}$$

Le système (C.68) devient maintenant,

$$\begin{cases} \dot{z}_1 = -\dfrac{k_1}{k_2^2 A_{11}^2} z_1 - \dfrac{k_1}{k_2} z_2 - \dfrac{k_1 A_3}{k_2 A_{11}} e_4 - A_{150} Y_r \\ \dot{z}_2 = -\dfrac{k_1}{k_2} z_1 - A_{19} z_2 - A_{20} e_4 + A_{11} e_5 + A_{10} Y_r \\ \dot{e}_3 = -k_3 e_3 + e_4 \\ \dot{e}_4 = -\dfrac{k_1 A_3}{k_2 A_{11}} z_1 - A_{21} z_2 - e_3 - A_{22} e_4 + A_3 e_5 + Y_r \\ \dot{e}_5 = -A_{11} z_2 + A_3(.) e_4 - k_5 e_5 + e_6 + A_{160} Y_r \\ \dot{e}_6 = V(.) - A_{34}(.)z_1 - A_{35}(.)z_2 - A_{36}(.)e_3 - A_{37}(.)e_4 - A_{38}(.)e_5 - A_{39}(.)e_6 + Z(.)u + A_{170}(.)Y_r \end{cases} \quad \text{(C.90)}$$

Considérons maintenant la fonction de Lyapunov globale,

$$V_6 = V_5 + \frac{1}{2}e_6^2 = \frac{1}{2}e_3^2 + \frac{1}{2}e_4^2 + \frac{1}{2}z_2^2 + \frac{1}{2}z_1^2 + \frac{1}{2}e_5^2 + \frac{1}{2}e_6^2 \quad \text{(C.91)}$$

Alors,

$$\begin{aligned} \dot{V}_6 &= \dot{V}_5 + e_6\dot{e}_6 \\ &= \underbrace{(.....)}_{<0 \text{ depuis l'étape 5}} + e_6 \begin{Bmatrix} V(.) - A_{34}(.)z_1 - A_{35}(.)z_2 - A_{36}(.)e_3 - A_{37}(.)e_4 \\ -A_{38}(.)e_5 + e_5 - A_{39}(.)e_6 + Z(.)u + A_{170}(.)Y_r \end{Bmatrix} \end{aligned} \quad \text{(C.92)}$$

Alors finalement, la commande u qui va assurer la stabilité du système et qui n'est que le signal de commande envoyé à la servovalve est :

$$u = \frac{1}{Z(.)}\left(-V(.) + A_{34}(.)z_1 + A_{35}(.)z_2 + A_{36}(.)e_3 + A_{37}(.)e_4 + \left(A_{38}(.) - 1\right)e_5 + A_{39}(.)e_6 - k_6 e_6\right) \quad \text{(C.93)}$$

Ce qui donne, $\dot{V}_6 = \dot{V}_5 - k_6 e_6^2 + A_{170}(.)Y_r$ (C.94)

Il est simple de vérifier que $\dot{V}_6$ est négative pour de valeurs assez grandes de k_1, k_2, k_3, k_4, k_5, k_6 ou plus précisément si : $Y_r \le \dfrac{k_6}{A_{170}(.)} e_6^2$ (C.95)

Alors, en replaçant u dans $\dot{e}_6$ nous obtenons :

$$\dot{e}_6 = -e_5 - k_6 e_6 + A_{170}(.)Y_r \tag{C.96}$$

Pour terminer, la dynamique du système de départ (C.3), en boucle fermée, est donnée par :

$$\begin{cases} \dot{z}_1 = -\dfrac{k_1}{k_2^2 A_{11}^2} z_1 - \dfrac{k_1}{k_2} z_2 - \dfrac{k_1 A_3}{k_2 A_{11}} e_4 - A_{150} Y_r \\ \dot{z}_2 = -\dfrac{k_1}{k_2} z_1 - A_{19} z_2 - A_{20} e_4 + A_{11} e_5 + A_{10} Y_r \\ \dot{e}_3 = -k_3 e_3 + e_4 \\ \dot{e}_4 = -\dfrac{k_1 A_3}{k_2 A_{11}} z_1 - A_{21} z_2 - e_3 - A_{22} e_4 + A_3 e_5 + Y_r \\ \dot{e}_5 = -A_{11} z_2 + A_3(.) e_4 - k_5 e_5 + e_6 + A_{160} Y_r \\ \dot{e}_6 = -e_5 - k_6 e_6 + A_{170}(.) Y_r \end{cases} \tag{C.97}$$

BIBLIOGRAPHIE

Abdellahi, E., D. Mehdi, and M. Saad (2000). On the design of active suspension system by H_{oo} and mixed H_2/H_{oo}: an LMI approach. 2000 American Control Conference, Jun 28-Jun 30 2000, Chicago, IL, USA, Institute of Electrical and Electronics Engineers Inc., Piscataway, NJ, USA.

Acarman, T. and K. A. Redmill (2002). A robust controller design for drive by wire hydraulic power steering system. 2002 American Control Conference, May 8-10 2002, Anchorage, AK, United States, Institute of Electrical and Electronics Engineers Inc.

Alleyne, A. and J. K. Hedrick (1995). "Nonlinear adaptive control of active suspensions." Control Systems Technology, IEEE Transactions on **3**(1): 94-101.

Alleyne, A. and R. Liu (2000). "Simplified approach to force control for electro-hydraulic systems." Control Engineering Practice **8**(12): 1347-1356.

Ando, Y. and M. Suzuki (1996). "Control of active suspension systems using the singular perturbation method." Control Engineering Practice **4**(3): 287-293.

Astrom, K. J. and B. Wittenmark (1989). Adaptive Control. Addison-Wesley, United States.

Ayalew, B. and B. T. Kulakowski (2005). Nonlinear decentralized position control of electrohydraulic actuators in road simulation. Proceedings of the ASME Design Engineering Division 2005, Nov 5-11 2005, Orlando, FL, United States, American Society of Mechanical Engineers, New York, NY 10016-5990, United States.

Ayalew, B., B. T. Kulakowski, and K.W. Jablokow (2005). A near input-output linearizing force tracking controller for an electrohydraulic actuator. 2005 ASME International Mechanical Engineering Congress and Exposition, IMECE 2005, Nov 5-11 2005, Orlando, FL, United States, American Society of Mechanical Engineers, New York, NY 10016-5990, United States.

Chen, H.-M., J.-C. Renn, and J. P. Su (2005). "Sliding mode control with varying boundary layers for an electro-hydraulic position servo system." International Journal of Advanced Manufacturing Technology **26**(1-2): 117-123.

Deticek, E. (1999). "Intelligent position control of electrohydraulic drive using hybrid fuzzy control structure." Proceedings of the 1999 IEEE International Symposium on Industrial Electronics (ISIE'99), Jul 12-Jul 16 1999. **3**: 1008-1013.

Fialho, I. and G. J. Balas (2002). "Road adaptive active suspension design using linear parameter-varying gain-scheduling." Control Systems Technology, IEEE Transactions on **10**(1): 43-54.

Fink, A. and T. Singh (1997). Saturating controllers for pressure control with an electrohydraulic servovalve. Control Applications, 1997., Proceedings of the 1997 IEEE International Conference on.

Fink, A. and T. Singh (1998). Discrete sliding mode controller for pressure control with an electrohydraulic servovalve. Proceedings of the 1998 IEEE International Conference on Control Applocations. Part 1 (of 2), Sep 1-4 1998, Trieste, Italy, IEEE, Piscataway, NJ, USA.

Foo, E. and R. M. Goodall (2000). "Active suspension control of flexible-bodied railway vehicles using electro-hydraulic and electro-magnetic actuators." Control Engineering Practice **8**(5): 507-518.

Gaspar, P., I. Szaszi, J. Bokor (2002). Nonlinear Active Suspension Modelling Using Linear Parameter Varying Approach. Presented at Proceedings of the 10th Mediteranean Conference on Control and Automation - MED 2002, Lisbon, Portugal 2002.

Ha, Q. P., H. Q. Nguyen, and D. C. Rye (1998). "Sliding mode control with fuzzy tuning for an electro-hydraulic position servo system." Proceedings of the 1998 2nd International Conference on knowledge-Based Intelligent Electronic Systems (KES '98), Apr 21-Apr 23 1998

Habibi, S. and A. Goldenberg (2000). "Design of a new high-performance electrohydraulic actuator." Mechatronics, IEEE/ASME Transactions on **5**(2): 158-164.

Hahn, H., A. Piepenbrink, and K. D. Leimbach (1994). Input/output linearization control of an electro servo-hydraulic actuator. Proceedings of the 1994 IEEE Conference on Control Applications. Part 2 (of 3), Aug 24-26 1994, Glasgow, UK, IEEE, Piscataway, NJ, USA.

Hahn, J.-O., J.-W. Hur, Y. M. Cho, and K. I. Lee (2002). "Robust observer-based monitoring of a hydraulic actuator in a vehicle power transmission control system." Control Engineering Practice **10**(3): 327-335.

Hwang, C.-L. (1996). "Sliding mode control using time-varying switching gain and boundary layer for electrohydraulic position and differential pressure control." IEE Proceedings: Control Theory and Applications **143**(4): 325-332.

Ionescu, F. and F. Haszler (1996). Comparison between classical and fuzzy-controller for electrohydraulic axes. Proceedings of the 1996 1st International Symposium on Neuro-Fuzzy Systems, AT'96, Aug 29-31 1996, Lausanne, Switz, IEEE, Piscataway, NJ, USA.

Janas, D. (1995). Electro-hydraulic suspension control for low floor light rail vehicles. Railroad Conference, 1995., Proceedings of the 1995 IEEE/ASME Joint.

Jiang, Z.-P. and L. Praly (1998). "Design of robust adaptive controllers for nonlinear systems with dynamic uncertainties." Automatica **34**(7): 825-840.

Jung-Shan, L. and I. Kanellakopoulos (1997). "Nonlinear design of active suspensions." Control Systems Magazine, IEEE **17**(3): 45-59.

Kaddissi, C., J.-P. Kenné, and M. Saad (2005). Drive by wire control of an electro-hydraulic active suspension a backstepping approach. Control Applications, 2005. CCA 2005. Proceedings of IEEE Conference on.

Kaddissi, C., J.-P. Kenné, and M. Saad (2006). Indirect Adaptive Control of an Electro-Hydraulic Servo System Based on Nonlinear Backstepping. Industrial Electronics, 2006 IEEE International Symposium on, Montreal, Qc, Canada.

Kaddissi, C., J.-P. Kenné, and M. Saad. (2004). Position Control of an Electro-Hydraulic Servosystem - A Non-Linear Backstepping Approach. Int. Conf. of Informatics in Control, Automation and Robotics - ICINCO, Setubal, Portugal.

Kaddissi, C., J.-P. Kenné, and M. Saad (2007). "Identification and Real-Time Control of an Electrohydraulic Servo System Based on Nonlinear Backstepping." Mechatronics, IEEE/ASME Transactions on **12**(1): 12-22.

Kandil, N., S. LeQuoc, and M. Saad (1999). On-line Trained Neural Controllers for Nonlinear Hydraulic System. 14th World Congress of IFAC, pp.323-328.

Khalil, H. K. (2002). Nonlinear systems. New Jersey, Upper Saddle River, N.J: Prentice Hall, c2002.

Khoshzaban Zavarehi, M., P. D. Lawrence, and F Sassani (1999). "Nonlinear modeling and validation of solenoid-controlled pilot-operated servovalves." Mechatronics, IEEE/ASME Transactions on **4**(3): 324-334.

Krstic, M. (2004). "Feedback linearizability and explicit integrator forwarding controllers for classes of feedforward systems." Automatic Control, IEEE Transactions on **49**(10): 1668-1682.

Krstic, M., I. Kanellakopoulos, and P. V. Kokotovic (1995). Nonlinear and Adaptive Control Design, J. Wiley and Sons, New York, N.Y.

Lee, S. J. and T.-C. Tsao (2002). Nonlinear backstepping control of an electrohydraulic material testing system. American Control Conference, Anchorage, AK, United States, Institute of Electrical and Electronics Engineers Inc.

Leite, V. J. S. and P. L. D. Peres (2002). Robust pole location for an active suspension quarter-car model through parameter dependent control. Proceedings of the 2002 IEEE International Conference on Control Applications, Sep 18-20 2002, Glasgow, United Kingdom, Institute of Electrical and Electronics Engineers Inc.

LeQuoc, S., R. M. H. Cheng, and M. Saad (1990). "Tuning an electrohydraulic servovalve to obtain a high amplitude ratio and a low resonance peak." Journal of Fluid Control **20**(3): 30-49.

Li, P. Y. (2001). Dynamic redesign of a flow control servo-valve using a pressure control pilot. 2001 ASME International Mechanical Engineering Congress and Exposition, Nov 11-16 2001, New York, NY, United States, American Society of Mechanical Engineers.

Lim, T. J. (1997). Pole placement control of an electro-hydraulic servo motor. Proceedings of the 1997 2nd International Conference on Power Electronics and Drive Systems, PEDS. Part 1 (of 2), May 26-29 1997, Singapore, Singapore, IEEE, Piscataway, NJ, USA.

Lin, J.-S. and C.-J. Huang (2003). "Nonlinear backstepping control design of half-car active suspension systems." International Journal of Vehicle Design **33**(4): 332-350.

Lin, J.-S. and I. Kanellakopoulos (1995). Nonlinear design of active suspensions. Proceedings of the 1995 34th IEEE Conference on Decision and Control. Part 4 (of 4), Dec 13-15 1995, New Orleans, LA, USA, IEEE, Piscataway, NJ, USA.

Lin, J.-S. and I. Kanellakopoulos (1997). "Nonlinear design of active suspensions." IEEE Control Systems Magazine **17**(3): 45-59.

Liu, R. and A. Alleyne (1999). Nonlinear force/pressure tracking of an electro-hydraulic actuator. Proceedings of 14th World Congress of IFAC 99, 5-9 July 1999, Beijing, China, Elsevier Sci.

Merrit, H. E. (1967). Hydraulic Control Systems, New York, N.Y.: J. Wiely and sons.

Miroslav, K., I. Kanellakopoulos, and P. V. Kokotovic (1995). Nonlinear and Adaptive Control Design, John Wiley & Sons, Inc.,605 Third Avenue, New York, NY 10158-0012.

Morselli, R., R. Zanasi, and P. Ferracin (2006). Dynamic model of an electro-hydraulic three point hitch. 2006 American Control Conference, Jun 14-16 2006, Minneapolis, MN,

United States, Institute of Electrical and Electronics Engineers Inc., Piscataway, NJ 08855-1331, United States.

Plahuta, M. J., M. A. Franchek, and S. Hansjoerg (1997). "Robust controller design for a variable displacement hydraulic motor." Proceedings of the 1997 ASME International Mechanical Engineering Congress and Exposition, Nov 16-21 1997 **4**: 169-176.

Rodden, J. (1960). "A mathematical representation of hydraulic servomechanisms." Automatic Control, IRE Transactions on **5**(2): 129-135.

Sam, Y. M., J. H. S. Osman, M. R. A. Ghani (2003). Active suspension control: Performance comparison using proportional integral sliding mode and linear quadratic regulator methods. Proceedings of 2003 IEEE Conference on Control Applications, Jun 23-25 2003, Istanbul, Turkey, Institute of Electrical and Electronics Engineers Inc.

Sepulchre, R., M. Jankovic, and P. V. Kokotovic (1997). Constructive nonlinear control. Springer-Verlag New York , c1997.

Sepulchre, R., M. Jankovic, and P. V. Kokotovic (1997). "Integrator forwarding: a new recursive nonlinear robust design." Automatica **33**(5): 979-984.

Sepulchre, R. and P. V. Kokotovic (1997). Interlaced Systems and Recursive Designs for Global Stabilization. Presented at the 4th European Control Conference ECC, Brussels, 1997.

Sirouspour, M. R. and S. E. Salcudean (2000). On the nonlinear control of hydraulic servo-systems. ICRA 2000: IEEE International Conference on Robotics and Automation, Apr 24-Apr 28 2000, San Francisco, CA, USA, Institute of Electrical and Electronics Engineers Inc., Piscataway, NJ, USA.

Sun, H. and G. T.-C. Chiu (1999). Nonlinear observer based force control of electro-hydraulic actuators. Proceedings of the 1999 American Control Conference (99ACC), Jun 2-Jun 4 1999, San Diego, CA, USA, Institute of Electrical and Electronics Engineers Inc., Piscataway, NJ, USA.

Sun, W., H. He, W. Shulian (1998). Continuous CMAC and its application in identification of electrohydraulic servo system. Proceedings of the 1998 ASME International

Mechanical Engineering Congress and Exposition, Nov 15-20 1998, Anaheim, CA, USA, ASME, Fairfield, NJ, USA.

Ursu, I., F. Popescu (2003). Control synthesis for electrohydraulic servo mathematical model. 11th Int. Conf. Applied and Industrial Mathematics CAIM, Oradea, Romania.

Ursu, I. and F. Ursu (2004). "New results in control synthesis for electrohydraulic servos." International Journal of Fluid Power **5**(3): 25-38.

Ursu, I., F. Ursu, and F Popescu (2006). "Backstepping design for controlling electrohydraulic servos." Journal of the Franklin Institute **343**(1): 94-110.

Woo, Z.-W., H.-Y. Chung, and J. Lin (2000). "PID type fuzzy controller with self-tuning scaling factors." Journal of Fuzzy Sets and Systems **115**(2): 321-326.

Yongqian, Z., S. LeQuoc, and M. Saad (1998). Nonlinear fuzzy control on a hydraulic servo system. American Control Conference. Proceeding of the.

Yoshimura, T., Y. Isari, and J. Hino (1997). "Active suspension of motor coaches using skyhook damper and fuzzy logic control." Control Engineering Practice **5**(2): 175-184.

Yu, W.-S. and T.-S. Kuo (1996). "Robust indirect adaptive control of the electrohydraulic velocity control systems." IEE Proceedings: Control Theory and Applications **143**(5): 448-454.

Yu, W.-S. and T.-S. Kuo (1997). "Continuous-time indirect adaptive control of the electrohydraulic servo systems." IEEE Transactions on Control Systems Technology **5**(2): 163-177.

Zeng, W. and J. Hu (1999). "Application of intelligent PDF control algorithm to an electrohydraulic position servo system." Proceedings of the 1999 IEEE/ASME International Conference on Advanced Intelligent Mechatronics (AIM '99), Sep 19-Sep 23 1999: 233-238 BN - 0-7803-5038-3.

Zhiming, J., W. Shengwei, and L. Tinggi (2003). "Variable structure control of electrohydraulic servo systems using fuzzy CMAC neural network." Transactions of the Institute of Measurement and Control **25**(3): 185-201.